UNIVERSITÀ
DEGLI STUDI
DI PADOVA

# UNIVERSITA' DEGLI STUDI DI PADOVA

## DEPARTMENT OF PHARMACEUTICAL SCIENCE

Doctoral School in Regeneration Biology and Medicine

Curriculum in Tissue and Transplant Engineering

Cycle XXIV

# *STUDIES ON POLYMER CONJUGATION AS VERSATILE TOOL FOR DRUG DELIVERY*

**School Director :** Ch.mo Prof. Mariateresa Conconi

**Supervisor** : Ch.mo Prof. Oddone Schiavon

**PhD Student** : Chiara Clementi

*31 Gennaio 2012*

*Al mio entusiasmo e alla mia volontà!!!!*

# INDEX

# ABBREVIATIONS & SYMBOLS

*Studies on polymer conjugation as versatile tool for drug delivery*

| | |
|---|---|
| **A** | Absorbance |
| **AA** | Amino acid |
| **ACN** | Acetonitrile |
| **ALN** | Alendronate |
| **ATP** | Adenosine triphosphate |
| **AUC** | Area Under the Curve |
| **BSA** | Bovine Serum Albumins |
| **β-Glu** | β-glutamic acid |
| **BPs** | Bisphosphonates |
| **° C** | Degree Celsius |
| **CDI** | Carbonyldiimidazole |
| **$C_0$** | Initial concentration |
| **Cl** | clearance |
| **$C_t$** | Concentration at time t |
| **d** | Density |
| **D** | Dose |
| **Da** | Dalton |
| **DAPI** | 4',6-diamidino-2-phenylindole |
| **DCC** | *N,N'*-Dicyclohexylcarbodiimide |
| **DMEM** | Dulbecco's Modified Eagle's Medium |
| **DMF** | N, N-dimethylformamide |
| **DMSO** | Dimethylsulfoxide |
| **DNA** | Deoxyribonucleic Acid |
| **ECM** | Extra Cellular Matrix |
| **EPI** | Epirubicin |
| **EPR** | Enhanced Permeability and Retention Effect |
| **$ET_3N$** | Triethylamine |
| **FBS** | Fetal Bovine Serum |
| **FDA** | Food and Drug Administration |
| **FITC** | Fluorescein isothiocyanate |
| **FR** | Folate Receptor |
| **G-CSF** | Granulocyte Colony-Stimulating Factor |
| **GH** | Growth Hormone |
| **GG** | Glycine-Glycine |
| **GPLG** | Glycine-Phenilalanine-Leucine-Glycine |
| **GPC** | Gel Permeation Chromatography |
| **HOBT** | 1-Hydroxybenzotriazole |
| **HPMA** | Poly-hydroxypropyl-methacrylamide |
| **HUVEC** | Human umbilical vein endothelial cells |
| **$IC_{50}$** | 50% Inibition Concentration |
| **IFN** | Interferon |
| **J** | Dissociation constant |
| **Ke** | Elimination rate constant |
| **LHRH** | Luteinizing Hormone-Releasing Hormone |
| **MCF-7** | Human breast cancer cell line |
| **MCF-7/Dx** | Human breast cancer cell line with multidrug resistence |
| **MeCN** | Acetonitrile |
| **MDA-MB-231** | Human mammary adenocarcinoma cell line |
| **Mn** | Nominal molecular weight |

| | |
|---|---|
| **mPEG-** | Metossi poly-(ethylene glycol) |
| **mQ** | Deionized water and filtered through Millipore filter ® |
| **MTT** | 3 - (4,5-Dimethylthiazole-2-yl) -2,5-diphenyl-tetrazolium bromide |
| **Mw** | Molecular weight |
| **NHS** | *N*-Hydroxysuccinimide |
| **NMR** | Nuclear Magnetic Resonance |
| **PBS** | Phosphate Buffer Solution |
| **PC3** | Human prostate adenocarcinoma cell line |
| **PEG-** | Poly (ethylene glycol) |
| **PGA** | Polyglutamic acid |
| **PPi** | Inorganic pyrophosphate |
| **ppm** | Parts per million |
| **PSA** | Polysialic acid |
| **PTX** | Paclitaxel |
| **RES** | Reticuloendothelial system |
| **RGD** | Argininina-Glycine-Aspartic |
| **RI** | Refraction Index (refractive index) |
| **RNA** | Ribonucleic acid |
| **RP-HPLC** | Reverse Phase-High Performance Liquid Chromatography |
| **RPM** | Revolutions Per Minute |
| **SCID** | Severe Combined Immuno Deficiency |
| **SDS** | Sodium dodecyl sulphate |
| **SMA** | Styrene-maleic anhydride |
| **SMANCS** | Styrene-maleic anhydride-neocarcinostatina |
| **4T1** | Murine mammary adenocancinoma cell line |
| **t ½** | Half-life |
| **TEA** | Triethylamine |
| **TFA** | Trifluoroacetic acid |
| **TNBS** | Acid 2,4,6-trinitro-benzenesulfonic |
| **TNF** | Tumor Necrosis Factor |
| **$t_R$** | Retention time |
| **UV** | Ultraviolet |
| **VD** | Apparent volume of distribution |
| **VEGF** | Vascular Endothelial Growth Factor |
| **VIS** | Visible |
| **ø** | diameter |

# ABSTRACT

*Studies on polymer conjugation as versatile tool for drug delivery*

Drug delivery is a rapidly evolving field aimed to maximize the potential and safety of therapeutic agents.

The project of this thesis focused on development and characterization of drug delivery systems (*DDSs*), based on polymeric carriers. Among, the advantages of these systems it is possible to list an increased solubility, a prolonged exposure of the drug, a protection from enzymatic degradation and a controlled release of drug and an accumulation in diseased tissues. The *DDSs* developed here were firs tested in the context of cancer therapy where the delivery, controlled release and targeting are important issues. Nevertheless these systems can also be applied to tissue engineering where the same issues are important for the development of scaffolds capable of releasing growth factors for cells.

This work was divided into two studies. The first study focused on the comparison of the biological behavior (*in vitro* cytotoxicity, cellular uptake and pharmacokinetic properties *in vivo*) of five polymer-drug conjugates diversified for the types of polymeric carrier and containing Epirubicin as a model anticancer drug, conjugated via amide bond. The carriers were distinguished on: non-biodegradable (N-(2-hydroxypropyl) metacrylamide copolymers (HPMA) with either the enzymatic cleavable linker GPLG or the stable GG and poly(ethylene glycol) (PEG)) and biodegradable polymers (poly(L-glutamic acid) (PGA) and polysialic acid (PSA)). After characterisation in terms of purity and stability under physiological conditions, all conjugates were tested *in vitro* on MCF-7 (human breast cancer cells) and MCF-7/Dx (human breast cancer cells with resistance to anthracyclines). In MCF-7, all conjugates were relatively non-cytotoxic at the concentrations tested as expected for the type of conjugates synthesized. In the case of the two biodegradable conjugates some cytotoxic activity degree was still observed (approximately 40% reduction of viability at a concentration of 1μM, for both polysialic acid and polyglutamic acid). PEG-EPI, HPMA-GPLG-EPI, HPMA-GG-EPI and PGA-EPI were also inactive in multidrug-resistant sub-line (MCF 7/Dx), while PSA-EPI reduces of 30% cell viability at the concentration of 1 μM. Studies performed with FACS, in the presence of selective inhibitors of different mechanisms of endocytosis, allowed to understand that all conjugates were internalized by endocytosis cholesterol-dependent suggesting that uptake is not responsible for the different pattern of cytotoxicity observed. Finally, pharmacokinetic studies performed *in vivo* in mice Balb/c, shown a significantly increased half-life of the conjugates compared to free drug.

The second study focused on the synthesis and characterization of target polymer-drug conjugates, based on a PEG with a defined dendritic structure for delivery of the anticancer drug paclitaxel (PTX). The structure of PEG Dendron offer the possibility to obtain defined chemical structure in terms of drug and targeting moiety contents. Furthermore, it was hypothesized that by synthesizing a heterobifunctional PEG-dendrimer, namely $NH_2$-PEG-βGlu-$(βGlu)_2$-$(COOH)_4$, it could be possible to obtain a conjugate with a high degree of homogeneity, thus impacting positively on both the targeting and activity properties. The heterobifunctional PEG allows the subdivision of targeting and activity functions by linking PTX and ALN at the two different end chains of the polymers. This design leads to the obtainment of an amphiphilic conjugate, being PTX highly hydrophobic and ALN hydrophilic. The spatial separation of these drugs, besides offering the possibility to form self-assembled micelles, will maintain all ALN molecules exposed to the water, promptly available for binding to the bone mineral hydroxyapatite.

Paclitaxel was conjugated via ester bond, through a succinic spacer, at one end of PEG, while, at the opposite end, four molecules of alendronate were linked, to obtain a bone targeting. In addition, the conjugates can accumulate in tumor by passive targeting, because their high molecular weight allows to accumulate in the tumor tissue thanks to a preferential extravasation in solid tumors due to blood vessels high permeability, also known as EPR effect (Enhanced Permeability and Retention).

All conjugates synthesized were characterized in terms of amount of PTX and ALN content, purity and stability under physiological conditions. These conjugates showed a 50% of degradation after 1 hour of incubation at pH 7.4 and in plasma, confirming that, the type of bond, allows the drug release under physiological conditions. The conjugates-based PTX and ALN have also been shown high affinity for hydroxyapatite *in vitro*, confirming the potential of alendronate as target agent, and cytotoxic activity similar to free drug or in combination with alendronate in 4T1 cells (murine mammary adenocarcinoma cells line), MDA-MB-231 (human mammary adenocarcinoma cells line) and PC3 (human prostate adenocarcinoma cells line). Anti-angiogenic properties of alendronate in combination with paclitaxel were also evaluated, testing conjugates in HUVEC (human umbilical vein endothelial cells). PTX and ALN in free form and conjugated, showed a inhibition of proliferation and migration of HUVEC and also, after 8 hours of incubation, a reduction of capillary structures formation by 50-60%.

*In vivo* an improve of pharmacokinetic profile compared to free drug was found, which was confirmed by an increase of half-life. In addition tumor activity studies *in vivo* were performed by inoculating both 4T1 cells (syngeneic mouse) and MDA-MB-231 (xenograft mouse) in tibia mice. These studies shown that PTX-PEG-ALN conjugate has a greater antitumor effect compared to PTX alone at the same dose. This enhanced antitumor activity was attributed to preferential accumulation of the conjugate in the tumor tissue, as confirmed by the analysis of distribution in the body, performed with FITC-labeled conjugates. Furthermore, treatment with the conjugate did not result in weight loss or death of the animal in contrast to what was found for mice treated with paclitaxel and paclitaxel in combination with alendronate.

This type of bone targeting was studied with the prospects of using these derivatives PEG-alendronate in order to target growth factor for the preparation of scaffolds in the area of bone tissue reconstruction.

# RIASSUNTO

*Studies on polymer conjugation as versatile tool for drug delivery*

Il *Drug Delivery* è un campo in rapida evoluzione a cui si fa sempre più ricorso per massimizzare le potenzialità e la sicurezza degli agenti terapeutici.

Il progetto di questa tesi è focalizzato sullo sviluppo e la caratterizzazione di sistemi di veicolazione di molecole biologicamente attive. Sono stati studiati sistemi di d*rug delivery (DDSs)* basati sui carrier polimerici. Fra i vantaggi di questi sistemi è possibile elencare un aumentata solubilità, una prolungata esposizione del farmaco, una protezione dalla degradazione enzimatica un rilascio controllato del principio attivo e un accumulo preferenziale nel tessuto malato. I *DDSs* qui sviluppati sono stati prima testati nell'ambito della terapia antitumorale dove sono importanti le problematiche di *delivery*, rilascio controllato e *targeting*. Tuttavia questi potranno essere applicati anche al campo dell'ingegneria tissutale dove le medesime problematiche sono di basilare importanza per lo sviluppo di *scaffold* per cellule in grado di rilasciare fattori di crescita.

Questo lavoro si è articolato in due studi. Il primo studio si è focalizzato sulla comparazione del comportamento biologico (citotossicità *in vitro*, *uptake* cellulare e farmacocinetiche *in vivo*) di cinque coniugati polimero-farmaco diversificati per il tipo di carrier polimerico e contenenti epirubicina come farmaco antitumorale modello, coniugato via legame amidico. I *carrier* presi in considerazione si distinguono in: polimeri non-biodegradabili (poli-idrossipropilmetacrilamide (*HPMA*) sia con GFLG come spaziatore degradabile che GG come spaziatore stabile, e polietilenglicole (*PEG*)) e polimeri biodegradabili (acido poliglutammico (*PGA*) e acido polisialico (*PSA*)).

Dopo essere stati caratterizzati dal punto di vista della purezza e della stabilità in condizioni fisiologiche, tutti i coniugati sono stati testati *in vitro* su cellule MCF-7 (cellule umane di adenocarcinoma al seno) e MCF-7/Dx (cellule umane di adenocarcinoma al seno con resistenza alle antracicline). Nelle cellule MCF-7, tutti i coniugati risultano relativamente non citotossici alle concentrazioni testate come ci si attendeva per il tipo di coniugati sintetizzati. Nel caso dei due coniugati biodegradabili è stata comunque osservata una certa attività citotossica (circa 40% di riduzione della vitalità alla concentrazione 1µM sia per acido polisialico che poliglutammico). PEG-Epi, HPMA-GFLG-Epi, HPMA-GG-Epi e PGA-Epi sono risultati inattivi anche verso le cellule resistenti alle antracicline, mentre il PSA-Epi alla concentrazione 1µM riduce del 30% la vitalità. Gli studi eseguiti con *FACS* in presenza di inibitori selettivi dei diversi meccanismi di endocitosi hanno permesso di capire che tutti i

coniugati sono stati internalizzati attraverso endocitosi colesterolo-dipendente suggerendo quindi che l'*uptake* non è responsabile del diverso comportamento di citotossicità osservato. In fine, sono stati eseguiti studi farmacocinetici *in vivo* su topi Balb/c, attraverso i quali è stato dimostrato un significativo aumento del *half-life* dei coniugati rispetto al farmaco libero.

Il secondo studio si è focalizzato sulla sintesi e caratterizzazione di coniugati polimero-farmaco direzionati basati sul PEG, con struttura dendrica ben definita, per la veicolazione del farmaco antitumorale paclitaxel (PTX). La conformazione del PEG dendrone offre la possibilità di ottenere una struttura chimica definita in termini di contenuto di farmaco e agente di *targeting*. Inoltre, è stato ipotizzato che sintetizzando un PEG dendrone eterobifunzionale, chiamato $NH_2$-PEG-βGlu-$(βGlu)_2$-$(COOH)_4$, è possibile ottenere un coniugato con un alto grado di omogeneità che condiziona positivamente sia le proprietà di targeting sia l'attività. Il PEG eterobifunzionale permette la suddivisione della funzione di targeting da quella dell'attività attraverso il legame del paclitaxel e dell'alendronato alle due estremità del polimero. Una struttura così disegnata porta ad ottenere un coniugato anfifilico, date le caratteristiche idrofobiche del paclitaxel e quelle idrofiliche dell'alendronato. Inoltre, la separazione spaziale dei due farmaci, oltre ad offrire la possibilità di formare micelle, permette di mantenere tutte le molecole di alendronato esposte all'acqua e quindi immediatamente disponibili per il legame con i minerali di idrossiapatite dell'osso. Il paclitaxel è stato quindi coniugato via legame estereo, attraverso uno spaziatore succinico, ad una estremità del PEG mentre all'estremità opposta sono state legate quattro molecole di alendronato, per ottenere un *targeting* mirato all'osso. I coniugati possono, inoltre, accumularsi nel tumore per *targeting* passivo*,* in quanto il loro elevato peso molecolare ne permette l'accumulano nel tumorale grazie ad una extravasazione preferenziale nei tumori solidi per l'elevata permeabilità dei vasi sanguigni in questa sede, noto anche come effetto EPR (*Enhanced Permeability and Retention*).

Tutti i coniugati sintetizzati sono stati caratterizzati dal punto di vista della quantità di PTX e ALN legati, della purezza e della stabilità in condizioni fisiologiche. Tali coniugati hanno dimostrato una degradazione del 50% dopo 1h di incubazione a pH 7.4 e in plasma confermando così che il tipo di legame permette il rilascio del farmaco in condizioni fisiologiche. I coniugati a base di PTX e ALN hanno inoltre dimostrato di avere elevata affinità per l'idrossiapatite, *in vitro*, permettendo così di confermare le potenzialità dell'alendronato

come agente direzionante, e attività citotossica simile a quella del farmaco libero o in combinazione con alendronato in cellule 4T1 (cellule murine di adenocarcinoma mammario), MDA-MB-231 (cellule umane di adenocarcinoma mammario) e in PC3 (cellule umane di adenocarcinoma prostatico). Sono state inoltre valutate le proprietà anti-angiogeniche dell' alendronato in combinazione con il paclitaxel testando i coniugati in HUVEC (cellule endoteliali umane del cordone ombelicale). PTX e ALN in forma libera e i coniugati hanno mostrato inibizione sia della proliferazione che della migrazione di tali cellule, inoltre dopo 8 ore di incubazione, è stata osservata riduzione della formazione di strutture capillari del 50-60%. *In vivo* è stato riscontrato un miglioramento del profilo farmacocinetico, comparato a quello del farmaco libero, confermato da un incremento dell' *half life*. Sono stati eseguiti, inoltre, studi di valutazione dell'attività tumorale *in vivo*, inoculando sia cellule 4T1 (*syngeneic mouse*) sia MDA-MB-231 (*xenograft mouse*) a livello tibiale nel topo. Questi studi hanno dimostrato che il coniugato PTX-PEG-ALN presenta un effetto antitumorale superiore comparato a quello del PTX da solo alla stessa dose. Questa migliore attività antitumorale è stata attribuita all'accumulo preferenziale del coniugato nel tessuto tumorale, come confermato dall'analisi di distribuzione nel corpo eseguita con gli stessi coniugati ma fluoresceinati. Inoltre, il trattamento con il coniugato non ha comportato né perdita di peso né mortalità dell'animale diversamente da quanto riscontrato per i topi trattati con paclitaxel e paclitaxel in combinazione con alendronato.

Questo tipo di *targeting* all'osso è stato studiato con le prospettive di impiegare questi derivati PEG-Alendronato al fine di veicolare agenti di crescita per la costituzione di *scaffold* nell'area di ricostruzione del tessuto osseo.

# INTRODUCTION

*Studies on polymer conjugation as versatile tool for drug delivery*

## 3.1 DRUG DELIVERY SYSTEMS (DDSs)

Drug delivery can be divided into a variety of subjects: micro- and nanoparticles, liposomes, release from matrix or gel, association with cyclodextrine and conjugation with natural or synthetic polymer. These systems, containing polymers, can be seen as the first generation of "*nanomedicines*"[1].

Drug delivery systems (DDSs) technology is particularly promising to improve the *in vivo* efficiency of active molecules. Moreover, it is possible to stabilize and prolong the half life at biologically active molecules, thus prolonging the in vitro activity. DDSs can be used either for the delivery of anticancer drug but also for the controlled release of growth factors essential for the tissue engineering.

### 3.1.1 Tissue Engineering

As a consequence of disease or trauma, the tissues and organs in our bodies may be unable to perform their anatomical and metabolic functions. Until recently the use of implants, and in severe cases transplants, is the only way to deal with these pathological conditions [2]. In recent years, a new branch of regenerative medicine called tissue engineering is under development. This term, officially coined in 1988 by the National Science Foundation, indicates that this multidisciplinary field produces biological substitutes containing living and functional cells for regeneration, maintaining or improving performance of the tissue [3].

Tissue engineering represents the meeting point of different disciplines such as medicine, biology, engineering, and chemistry with the common purpose for obtaining or replacing organs or parts of organs in the human body. This will make possible to have a viable alternative to transplantation, as this can have many fundamental problems such as the chronic shortage of donors, the phenomena of organ rejection and the continued need to take immunosuppressive drugs [2]. In general, a tissue engineering construct is formed by cellular component and a basic structure with function support. By production of extracellular matrix, the cells promote the interaction with the implantation site. A great advantage of this technique is that the cells can be donated from the patient himself; once

selected they are grown *in vitro* and subsequently replanted [4]. The basic structure can be by an artificial component, polymer type, or from natural component that can ensure the support to the cell populations of interest.

Therefore, the aims of tissue engineering are to design organs and prostheses, and to assess the interaction between biomaterial and cellular component facilitating the rapid and efficient regeneration of the original tissue. Moreover, the support must be biocompatible and biodegradable. To optimize the adhesion and cell growth, adhesion peptides are derived from the sequence RGD (arginine, glycine, aspartic acid), or the proteoglycan KSRS type (lysine, serine, arginine, serine). Another way to allow cell proliferation is to add sequences to the culture medium that belong to active growth factors specific for the type of cells used. When the tissue around the defect has no inherent potential to regenerate, the tissue regeneration cannot always be expected by providing the scaffolding technology and space mentioned above. In this case, it would be better to combine the technology with cells and/or a growth factor which has the potential to accelerate tissue regeneration. It is possible to use cells which were proliferated *in vitro* by the method described above.

To overcome the problem of the *in vivo* instability of biological substances such as protein and genes that are used to induce tissue regeneration, it is vital to use technology to develop the administration form. Indeed, when a solution of the growth factor is injected into the site requiring regeneration, the biological effect cannot be always predicted. This is because the growth factor is rapidly diffused away from the injection site. To enhance the *in vivo* efficacy of the growth factor, the drug delivery system (DDS) is promising. It is possible that when used in combination with an appropriate DDS technology, the growth factor enhances the *in vivo* proliferation and differentiation of key cells which promotes tissue regeneration. For example, the controlled release of the growth factor at the site of action over an extended time period is performed by incorporating the factor into an appropriate carrier. It is also possible that the growth factor is protected against proteolysis, as it is incorporated in the release carrier for prolonged retention of the activity *in vivo.* Other than the controlled release method, this DDS technology for half-time prolongation, absorption improvement and targeting are also applicable in tissue engineering using protein and genes.

### 3.1.2 Antitumor therapy

Cancer is a leading cause of death in the United States and about one person in three is affected [5]. The diagnosis of cancer has always been considered fatal, but the recent development of new cares in the treatment of solid tumors has improved the life expectancy of cancer patients. In recent years it was developed and approved for clinical use a number of chemotherapeutic agents, and the lines of research were developed in the following directions [6]:

- development of new anticancer agents with low molecular weight [7] obtained with a screening program among the natural compounds, synthetic and combinatorial chemistry;
- identification of new tumor targets (such as the processes of apoptosis and angiogenesis) for chemotherapy [8,9];
- development of gene therapy and antisense oligonucleotides [10];
- development of better drug delivery systems for anticancer drugs selectively localize in diseased tissues, using as a carrier: liposomes, immune-conjugated, proteins, peptides and polymers for therapeutic use [11].

Drug delivery is an area of research developed to overcome the problems associated with the use of traditional chemotherapeutic agents which, although often very powerful, have low specificity, resulting in the destruction of cancer cells and also healthy ones. This lack of specificity involves, also, the use of higher doses resulting in increased toxic side effects. Another problem that should not be underestimated is the emergence of drug resistance in cancer cells, which reduces the possibility of intervention. Many experts believe that was identified a sufficient number of anticancer agents, but an effective cancer therapy will be reached only by obtaining a suitable drug delivery systems, able to direct into target site. Despite this technology, it’s impossible that only a single treatment may be the cure for all different types of tumors, but the therapeutic polymers seem to be a good starting point to modify and improve the physical-chemical characteristics and pharmacokinetic profiles of anticancer agents.

## 3.2 THERAPEUTIC POLYMERS

The term "polymer therapeutics" [12,13] describes the family of compounds and drug delivery technology that uses a polymer soluble in water as a common central component (core component). The term includes polymeric drugs, polymer-drug conjugates, polymer-protein conjugates, non-viral vectors for intra-cytoplasmatic transportation and polymeric micelles that trap covalently bound drugs [1].

The compounds obtained with these technologies often regarded as "new chemical entities" or "pro-drugs", according to fact that the conjugate is already active or that the drug bound needs to be freed in order to explain its action. A pro-drug is, in fact, a form of drug that remains inactive until it reaches the site of action where is activated by specific conditions in the target site. The conjugation of drugs with polymers form the so-called "Polymeric pro-drugs" which are part of the category of "Polymeric Drug Delivery System (PDDs)" [14]. The task of these systems is to improve drug distribution, bioavailability, targeting, and provide a controlled release of therapeutic agent over time.

### 3.2.1 Use of polymers for the controlled release of biological active molecules

The delivery of biologically active molecules, especially with various types of polymeric systems has several advantages:

- less frequent dosing
- lower doses, and below the minimum toxic concentration
- protection of the drug from inactivation resulting in prolonged half life [15].

Drug release from polymeric systems may be due to a physical or chemical mechanism:

- physically controlled-release system: the drug can be found surrounded by an insoluble polymer membrane or dispersed in a in soluble polymer matrix; therefore there is a release by diffusion. In other cases the initially dry polymer can swell, implicating the osmotic process, especially in the membrane system;

- chemically controlled release system: there is a link between the active molecule and biodegradable polymer, or the active molecule is dispersed in a matrix bioerodible [16].

Then there are delivery systems implanted *in situ*, where there is local release of the active substance from insoluble polymer.

The bioactive molecule field has had great developments in bioconjugation, which provides the formation of a covalent bond between a macromolecule of polymer and the active molecule, creating a new chemical entity that has typical characteristics [16].

### 3.2.2 Experimental model of conjugated polymeric

The use of a soluble macromolecular carrier for bioactive molecules delivery can alter the pharmacokinetic characteristics without altering the activity and bioavailability in the target site. The only characteristics modified are the half-life, its distribution in various body areas and its elimination.

The use of carrier systems based on synthetic water-soluble polymers defined as polymeric drug carriers, was proposed for the first time in 1975 by Helmut Ringsdorf [17]. He suggested combining the drug covalently-bonded with water-soluble polymer chains, subject to enzymatic or hydrolytic cleavage in the target site (Fig. 3.1).

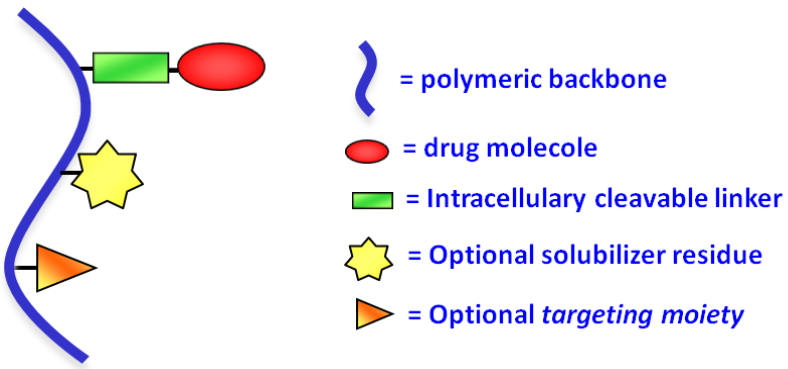


**Figure 3.1:** Model of polymeric carrier

This model suggested by Ringsdorf (summarized in figure 3.1) must have particular characteristics and was made by:

- an inert water-soluble polymeric carrier (polymer backbone), with certain characteristics;
- a spacer interposed between biodegradable polymer and active molecules (intracellulary cleavable linker) capable of giving a bond that is broken only at the site of action, releasing the active biomolecules;
- the bioactive molecule covalently linked to the linker;
- targeting ligand that may or may not be linked to the polymer structure, promoting the direction and specific uptake by target cells while minimizing nonspecific interactions;
- functional group additives, which influence the solubility of the conjugate.

### 3.2.3 Characteristics of polymeric carrier

As mentioned earlier [17,18], the Ringsdorf polymer carrier model must have certain characteristics, and it has been tried in various polymers for drug delivery, both natural and synthetic. This has resulted in identification of requirements for an ideal carrier:

- the polymer must be biocompatible and not induce significant toxicity or immunogenicity;
- must be biodegradable by hydrolytic or enzymatic activity, and not have a molecular weight greater than 40kDa to aid elimination from the kidneys or liver to avoid accumulation;
- must have low polydispersity;
- the polymer must be found in large-scale, low cost and made by simple economic processes;
- must be hydrophilic to ensure its solubility in body fluids and to increase the solubility of the bound drug;
- must possess the functional groups that allow binding of the drug and the residue targeting with simple chemical reactions, not involving toxicity or immunogenicity;

- the link between the polymer and drug must be sufficiently stable in the bloodstream and easily hydrolysable in the target cells, in order to have a controlled release of the drug;
- the conjugate must present a sufficient carrying capacity, to ensure the correct amount of drug at the site of action;
- the conjugate must have a molecular weight that ensures the accumulation in the tumor tissue by EPR effect (Enhanced Permeability and Retention) and any excess drug should be removed quickly without reaching places where it can exert toxic action;
- industrial production of the conjugate must be reproducible, economic and its analytical characterization must be complete and validated;
- the characteristics of the conjugate must be sufficient for an appropriate formulation with an high stability and easy administration.

### 3.2.4 Bioactive molecules release

The bioactive molecules bound to macromolecular carrier may be release as following:

- passive hydrolysis
- pH-dependent hydrolysis
- enzymatic hydrolysis

The steps of hydrolysis mainly involve those bonds more sensitive to normal hydrolytic action, such as esters, amides, carbonates and urethanes. The percentage of the drug released will depend on the stability of the bonds themselves. This will be greater for the ester groups because they are very sensitive to hydrolysis, and decrease progressively with carbonates, urethanes and amides.

The acidic environment of lysosomes (pH of about 4.5-5.5) can be exploited to obtain pH dependent hydrolysis by linking of the bioactive molecules to the polymer through a linker sensitive to this environment [16, 19]. Last enzymatic hydrolysis may occur in conjugates that present a polypeptides spacer between the active molecule and carrier,

sensitive to the action of many enzymes present in the lysosomal level, such as phosphatases, esterases, glycosidases and peptidases [20, 21]. Different peptide spacers have been studied, especially for the peptide and protein conjugates, and according to the amino acid sequence chosen, there is an action of either enzyme. In the literature there are examples of conjugated polymers designed to be sensitive to cathepsins, cysteine peptidase-dependent present in large quantities and with high activity at lysosomal level.

### 3.2.5 Problems and advantages of bioconjugates

The bioconjugates is certainly an encouraging strategy to increase the effectiveness of injectable drugs because it allows us to obtain new chemical entities with specific chemical, physical and biological characteristics that positively affect the pharmacokinetics and pharmacodynamics of the therapeutic agent. There are issues to overcome before we obtain the ideal bioconjugate including the improvement of the chemical bond to obtain activation, conjugation that does not affect the stability of the polymer and the active site of the drug remains available. Development of analytical methods for the characterization of the conjugate and its components, the achievement of well defined polymers with low polydispersivity, the polymer have been already approved by the FDA.
Apart from these problems that are still being resolved, the bioconjugates certainly presents many advantages:

- masking of antigenic sites of the drug, especially for protein drugs with resulting reduced uptake by the immune system;
- reduction of renal excretion, due to the high hydrodynamic volume;
- increased plasma half-life, linked to previous point;
- increased the solubility of normally low solubility drugs in biological fluids;
- specific direction of the drug in tumor tissue due to the presence of targeting residues;
- greater retention of the conjugate with subsequent release of drug in tumor tissue by EPR effect;
- possibility of less frequent, and lower doses;

- reduced toxicity in other tissues and organs, as a result of the previous point;
- increased patient compliance and with improvement of quality of life;
- new internalization mechanism for the bioactive molecules into cells.

However, the main advantage is the direction of the drug only to the target site, exploiting the characteristics of the tumor tissue and the bond polymer-drug [22].

## 3.3 TARGETING

The toxicity of the chemotherapy that uses anticancer compounds with low molecular weight is due to the large distribution volume which have after intravenous administration. Low molecular weight drugs enter the cell mainly by diffusion, then, in the first minutes following intravenous administration, a high percentage of injected drug leaves the bloodstream and is distributed in the body in ubiquitous manner. The conjugation of low molecular weight drugs with high molecular weight carrier results in a substantial change in the mechanism of cell entry of the drug. The conjugation technique also offers the drugs delivery to solid tumors by EPR effect also known as passive targeting (see section 3.3.1). Further direction can be obtained by conjugation of polymer-dugs with specific target molecules obtaining a specific direction to the tumor (see section 3.3.3)

### 3.3.1 Passive targeting or EPR Effect

Cancer drugs with low molecular weight were distributed equally in healthy and diseased tissue, while macromolecular drugs as well as natural macromolecules such as albumin, could only passively accumulate in cancer tissue. This phenomenon, observed for the first time by H. Maeda, has been called Enhanced Permeability and Retention effect, or more commonly EPR effect (Fig. 3.2) [23].

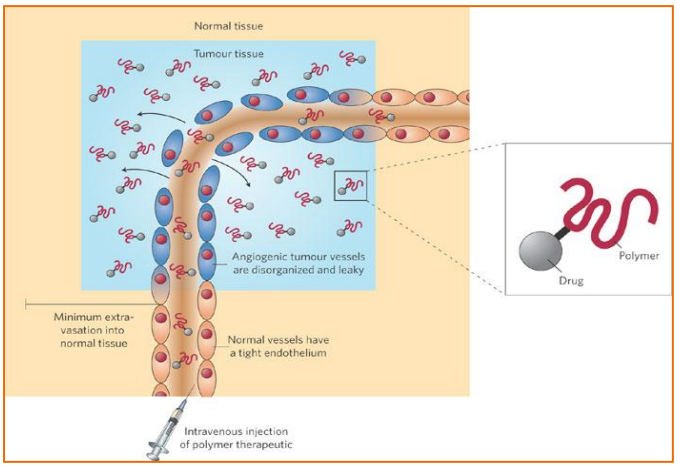


**Figure 3.2:** EPR Effect

The EPR effect is due to two main phenomena:

- increased vascular permeability (Enhanced Permeability) compared with normal tissue, due to irregular blood vessel architecture (endothelium discontinuous) in tumor tissue [24]; extensive production of vascular mediators that facilitate the extravasations, including bradykinin, prostaglandins, NO, peroxynitrite, VEGF/VPF (vascular endothelial growth factor/vascular permeability factor) [25], active angiogenesis and high vascular density. All of these factors allow massive macromolecules and small particles extravasations, with molecular mass between 20 and 800 kDa;
- decreased drainage of the lymphatic system in tumor tissue (Enhanced Retention) which reduces the clearance of macromolecules resulting in accumulation in the tissue itself [26].

By exploiting these tumor tissue characteristics can be selectively delivered on it the antineoplastic agents like bioconjugates, thus limiting the diffusion in normal tissues, because their blood vessels structure are less permeable than the macromolecular construct still on the blood stream.

### 3.3.2 Endocytosis uptake

Traditional chemotherapy uses drugs with low molecular weight, and is often accompanied by high toxicity as the molecules are spread rapidly throughout the body, entering by simple diffusion in cells. This occurs in the first minutes following intravenous administration as there is high percentage of the injected dose which leaves the circulatory system to be distributed ubiquitously around the body. This results in the need for an increased dose; in addition there is an inevitable damage to healthy tissue.

The bioconjugation technique can partially limit the damage because the accumulation in solid tumors due to the EPR effect mentioned earlier, is facilitated by the high molecular weight of the conjugate. This can limit the cellular uptake only at the endocytosis mechanism, predominantly in tumor cells [16].

The interaction with the plasma membrane, depending on the conjugates structure could have three mechanisms of pinocytosis, summarized in figure 3.3:

- a fluid phase;
- adsorption
- receptor-mediated [18]

In the fluid phase pinocytosis do not have any interaction with the plasma membrane and it is the conjugate concentration in the extracellular fluid that determines the speed and extent of the process. Adsorption occurs after non-specific interactions with the membrane due to the presence of hydrophobic groups or positive charges on the surface of the conjugate, and it can increase the endocytosis. Finally, receptor-mediated pinocytosis occurs when the macromolecules are linked with the residues complementary to the receptors or surface antigens: in this way the conjugate is recognized and endocytic only by the target cells. Figure 3.3 shows the internalization process of the drug-polymer conjugate and the target drug-polymer conjugate.

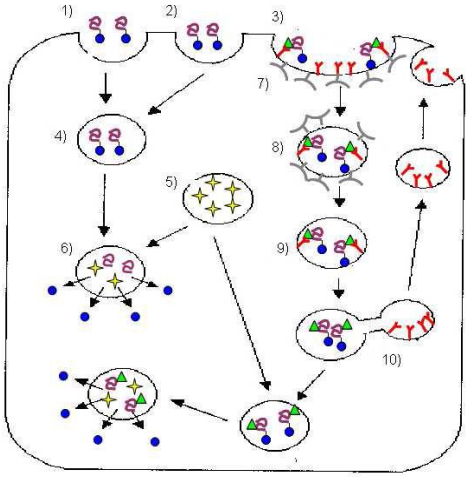


**Figure 3.3:** Uptake by endocytosis of conjugates polmerici

Figure 3.3 showed all three mechanisms of pinocytosis: a fluid phase (1), by adsorption (2) and receptor-mediated (3). In the first 2 cases (1 and 2) the pinocytic capture occurs with invagination of the plasma membrane, which captures the macromolecules present in the extracellular fluid, or deposited on the membrane. The conjugates are enclosed in vesicles and delivered to the endosomal compartment which is a pH about 6 (4). Here we can check the hydrolysis of the links or spacers susceptible to acid pH, following the endosome merges with a primary lysosome (5) to give a secondary lysosome (6). In the lysosomal compartment the macromolecules are exposed to more acidic environment (pH 4.5-5.5), and there are many enzymes capable of hydrolyzing specific bonds. The lysosomal membrane, such as plasmatic membrane, is impermeable to macromolecules and allows only products with a low molecular weight from enzyme degradation passage into the cytoplasm: so at this point the molecules of the active substance are released from the carrier and can diffuse into the cytoplasm giving their pharmacological action. In the latter case (3) i.e the receptor-mediated pinocytosis, the conjugate is linked with targeted residues bound to receptors and the cell surface antigens (Y), which are found inside clathrin-coated dimples (ب) (7). It forms a primary endosome (8) which subsequently loses the clathrin coating and becomes CURL (Compartment for Uncupling Receptor and Ligand) (10). Inside this organelle, the conjugates separate from the receptors which return to the cell surface. The endosome containing the conjugate then merges with lysosomes and as described in the mechanisms (1) and (2), gives rise to the secondary lysosome. The drug released from the carrier can now spread in the cytoplasm of treated cells.

### 3.3.3 Active targeting

In addition to passive targeting mechanisms described above, the bioconjugates can be selectively directed to tumor tissue with an active targeting mechanism. Linking a targeting residue to polymeric structure encourages the uptake by cells that have surface receptors which able to recognize the target moiety, thereby obtaining a target internalization [27].
The main objectives of the targeted drug delivery are:

- reducing the indiscriminate uptake of toxic agents;
- improvement of the accumulation of the drug at the site of action;
- limitation of the phenomenon of Multi-Drug Resistance associated transporters (eg P-glycoprotein) that are often over-expressed in cancer cells.

Many molecules have been studied as targeting agents and some of these have been exploited to direct anticancer drugs (see Table 3.1).

**Table 3.1**: Target residue commonly use

| ***Target residues*** | ***Receptor*** | ***Vehicle*** | ***Therapeutic agent delivered*** |
|---|---|---|---|
| Folic Acid | FR (Folic receptor) | Nanoparticles | Camptotecin |
| Folic Acid | FR (Folic receptor) | PEG | Doxorubicin |
| Galactosamine | Glycoprotein receptor | HPMA | Doxorubicin |
| RGD | Integrine | Nanoparticles | Doxorubicin, Paclitaxel |
| LH-RH | Estrogen receptor | PEG | Camptotecin |
| Transferrin | TFR (transferrin receptor) | Stealth Liposomes | Doxorubicin |

## 3.4 TYPES OF POLYMERS USED AS DRUG CARRIERS

### 3.4.1 Poly(ethylene glycol) (PEG)

Poly(ethylene glycol) (PEG) [28] is a synthetic amphiphilic polymer constituted by repeating oxyethylene units with molecular weight of 44 Da, and has the following structure:

$$HO[CH_2CH_2O]_nH \text{ or } CH_3O[CH_2CH_2O]_nH$$

**Figure 3.4:** Structure of poly(ethylene glycol)

Its synthesis is shown schematically in figure 3.5. This involves three steps:

I. this begins with the nucleophile attack to ethylene oxide cyclic opening the epoxy ring and the formation of oxygen reactive alcohol;
II. follows the propagation of the reaction by the addition of other ephossidic molecules;
III. finally, the cessation of the reaction by the action of a terminator.

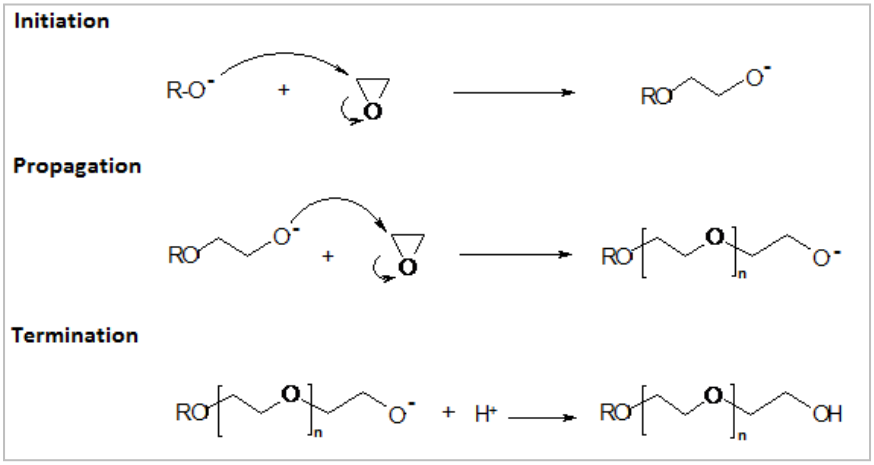


**Figure 3.5:** Synthesis of poly-ethylene glycol.

The PEG is a polymer suitable for the bioconjugates, as it characteristics include being biocompatible, it is neither toxic, allergenic nor immunogenic [29], is not charged and has only one functional group giving a clean chemistry. It is soluble in both aqueous and organic solutions [30, 31], it is not biodegradable except for molecular weights below 40 kDa, it is

easily eliminated by the kidney or liver function and does not accumulate [32]. It is also readily commercially available and is of low cost in a wide range of molecular weights and structures. All these features would allow its wide use in the biomedical field. Finally it was approved by the Food and Drug Administration (FDA) as a constituent of foods, cosmetics and pharmaceutical preparations, injections, topical, rectal and nasal applications.

The type of polymer that is formed depends on the initiator used: in aqueous solution, ethylene oxide reacts with a hydroxyl giving a bi-functional PEG-diol HO-$[CH_2CH_2\text{-}O]_nH$; in presence of a methoxy anion, in DMF, gives the mono-methoxy PEG (mPEG) mono-functional: $CH_3O\text{-}[CH_2CH_2\text{-}O]_nH$; using an initiator bi-or poly-functional, branched polymers are obtained.

#### 3.4.1.1 Uses and applications

Polyethylene glycol is used in the pharmaceutical field to obtain bioconjugates as it modifies the chemical and physical characteristics, the pharmacokinetic and pharmacodynamic therapeutic agents without drastically altering the biological activity [33, 34]. Generally, the following are observed in the pegylated active molecules:

- increased plasma half life;
- reduction of renal excretion and biodistribution for the increase of the molecular weight;
- reduction of the hydrolytic and enzymatic degradation;
- reduction of uptake into the reticulo-endothelial system [35];
- increased solubility in water [36];
- reduction of immunogenicity and antigenicity [29,37,38].

The pegylation was initially used to conjugate peptides and proteins, however there were some problems. Mild chemistry is needed so not to disable or denature the protein. The presence of many functional groups means that it is difficult to determine the exact position of binding, then is necessary to use PEG mono-functional, and the active sites of the protein will be left intact [22,40]. However there are several conjugates in both clinical trials and market which include:

- ADAGEN: conjugate between PEG and bovine adenosine deaminase [41] is marketed by Enzon, Inc., for the treatment of combined immunodeficiency syndrome;
- ONCOSPAR®: conjugate between PEG and L-asparaginase [41], used in the treatment of cancer Acute lymphocytic leukemia;
- PEG-INTRON: conjugate between PEG 12000 Da and a interferon (a-IFN) to treat hepatitis C.

In this advanced stage of research there are PEG conjugated with insulin, superoxide dismutase, interleuchine-2, hemoglobin and many others.

The pegylation technique also has been widely used in cancer therapy in order to direct the drug specifically within the tumor tissue, preventing the distribution to other areas to avoid side effects, and also to avoid circulation inactivation.

Examples of PEG conjugated with anticancer drugs include camptothecin, which is an antitumor alkaloid whose solubility is increased by binding to the polymer. There is also doxorubicin, which substantially reduced the cardiotoxic effects. In addition, there are Ara-C, methotrexate and taxanes conjugates currently being researched aiming to target the antineoplastic agent in the tumor tissue, thus reducing systemic toxicity and improving the pharmacodynamic and pharmacokinetic profiles [41].

The pegylation technique is used with antiviral, antimalarial and anti-AIDS drugs to improve their pharmacological properties [41].

However, PEG has significant applications in other areas than in the pharmacological discipline [36]. PEG is very flexible and has a strong ability to coordinate water molecules [42] and a high hydrodynamic volume that is exploited in the "two phases partitioning" purification technique, which usually employs PEG and dextran. In cyclic form it can form complexes with the transition metals; this characteristic is exploited to transfer the metals in the organic phase by allowing a new type of catalysis called phase-transfer catalysis.

The PEG is also used for the precipitation of proteins and nucleic acids, and for the synthesis of peptides and oligonucleotides in liquid and solid phase for the enzymatic catalysis in organic solvents. It can induce cell fusion and can make the bound surface materials biocompatible thus reducing the thrombogenicity. It also used in cosmetic material production.

Lately it is also widely used in the pharmaceutical industry for the preparation of drug delivery systems such as liposomes, nanoparticles, nano-and microspheres, dendrimers and

hydrogels [37] and for the preparation of prodrugs with the bioconjugation technique of peptides, proteins and low molecular weight drugs [38].

### 3.4.2 N-(2-hydroxypropyl)methacrylamide copolymers (HPMA)

HPMA is one of the most extensively studied polymers in this field. It is a synthetic, multiple pendant side chain to carry the drug/targeting residue payload, non biodegradable and non toxic polymer that has been conjugated to a variety of known anticancer compounds. The development of HPMA copolymer drug conjugates is recognized as one of the pioneering works for today's nanomedicine, a broad field of biomedical science using macromolecules and other nanosized materials for the treatment of human diseases.

The homopolymer, poly (HPMA) [43,44,45], was originally developed in the Czech Republic as a plasma expander. It was non-toxic in preclinical tests at doses up to 30 g/kg, did not bind blood proteins and was not immunogenic. Moreover like PEG, grafting of HPMA copolymer chains to proteins reduces their immunogenicity [46]. From the outset there was likelihood that this hydrophilic polymer would display minimal inherent toxicity with its main limitation being lack of biodegradability of the polymer main chain. To introduce the functionality needed for drug conjugation, and also to insert biodegradable linkers for drug liberation, HPMA copolymers were prepared.

The synthesis of the HPMA copolymer intermediates used to create conjugates tested clinically involves free radical polymerisation using HPMA and methacryloylated (MA)-peptidyl-nitrophenylester (ONp) as the co-monomers (Fig. 3.6) [43]. Normally the monomer feed ratio of HPMA:MA-peptide-ONp is 95:5, although this is changed to 90:10 in certain conjugates. Selection of optimal co-monomer chemistry/composition, and careful control of the reaction conditions to regulate polymerisation kinetics made it possible to synthesis HPMA copolymer precursors of relatively narrow molecular weight distribution (Mw/Mn=1.2–1.5).

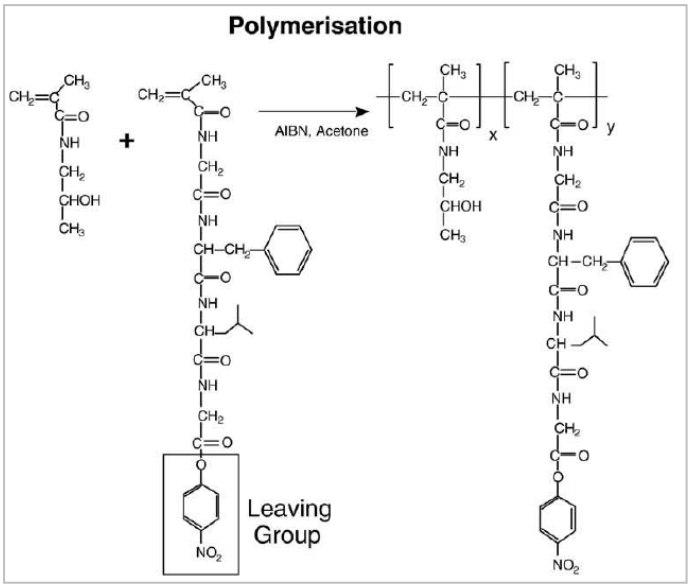


**Figure 3.6**: polymer intermediate synthesized by co-polymerisation

Drugs (and where needed targeting residues) have been generally bound to such "key" polymeric intermediates using an aminolysis reaction. It is noteworthy however, that general research studies have explored a much broader range of synthetic routes (e.g. use of drug-bearing co-monomers, binding of drugs directly to poly(HPMA) homopolymer, and use of well characterized low molecular weight functionalized drug intermediates for conjugation). Each synthetic route brings a unique profile of conjugate heterogeneity, challenges for purification and indeed impurity characterization. Early studies showed that doxorubicin conjugation to the hydrophilic HPMA copolymer led to a >10-fold increase in its aqueous solubility. Since, this "solubilising" opportunity has also been used to improve the formulation properties of other lipophilic drugs including paclitaxel. It should be emphasized that the –C–C–HPMA copolymer main chain is not biodegradable so the conjugates developed clinically have been limited to a molecular weight of < 40,000 g/mol to ensure eventual renal elimination.

Many HPMA copolymer conjugates tested clinically contain the peptidyl linker Gly-Phe-Leu-Gly [43]. This tetrapeptide was designed for stability in the circulation [47], and for degradation by the lysosomal thiol-dependant proteases, particularly cathepsin B [48]. It liberates 100% of conjugated doxorubicin over a 24–48 h period in vitro, in animals and apparently also in man.

### 3.4.2.1 Use and application

The preparation of various drug-HPMA conjugates shown that the polymer:

- increases the water solubility of the linked drug;
- guarantee the stability by decreasing the toxicity;
- the specific link with targeting compounds specifically recognized the cells, this also allows administration of lower and less frequent, due to reduced renal excretion and decreased inactivation.

The HPMA copolymer–drug conjugates that have progressed into clinical trial are summarized in table 3.2 [44].

**Table 3.2:** HPMA copolymer–conjugates that have entered clinical trials as anticancer agents.

| *Code* | *Composition* | *~MW (g/mol)* | *Status* |
|---|---|---|---|
| **FCE 28068** | HPMA copolymer-GFLG-doxorubicin | 30,000 | Phase I/II |
| **FCE 28069** | HPMA copolymer-GFLG-doxorubicin-galoctosamine | 25,000 | Phase I/II |
| **PNU 166945** | HPMA copolymer-paclitaxel | NS | Phase I-stopped |
| **MAG-CPT, PCNU166148** | HPMA copolymer-camptotecin | 18,000 | Phase I-stopped |
| **AP5280** | HPMA copolymer-carboplatinate analogue | 25,000 | Phase I/II |
| **AP5346** | HPMA copolymer-DACH palatinate analogue | 25,000 | Phase II trial as a single agent combination ongoing |

## 3.4.3 Polyglutamic acid (PGA)

Poly(L-glutamic acid) (Fig. 3.7) is naturally polymer occurring L-glutamic acid linked together through amide bonds rather than a non-degradable C-C backbone [49]. The pendent free γ-carboxyl group in each repeating unit of L-glutamic acid is negatively charged at a neutral pH, which renders the polymer water soluble. The carboxyl groups also provide functionally for drug attachment. PGA is biodegradable and non toxic. These features make

PGA a promising candidate as carrier polymer-drug conjugates for selective delivery of chemioterapeutics agents.

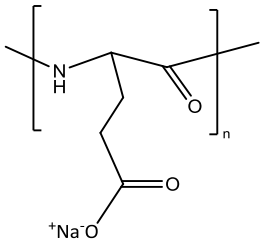

**Figure 3.7**: Structure of Poly(L-glutamic acid)

The production of PGA can be achieved by using chemical synthesis, extraction and microbial fermentation, while microbial fermentation is the most common method among the three methods. In fact, PGA was initially found in the cell wall of *Bacillus anthracis* and now obtained from *Bacillus subtilis*. The chemical strategy, instead, occur the synthesis of PGA starting from poly(γ-benzyl-L-glutamate) (PBLG) by removing the benzyl protecting group with the use of hydrogen bromide (Fig. 3.8) [49].

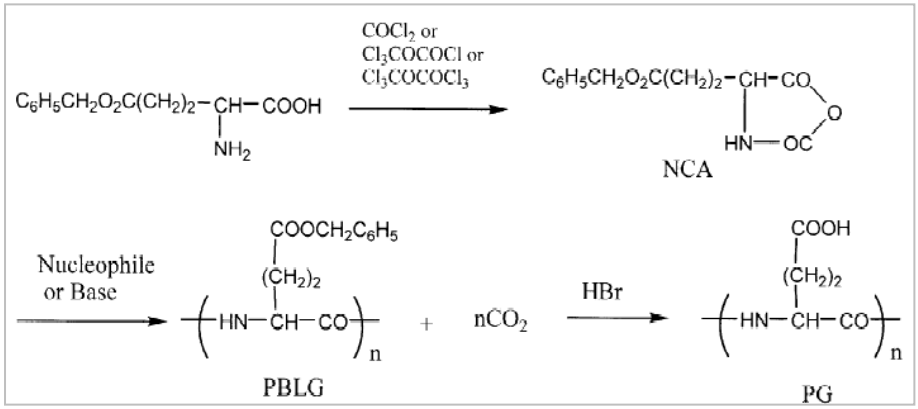


**Figure 3.8:** Reaction scheme for the synthesis of Poly(L-glutamic acid)

For the preparation of high-molecular-weight homopolymers and block or random copolymers of PBLG, triethylamine-initiated polymerization of the N-carboxyanhydride (NCA) of γ-benzyl-L-glutamate is the most frequently used methods.

The cellular uptake of negatively charged polymers can be hindered due electrostatic repulsion forces between the polymers and the rather negatively charged surface of the cells. Although PGA is no exception to this rule, it does not diminish the EPR effect and the accumulation and retention of PGA-drug conjugate in solid tumors. Specific receptor-

mediated interaction of PGA-drug conjugates containing targeting ligands may also increase the rate of polymer uptake into the target cells.

As already reported, PGA is a biodegradable polymer. PGA shows a conformational change that passes from a rod-like form in the a-helix state to a more random coil structure with increasing pH at midpoint of pH 5.5 . At neutral pH, PGA is expected to exist as a random coil. It is therefore not surprising to observe a strong effect of pH on the rate of enzymatic degradation of PGA. Indeed, a high helix content (at pH<5) and increasing charge density (at pH>5) decreased the degradation rate of PGA by papain [32]. Depending on the nature of bounds to link drug molecules to PGA, degradation of the polymer backbone may not necessarily always lead to the release of free drug. Digesting a PGA-Doxorubicin conjugate directly linked via amide bonds with papain resulted in the formation of oligomers of glutamic acid. No measurable free doxorubicin was detected in the incubation medium. Several studies have used isolated tissue lysosomal enzymes to investigate the degradability of PGA and its derivatives. PGA was found to be more susceptible to lysosomal degradation [50].

### 3.4.3.2 Uses and applications

In the past few years, PGA has been proposed for potential applications in wide areas including food, cosmetics, agriculture, sewer treatment, biodegradable plastics and other industrial applications. Today, given the structural characteristics of the polymer is more often used as polymeric carrier. In fact, the carboxylic group on the side chains of PGA offer attachment point for the conjugation of chemioterapeutic agents to the polymeric carrier. Various anticancer agents have been conjugated to PGA such as Doxorubicin [51,52,53], Ara-C [54], Paclitaxel (XYOTAX) [55,56,57] and Camptothecin [58]

### 3.4.4 Polysialic acid (PSA)

Polysialic acids (PSAs) are polymers of repeating N-acetyl neuraminic acid (Neu5Ac, sialic acid) a sugar abundantly present on the surface of cells and many proteins. Much is known about the structure and function of polysialic acids, of which there are several types depending on the linkage between each monomer. However, for the polysialylation of drugs, the α (2-8)-linked polysaccharide from group B *Neisseria meningitidis* or *E. coli* K1 and its shorter derivatives (also known as colominic acids, CAs) are the most suitable (Fig. 3.9). Other polysialic acids include the serogroup C capsular polysaccharide from *Neisseria meningitidis* group C (α 2-9) and the polysaccharide from *E. coli* K 92 (alternating α 2-8, α 2-9 Nacetylneuraminic acid links) [59].

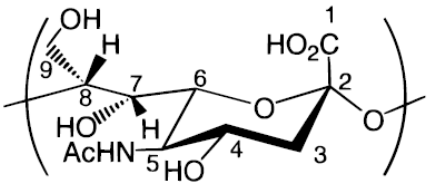


**Figure 3.9:** Structure of polysialic acid

Moreover, unlike other polymers (e.g. dextran, PEG), polysialic acids are biodegradable and their catabolic products (e.g. sialic acid) are not known to be toxic. PSAs are degraded by cellular neuraminidase. This is of particular importance where the polymer is used to improve the pharmacological profiles of therapeutics given chronically, especially when relatively large doses of the drug are required.

Polysialic acids are highly hydrophilic and highly hydrated, which is essential in order to maintain systemic inject ability. Moreover, they can be produced easily in large quantities from bacterial cultures using a non-pathogenic laboratory, adapted strain of *E. coli* K1.

Neuraminidases are responsible for the breakdown of PSA to non-toxic excretable products (i.e. Neu5Ac) of which intracellular (lysosomal) neuraminidases are particularly active upon (α 2-8)-linked PSAs. Mammalian neuraminidases catalyse the cleavage of non-reducing sialic acid residues glycosidically linked to another saccharide.

In the early 1990's, it was proposed that polysialic acids could be used to improve the pharmacokinetics and pharmacodynamics of therapeutic molecules. It was reasoned that by forming a watery "cloud" around the molecule, (via the highly hydrophilic PSA), interaction

with other molecules, whether proteolytic enzymes, opsonins, neutralising antibodies or receptors on phagocytic cells, would be hindered thus allowing the therapeutic to retain its integrity, preserve activity and prolong its presence in the body. For small peptides and drugs, a concomitant increase in size effected by PSA, together with the highly ionic state of the polymer, could also contribute to reduced loss through the kidneys. In the case of peptides and proteins (and, indeed, drug delivery systems such as liposomes), a number of polymer chains of appropriate length, attached randomly or strategically (polysialylation), would ensure protection (Fig. 3.10) [60].

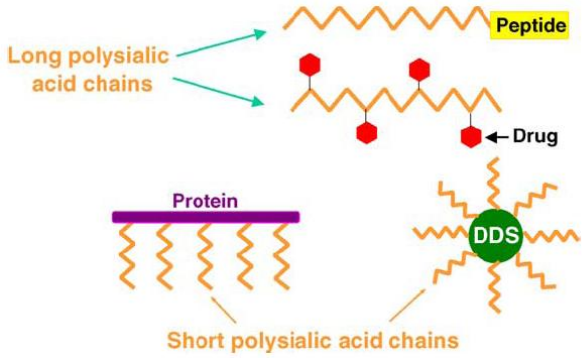


**Figure 3.10:** Schematic representation of polysialylated constructs.

The sites of possible conjugation include the amino groups that can be made available by deacetylation, carboxyl and hydroxyl groups and the reactive hemiketal group which can be activated. This enables a wide variety of drugs and other molecules to be covalently linked to PSA either directly or after mild chemical modification, with preservation of much of the drug's activity. In order to maximize the pharmacological benefits of polysialylation, an activated polysialic derivative is covalently linked to a reactive group on the polypeptide drug. The most common reactive sites on polypeptides for attaching polymers are ε amino groups of lysine, the N-terminal amino group, or thiol groups which can be selectively derivatised with maleimido forms of the polymer [59].

#### 3.4.4.1 Use and applications

Polysialylation techniques have been optimised to avoid the generation of unwanted side products and to enable attachment of PSA chains to areas in the molecule away from its active site. Promising properties of polysialylated therapeutics [59]:

- provides improved stability (polysialylation can prevent the loss of activity of a therapeutic in biological fluids);
- preserves functionality of therapeutics;
- reduces the clearance rate of therapeutics from the blood circulation (this prolonged circulation helps to reduce the classic 'sawtooth pattern' of plasma levels of drugs requiring repeated dosing, hence maintaining therapeutic concentrations of the drug for longer periods, in turn leading to reduced dosage, frequency of administration and toxicity);
- prolongs pharmacological action (results with some proteins [61,62] suggest that the presence of PSA chains on a therapeutic polypeptide allows retention of much of its activity, while providing greatly enhanced residence time in the circulation);
- reduces immunogenicity (some studies have shown that the immunogenicity of peptides and proteins can be markedly decreased by polysialylation [61,62]);
- reduces antigenicity [61,62].

## 3.5 TYPES OF ACTIVE MOLECULES USED AS DRUG MODELS

### 3.5.1 Epirubicin

#### 3.5.1.1 General aspect

Epirubicin (4'-or epidoxorubicin) is an anthracycline antibiotic that has antineoplastic activity similar to its epimer. More importantly doxorubicin is now used alone and in combination with other cytotoxic agents in a variety of leukemias and solid tumors [63,64,65].

Anthracyclines are formed by a core planar anthraquinone (aglicole) that is linked to aminoglicosidic (daunosamine) (Fig. 3.11).

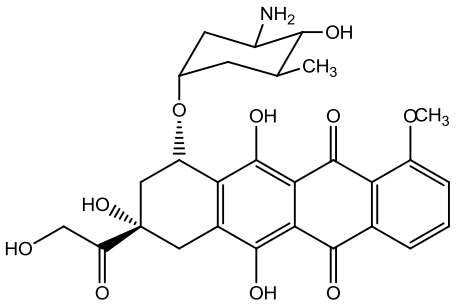


**Figure 3.11:** Structure of epirubicin

Epirubicin is closely related to doxorubicin with regard to its chemistry, which differs only by the spatial orientation of the 4'-hydroxyl group. In the epirubicin this is equatorial [66].

Epirubicin was marketed in 1984 and approved by the FDA in 1999. In clinics it is most commonly used in the form of hydrochloric acid, which is stable in both the solid state and in aqueous solution at a pH between 3 and 6.5. It decomposes at an increasing rate when the pH increases to a range of 6.5 to 12.

### 3.5.1.2 Mechanism of action

There are many biological actions of anthracycline antibiotics, all leading to a cytotoxic drug effect which is expressed predominantly at the level of tumor cells [63]. The mechanism of action of this drug is expressed at various levels:

- DNA intercalation with enzyme inhibition of DNA and RNA polymerases, topoisomerases, DNA helicases and DNA repair enzymes:
- intercalation in the cell and mitochondria membrane (vesicle formation, structural changes and interference with membrane activities);
- production of free radicals.

Intercalation between the two strands of DNA is possible due to the ability of the anthraquinon planar system to fit between the base pairs. When the drug intercalates, the

aromatic system planar inserts perpendicular to the axis of the double helix and establish interactions between the nucleotide bases and anthracycline rings B, C, D. The aminoglicosidic remains outside and adds stability to this complex by ionic interactions with the sugar and phosphate backbone of DNA. This binding induces stiffening, bending and elongation of the double helix, and forms the basis of the inhibition of nucleic acid synthesis in cancer cells, and induction of DNA fragmentation by inhibition of repair mechanisms.

The intercalation of the anthracycline antibiotics has been shown to interfere with the topoisomerase-DNA complex, with the formation of a ternary complex comprising of the drug leading to the inhibition of the topoisomerase catalytic activity. This is an intranuclear enzyme that transiently breaks one of the strands of DNA, rearrange and allowing relaxation of the double helix required for replication and transcription processes. The action of anthracyclines at this level stabilizes the cutting of DNA.

#### 3.5.1.3 Therapeutic uses

Epirubicin is usually administered by intravenous injection of various doses, either alone or in combination with other anticancer drugs. The epirubicin alone is now used for the treatment of breast cancer; administered in the usual doses ranging from 75 to 90 mg/m2 every three or four weeks. Doses over 180 mg/$m^2$ are also used. It is effective against many types of cancer including ovarian, stomach and lung cancer, non-Hodgkin's lymphoma and hepatocellular carcinoma.

#### 3.5.1.4 Toxicity

The epirubicin most important dose-limiting toxicity was myelosuppression, manifested primarily as leukopenia, which is related to dose and is reversible, and less commonly as thrombocytopenia and anemia [64,66]. Comparative studies *in vitro* using the same doses of doxorubicin and epirubicin has shown that epirubicin is less myelotoxic than doxorubicin. The lower hematologic toxicity of epirubicin allows for an intensified

therapeutic program, which is particularly important to define the dose-effect of anthracyclines.

The most important toxic chronic effect dose-limiting is cardiotoxicity, which manifests clinically as irreversible damage to the heart muscle, or as cardiomyopathy. Anthracycline cardiac damage can develop in several weeks after stopped of cancer therapy. The epirubicina has a lower cardiotoxic capacity when compared to doxorubicin, therefore its maximum recommended cumulative dose (1000 mg/m$^2$) is almost twice that dxorubicina (550 mg/m$^2$). This allows a greater number of cyclic treatments or an increased dose of the drug. The cardiac toxicity hypothesis could be explained by the transformation of anthracyclines in active radical species causing the formation of a superoxide which is highly toxic and harmful. It was observed that the presence of membrane P-450 reductase can promote this particular transformation in radical. Furthermore, the heart tissues lack the enzyme catalase, which converts hydrogen peroxide into water and oxygen; therefore there is no defense mechanism against the toxic metabolites of anthracyclines.

Other variable side effects that can occur following the administration of epirubicin include vomiting, nausea, alopecia, mucositis, stomatitis, diarrhoea, fever and hyperpigmentation.

### 3.5.2 Paclitaxel

#### 3.5.2.1 General aspect

Paclitaxel (PTX) has been proved to be a potent drug used to treat metastatic breast cancer, ovarian cancer, and other forms of cancer. PTX prevents division of cancer cells by stabilizing the mitotic spindle and inhibiting daughter cell separation, thereby causing toxicity and cell death [67,68]. However, several toxic side effects and clinical implications have been reported in PTX-treated patients [69,70]. In addition, because of the poor water-solubility of PTX, it is formulated in Cremophor EL which causes anaphylactic and hypersensitivity reactions [70]. Therefore, potential therapeutic strategies to improve the efficacy of PTX and reducing its side effects are needed.

The chemical name of paclitaxel is 5β, 20-epoxy-1,2α,4,7β,10β,13α-hexahydroxytax-11-en-9-one4, 10-diacetate 2-benzoate 13-ester with (2R,3S)-N-benzoyl-3-phenylisoserine (Fig. 3.12). The chemical formula of PTX is $C_{47}H_{51}O_{14}$, with a molecular weight of 853.9 Da. It is highly lipophilic and insoluble in water. The structure of paclitaxel is in the form of a complex ring system that is linked to a four-member oxetan ring at positions C4 and C5 and to an ester side chain at C13. Some studies suggested that this side chain is responsible for the unique effect of paclitaxel on microtubules. In contrast, other studies showed that the side chain is not an absolute requirement for the biologic activity of paclitaxel, but lack of this may confer a structure that is not as active as paclitaxel [71].

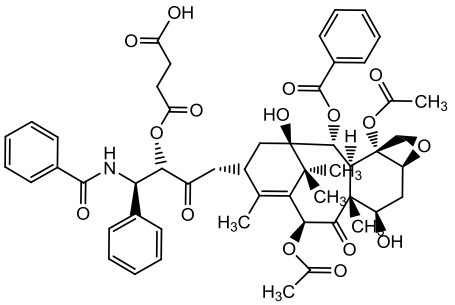

**Figure 3.11**: Structure of Paclitaxel

### 3.5.2.2 Mechanism of action

Microtubules play a key role in the initiation of DNA synthesis, mitosis, meiosis, motility, maintenance of cellular shape, and intracellular trafficking of macromolecules and organelles. Paclitaxel binds selectively and reversibly to the B subunit of tubulin, promoting tubulin polymerization and formation of stable microtubules even in the absence of the energy source, guanosine triphosphate. This effect leads to disruption of the equilibrium between the tubulin dimer-polymer in favor of polymer assembly. Paclitaxel induced microtubules have unusual stability and resist depolymerization by calcium, cold temperature, and dilution. Cells exposed to the drug exhibit an accumulation of arrays of disorganized microtubules which cause profound cell cycle arrest at the G2/M phase and eventually result in cell death through an apoptotic pathway. Paclitaxel induces two distinct microtubular structures, i.e., bundles and esters, which can be visualized by antitubulin antibody staining. Cells with esters produced by paclitaxel exposure are in mitosis and cells

with paclitaxel-induced bundles are in the G0/G1, S, and G2 phases. At high concentration, paclitaxel increases polymer mass and induces microtubule bundle formation, while at low concentration the principal effect is suppression of microtubule dynamics without altering the polymer mass. At a molecular level, paclitaxel-induced apoptosis and drug resistance is thought to be mediated through alteration in function of p53, p21, Bcl-2, and Bcl-xL. Specifically, apoptosis mediated by caspase 3 and caspase 8, hyperphosphorylation of Bcl-2, and increased expression of Bax have been shown to be partly responsible for paclitaxel-associated cytotoxicity [71].

#### 3.5.2.3 Toxicity

PTX is a potent anticancer drugs used for the treatment of several cancers, however it is associates with several toxic side effect as [71]:

- Hematologic

The major adverse effect of paclitaxel is myelosuppression, which mainly consists of neutropenia, whereas thrombocytopenia and anemia are uncommon. Neutropenia is more profound with higher doses, prolonged infusion, or if prior myelosuppressive therapy was used (e.g., paclitaxel given after cisplatin).

- Hypersensitivity reactions

The vast majority of these events are minor (dyspnea, bronchospasm, urticaria, hypotension, rash, and itching). They typically occur within the first 10 minutes after the first or second cycle, respond well to supportive measures, and do not require cessation of therapy. Major reactions on the other hand are generally severe, e.g., anaphylaxis, angioedema, or shock, and require cessation of therapy followed by emergent treatment.
Usually, minor reactions do not indicate development of a major event. The hypersensitivity reactions are most likely caused by the polyoxyethylated castor oil vehicle (Cremophor EL), but the taxane moiety may also be contributory.

- Neuromuscular

In contrast with myelosuppression, peripheral neuropathy is cumulative and progressive with increasing exposure to the drug, but usually disappears several weeks or

months after discontinuation of paclitaxel. Neuropathy due to paclitaxel presents as numbness and paresthesia in a gloveand-stocking distribution. It is usually symmetric, sensory as well as motor, and affects proprioception, vibration, temperature, and pinprick sensation.

The most commonly affected sites include the limbs, face, optic nerve, joints, and the autonomic nervous system. Risk factors include longer treatment, higher doses, alcohol, diabetes, and preexisting neuropathy. Transient muscle pains are common, unlike hematologic toxicity, neuropathy is observed more frequently with shorter infusion schedules (less than three hours).

- Cardiac

In the initial clinical trials of paclitaxel, routine cardiac monitoring was performed due to a high rate of hypersensitivity reactions. This led to the detection of a relatively high rate of cardiac rhythm disturbances, the relevance of which is doubtful because the vast majority of patients remained asymptomatic. Therefore, routine cardiac monitoring of patients receiving paclitaxel is no longer required. Nevertheless, the most common rhythm disturbance appears to be asymptomatic transient bradycardia.

There is no evidence that chronic paclitaxel use causes cardiac dysfunction. However, cardiac monitoring should be considered for patients with atrioventricular conduction disturbances or ventricular dysfunction. Doxorubicin used with paclitaxel increases cardiac toxicity more than what would be expected with the former alone.

- Gastrointestinal

Paclitaxel-induced gastrointestinal effects are generally uncommon and limited to mild nausea, mucositis, diarrhea, and elevated liver function tests, so routine use of antiemetics is not recommended.

- Dermatologic

Paclitaxel induces reversible alopecia of the scalp. Extravasations of large volumes can cause moderate soft tissue injury, and rare reports of nail disorders and recall reactions at previously irradiated sites have also been noted, although mostly with weekly schedules only.

## 3.6 ALENDRONATE FOR BONE TARGETING

Adult bone tissue is distinguished from the other tissues by the presence of calcium/phosphate-based mineral. The mineral is mainly hydroxyapatite, $Ca_{10}(PO_4)_6(OH)_2$ which incorporates other ions and salts in its structure. The mineral component is the main constituent of bone (per mass basis) and is the essential element responsible for the mechanical support function. In this type of tissue, the availability of molecules potentially exploitable as a target for drug delivery systems is very poor. The most logical solution to this problem is the synthesis of systems capable of binding to bone hydroxyapatite (HA).

The aminobisphosphonate, alendronate (ALN) has emerged in recent years as a highly effective therapeutic option for the prevention of skeletal complications caused by bone metastases. Like all bisphosphonates (BPs), it exhibits an exceptionally high affinity to the bone-mineral hydroxyapatite (HA) [72-74]. ALN is approved by the FDA for the treatment of bone related diseases and cancer associated hypercalcemia [75]. Because of the high bone affinity of BPs, much effort has been made to conjugate them with non-specific bone therapeutic agents in order to obtain osteotropicity [74,76,77]. Recently, ALN was successfully conjugated with polymer-drug delivery systems [76, 78,79].

In recent years, it has become evident that both ALN and PTX at low doses can selectively inhibit endothelial functions relevant to angiogenesis [80-82]. Angiogenesis, new capillary blood vessel growth from pre-existing vasculature, is now recognized as important control point in tumor progression and metastasis formation [83-88].

### 3.6.1 BPs chemical structure as basis for clinical activity

Structurally, bisphosphonates are chemically stable derivatives of inorganic pyrophosphate (PPi), a naturally occurring compound in which 2 phosphate groups are linked by esterification (Fig. 3.12 A) [89].

Pioneering studies from the 1960s demonstrated that PPi was capable of inhibiting calcification by binding to hydroxyapatite crystals, leading to the hypothesis that regulation of PPi levels could be the mechanism by which bone mineralization is regulated [90].

Like their natural analogue PPi, bisphosphonates have a very high affinity for bone mineral because they bind to hydroxyapatite crystals. Accordingly, bisphosphonate skeletal retention depends on availability of hydroxyapatite binding sites. Bisphosphonates are preferentially incorporated into sites of active bone remodeling, as commonly occurs in conditions characterized by accelerated skeletal turnover. Bisphosphonate not retained in the skeleton is rapidly cleared from the circulation by renal excretion. In addition to their ability to inhibit calcification, bisphosphonates inhibit hydroxyapatite breakdown, thereby effectively suppressing bone resorption [91]. This fundamental property of bisphosphonates has led to their utility as clinical agents.

Modification of the chemical structure of bisphosphonates has widened the differences between the effective bisphosphonate concentrations needed for antiresorptive activity relative to those that inhibit bone matrix mineralization, making the circulating concentrations of all bisphosphonates currently used in clinical practice active essentially only for the inhibition of skeletal resorption [92]. As shown in figure 3.12 A, the core structure of bisphosphonates differs only slightly from PPi in that bisphosphonates contain a central non-hydrolysable carbon; the phosphate groups flanking this central carbon are maintained. As detailed in figure 3.12 B, and distinct from PPi, nearly all bisphosphonates in current clinical use also have a hydroxyl group attached to the central carbon (termed the R1 position). The flanking phosphate groups provide bisphosphonates with a strong affinity for hydroxyapatite crystals in bone (and are also seen in PPi), whereas the hydroxyl motif further increases a bisphosphonate's ability to bind calcium. Collectively, the phosphate and hydroxyl groups create a tertiary rather than a binary interaction between the bisphosphonate and the bone matrix, giving bisphosphonates their remarkable specificity for bone [92]. Although the phosphate and hydroxyl groups are essential for bisphosphonate affinity for bone matrix, the final structural moiety (in the R2 position) bound to the central carbon is the primary determinant of a bisphosphonate's potency for inhibition of bone resorption. The presence of a nitrogen or amino group, such as in alendronate (Fig. 3.12 C) increases the bisphosphonate's antiresorptive potency by 10 to 10,000 relative to early non–nitrogen-containing bisphosphonates, such as etidronate (Fig. 3.12 B) [92,93]

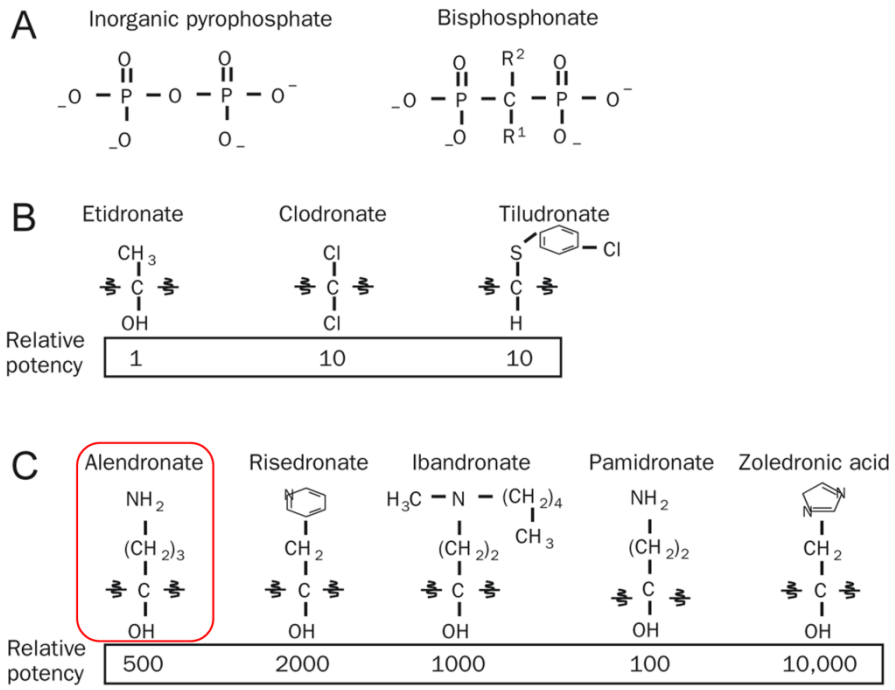


**Figure 3.12**: Bisphosphonate structures and approximate relative potencies for osteoclast inhibition.

This high affinity for bone mineral allows bisphosphonates to achieve a high local concentration throughout the entire skeleton. Accordingly, bisphosphonates have become the primary therapy for skeletal disorders characterized by excessive or imbalanced skeletal remodeling, in which osteoclast and osteoblast activities are not tightly coupled, leading to excessive osteoclast-mediated bone resorption.

# MATERIAL & METHODS

*Studies on polymer conjugation as versatile tool for drug delivery*

## 4.1 MATERIALS

Paclitaxel was from Indena (Milan, IT) and Epirubicin was from 21CEC PX Pharm Ltd (East Sussex, UK). The poly(ethylene glycol) Boc-NH-PEG-NHS and mPEG-CO-OSu were from Iris Biotech GmbH (Marktredwitz, Germany). HPMA was from Polymers Laboratories (UK), PGA was from Alamanda Polymers, Inc. (Huntsville, AL, USA). PSA, 1-Hydroxybenzotriazole (HOBt), N-(3-Dimethylaminopropyl)-3 N'-ethylcarbodiimide hydrochloride (EDC), Methanesulfonic acid ($CH_3SO_3H$), 1,1'-Carbonyldiimidazole (CDI), N-Hydroxysuccinimide (NHS), *N*,*N*-Dicyclohexylcarbodiimmide (DCC), succinic anhydride, β-glutamic acid (β-Glu), silica gel ($SiO_2$), sodium sulfate anhydrous ($Na_2SO_4$), triethylamine ($ET_3N$), trifluoroacetic acid (TFA), 2,4,6-trinitrobenzenesulfonic acid (TNBS), dimethylsulfoxide-d6, $CDCl_3$ and $D_2O$, 3-(4,5-Dimethyl-2-thiazolyl)-2,5-diphenyl- 2H-tetrazolium bromide (MTT), Cytochalasin B, Chlorpromazine hydrochloride, lovastatin and methyl-β-cyclodextrin, dichloromethane ($CH_2Cl_2$), chloroform ($CHCl_3$), N,N-dimethylformamide (DMF), acetonitrile, dimethylsulfoxide (DMSO), diethyl ether and salts of analytical grade were from Sigma-Aldrich Co (St Louis, MO, USA). Alendronate was purchased from Alcon Biosciences Ltd. (Mumbai, India; Petrus Chemicals, Israel). Glycil-glycine (Gly-Gly) was obtained from Merck (Darmstadt, Germany). Dulbecco's modified Eagle's medium (DMEM), RPMI 1640, Fetal bovine serum (FBS), Penicillin and Streptomicin were from Biological Industries Ltd. (Kibbutz Beit Haemek, Israel). Dextran (MW 70,000 Da) and all other chemical reagents, including salts and solvents were purchased from Sigma-Aldrich.

## 4.2 ANALYTICAL METHODS

Spectrophotometer analysis was performed with Perkin-Elmer (Northwolk, CT, USA). $^1$H-NMR spectroscopy was performed with Bruker 300MHz spectrometer and NMR data were processed using the program Topspin (Bruker GmbH, Karlsruhe, Germany). Reverse phase chromatography was performed with a Shimadzu analytical HPLC system using an Agilent 300-Extend $C_{18}$ (4.6 × 250 mm; 5 μm) column. Centrifugation was performed with Hettich Zentrifugen mod. MIKRO 200 for small volume and Centrikon T-42K, Kontron Company, for large volume solution. The freeze-drying was performed with freeze-Hetossic

Heto Lab Equipment. The dialysis membranes have been provided by Delchimica Scentific Glassware (Milan). Aqueous and organic solutions were evaporated with Rotavapor mod. R II BÜCHI (Switzerland).

## 4.3 SYNTHESIS AND CHARACTERIZATION OF EPIRUBICIN CONJUGATES

### 4.3.1 Synthesis of mPEG-EPI

mPEG-EPI was obtained coupling activated carboxylic groups of mPEG with the amino groups of Epirubicin, yielding an amide bond (reaction scheme 4.1).

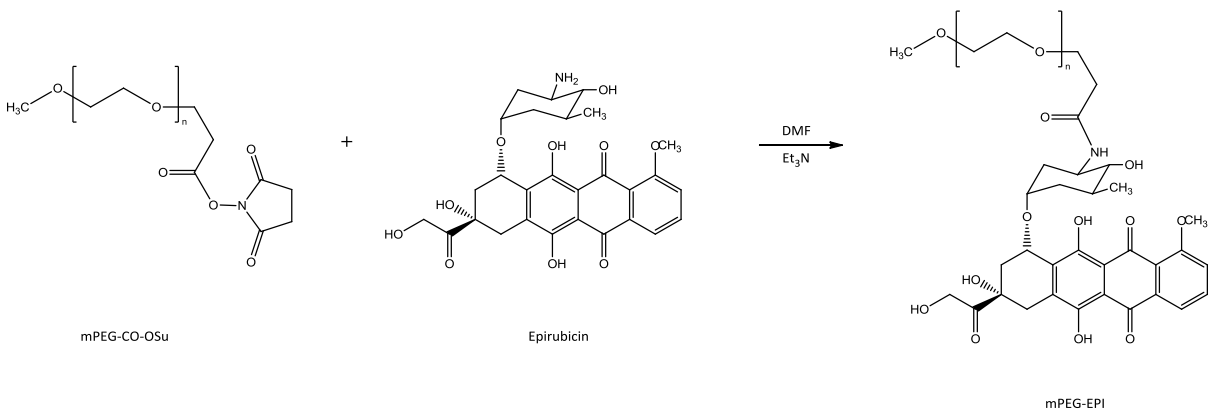


**Scheme 4.1**: Synthesis of mPEG-EPI

To 12 mg (0.02 mmol) of Epi·HCl (MW 580 Da; 1.2 equivalent excess for each activated carboxyl groups of PEG), dissolved in 5 ml of anhydrous DMF, 5 µl (0.035 mmol) of $Et_3N$ and 200 mg (0.018 mmol) of mPEG-COOSu (MW 11,193 Da; 74% of activated carboxylic groups) were added. The reaction was stirred at room temperature in the dark for 48 h. To the mixture 10 ml of $CH_2Cl_2$ was added and the excess of Epi was extracted with HCl 0.1 N (3 × 40 ml). The organic phase, dried over $Na_2SO_4$, was concentrated under vacuum and dropped into 150 ml of cold diethyl ether under stirring. The product was recovered by filtration and dried under vacuum (yield: 147 mg; 70%).

The purity of mPEG-EPI was evaluated by RP-HPLC using method reported in section 4.4. The amounts of free and total contents of EPI in the conjugate were evaluated as reported in the section 4.4.

## 4.3.2 Synthesis of HPMA-Gly-Gly-EPI

HPMA-GG-EPI was obtained, as for mPEG-EPI, by forming an amide bond between carboxylic groups of HPMA-Gly-Gly-OH and the amino groups of Epirubicin via EDC/HOBT (reaction scheme 4.2).

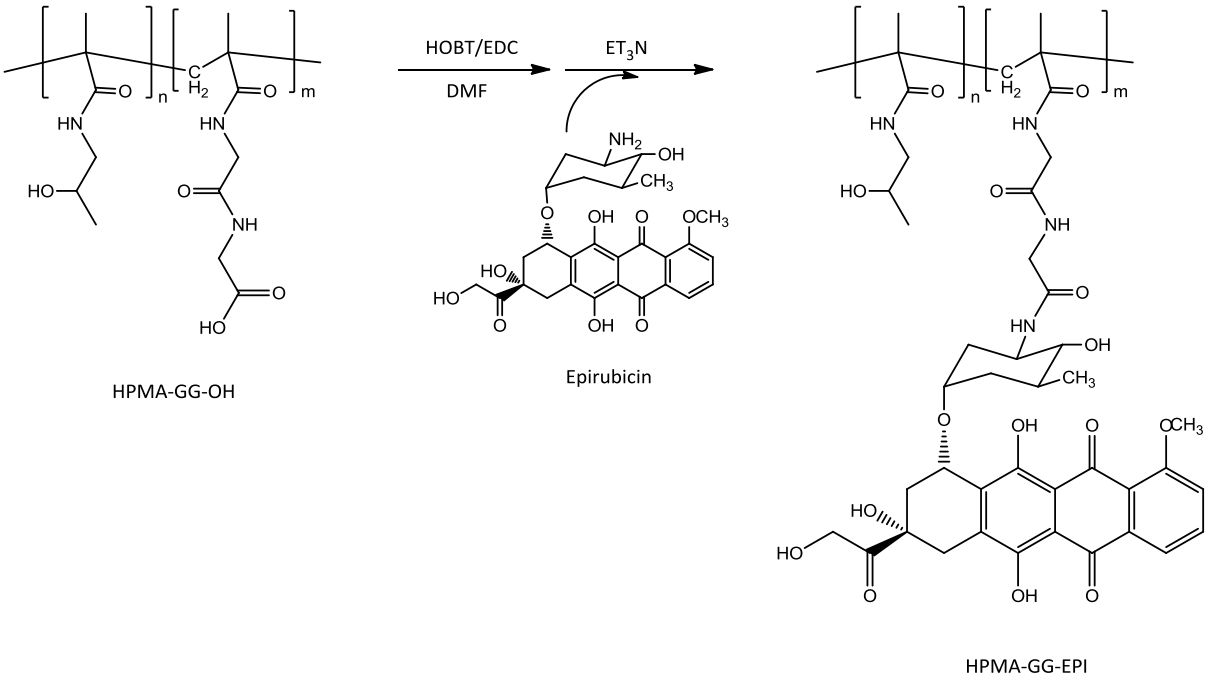


**Scheme 4.2**: Synthesis of HPMA-GG-EPI

To 6.5 mg (0.01125 mmol) of Epi·HCl (MW 580 Da) dissolved in 3 ml of anhydrous DMF, 2 µl (0.012 mmol) of $Et_3N$ were added. Separately, to 45 mg (0.15 mmol) HPMA-GG-COOH (MW of the monomer 300 Da, 5% of Gly-Gly content), dissolved in DMF, 1.52 mg (0.01125 mmol) of HOBT (MW 135.12 Da) and 2.15 mg (0.01125 mmol) of EDC (MW 191.7 Da) were added. After three hours the solutions were mixed and left to react under stirring at room temperature in the dark for 48 h. The reaction mixture was purified by precipitation into 50 ml of a cold mixture of acetone:diethyl ether (3:1). The product was recovered by centrifugation at 10,000 × g and dried under vacuum. The product was also purified from the excess of EPI by gel-filtration chromatography using Sephadex LH-20 resin (100 × 2.5 cm) eluted with DMF (flow rate of 0.5 ml/min). The fractions containing HPMA-GG-EPI were collected in a round bottom flask and DMF was evaporated under vacuum. The product was dissolved in $H_2O$ and lyophilized (yield: 62%).

The purity of HPMA-GG-EPI was evaluated by RP-HPLC using method reported in section 4.4. The amounts of free and total contents of EPI in the conjugate were evaluated as reported in the section 4.4.

### 4.3.3 Synthesis of HPMA-Gly-Phe-Leu-Gly-EPI

HPMA-GPLG-EPI was obtained with the same method used for the synthesis of HPMA-GG-EPI. The carboxylic groups of polymer were, first, activated via EDC/HOBT and then coupled with amine groups of epirubicin (reaction scheme 4.3).

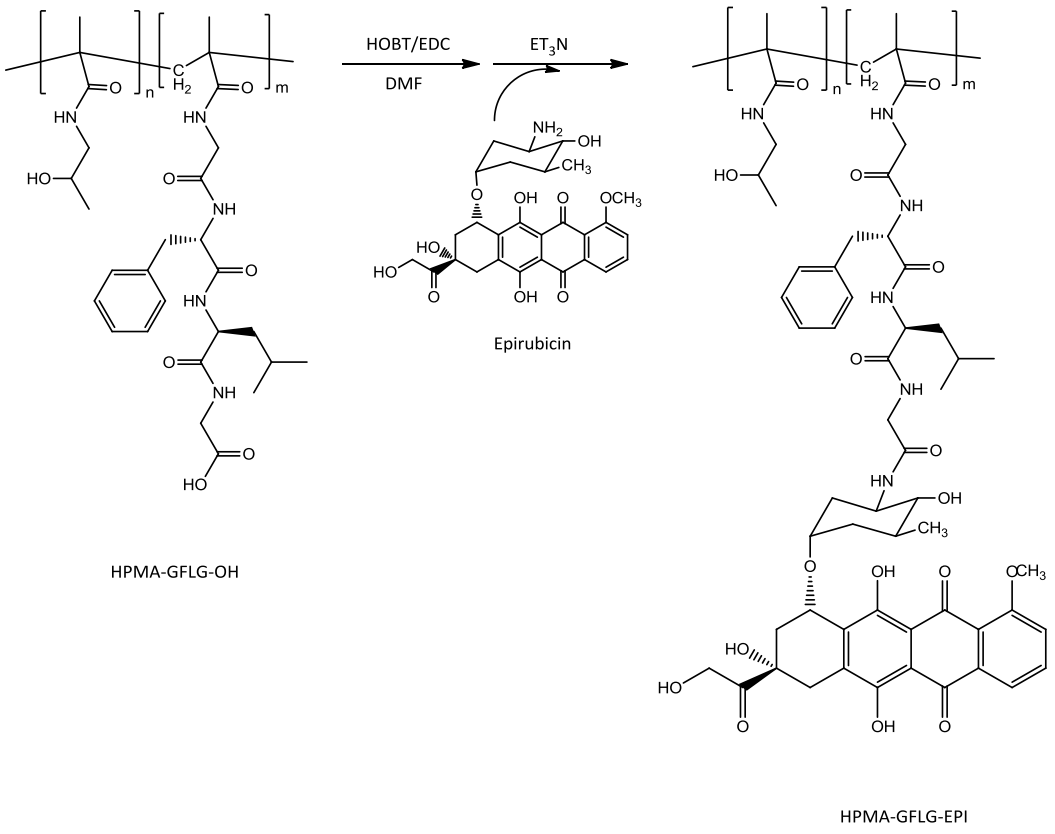


**Scheme 4.3**: Synthesis of HPMA-GPLG-EPI

To 6.5 mg (0.01125 mmol) of Epi·HCl (MW 580 Da) dissolved in 3 ml of anhydrous DMF, 2 µl (0.012 mmol) of $Et_3N$ were added. Separately, to 45 mg (0.15 mmol) HPMA-GG-COOH (MW of the monomer 300 Da, 5% of Gly-Phe-Leu-Gly content), dissolved in DMF, 1.52 mg (0.01125 mmol) of HOBT (MW 135.12 Da) and 2.15 mg (0.01125 mmol) of EDC (MW 191.7 Da) were added. After three hours the solutions were mixed and left to react under

stirring at room temperature in the dark for 48 h. The product was purified as reported in section 4.3.2.

The purity of HPMA-GPLG-EPI was evaluated by RP-HPLC using method reported in section 4.4. The amounts of free and total contents of EPI in the conjugate were evaluated as reported in the section 4.4.

### 4.3.4 Synthesis of PGA-EPI

#### 4.3.4.1 Sodium-tetrabutylamonium salts exchange from PGA

Before PGA-EPI synthesis, the polymer must be soluble in organic solvent. For this reasons, the sodium salts of PGA was exchanged with tetrabutylamonium salts (scheme 4.4) [94].

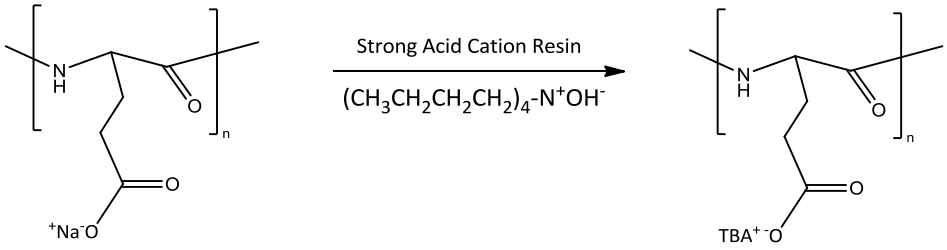


**Scheme 4.4**: Sodium-tetrabutylamonium salts exchange

Ion exchange resin (5 g of Dowex M-15) was washed with 500 ml of water and filtered to remove the supernatant three times. Then, 20 ml of $TBA^+OH^-$ solution (1M) were added to the resin and mixed for 30 min. TBA-resin was washed with 500 ml of water and filtered for three times before to fill a column. 100 mg (0.66 mmol) of PGA sodium salt (MW of the monomer 151 Da) were dissolved in 2 ml of water and loaded into the TBA-resin column. The polymer was left for 3 hours into the column and then the $PGA^-$ $TBA^+$ was collected, dialyzed against water, using a membrane with a cut-off of 3500 Da, and lyophilised.

### 4.3.4.2 EPI conjugation to $PGA^{-}TBA^{+}$

PGA-EPI was obtained, as for mPEG-EPI and HPMA-EPI, by forming an amide bond between carboxylic groups of $PGA^{-}TBA^{+}$ and the amino groups of Epirubicin via $CDI/CH_3SO_3H$ (reaction scheme 4.5).

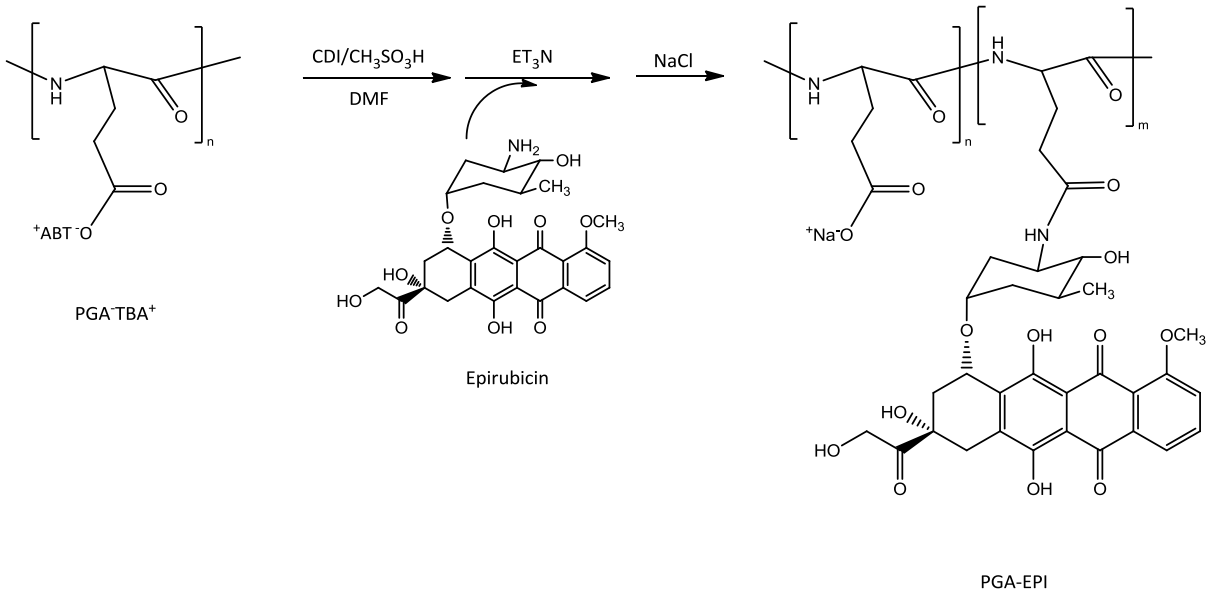


**Scheme 4.5**: Synthesis of PGA-EPI

To 50 mg (0.14 mmol) of $PGA^{-}TBA^{+}$ (MW of the monomer 370.47 Da), dissolved in 3 ml of anhydrous DMF, 9.52 µl (0.14 mmol) of $CH_3SO_3H$ (Mw 96.1 Da; d= 1,481 g/mL at 25°C; 1 eq. respect of PGA) 3.4 mg (0.021 mmol) of CDI (MW 162.15 Da; 0.15 eq. respect PGA) were added in order to activate 15% of carboxylic groups. After 1h, 4.4 µl (0.031 mmol) of $Et_3N$ and 18.3 mg (0.031 mmol) of EPI·HCl (MW 580 Da; 0.2 eq. respect PGA) were added. The reaction was stirred at room temperature in the dark for 48 h. To the mixture 300 µl of brine were added and the solution was stirred for 15 min, to exchange $TBA^{+}$ with $Na^{+}$. The conjugate was purified by precipitation into 20 ml of cold acetone, recovered by centrifugation at 10,000×g and dried under vacuum. The collected conjugate was dissolved in water and dialyzed against water using a membrane with a cut-off of 3,500 Da and then lyophilised. The product was eventually further purified by GPC using LH-20 resin (100 × 2.5 cm). The elution was performed with DMF at flow rate of 0.5 ml/min as already reported in section 4.2.2 (yield: 55%).

The purity of PGA-EPI was evaluated by RP-HPLC using method reported in section 4.4.The amounts of free and total contents of EPI in the conjugate were evaluated as reported in the section 4.4.

### 4.3.5 Synthesis of PSA-EPI

PSA-EPI was obtained, as for other EPI conjugates, by forming an amide bond between carboxylic groups of $PSA^- TBA^+$ and the amino groups of Epirubicin via $CDI/CH_3SO_3H$ (reaction scheme 4.6). The sodium salts of PSA was, first, exchanged with tetrabutylamonium salts as reported for PGA in section 4.3.4.1.

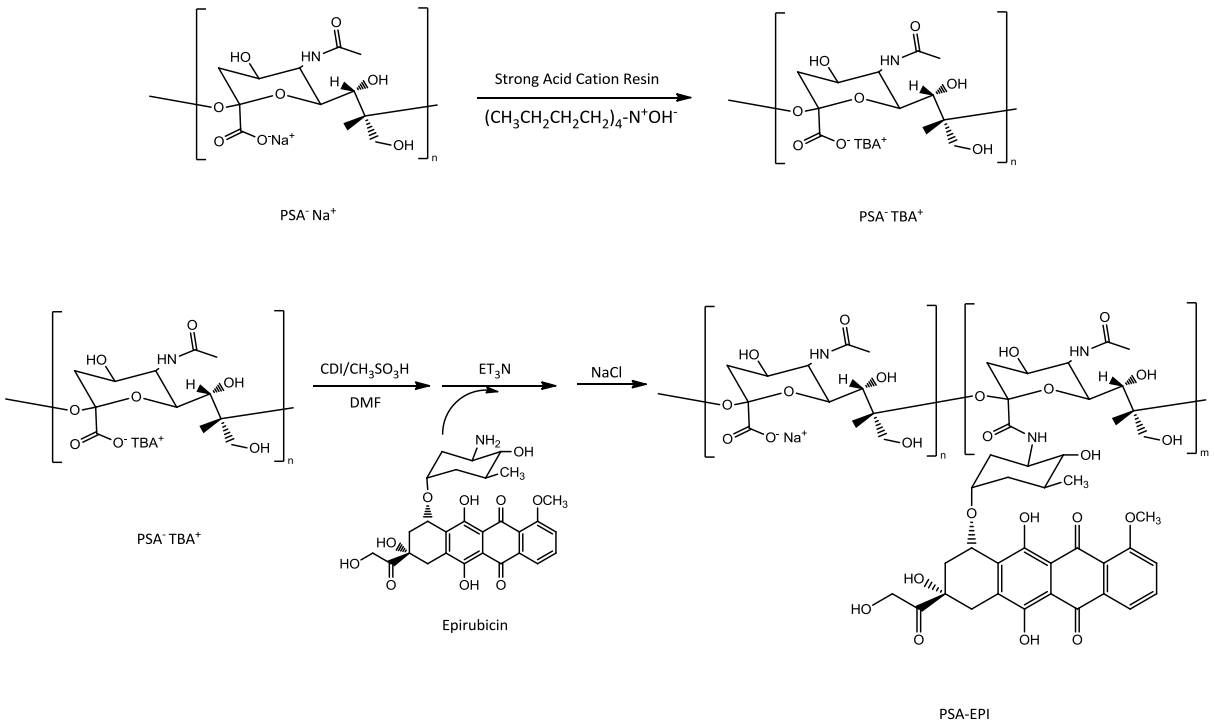


**Scheme 4.6**: Sodium-tetrabutylamonium salts exchange and synthesis of PSA-EPI

To 50 mg (0.096 mmol) of $PSA^- TBA^+$ (MW of the monomer 521.47 Da), dissolved in 3 ml of anhydrous DMF, 6.52 µl (0.096 mmol) of $CH_3SO_3H$ (Mw 96.1 Da; d= 1,481 g/mL at 25°C; 1 eq. respect of PSA) and 3 mg (0.019 mmol) of CDI (MW 162.15 Da; 0.2 eq. respect PSA) were added. After 1h, 4 µl (0.028 mmol) of $Et_3N$ and 16.24 mg (0.028 mmol) of EPI·HCl (MW 580 Da; 0.3 eq. respect PGA) were added. The reaction was conducted as for PGA-Epi and the product was purified by the same method (yield: 54%).

The amounts of free and total contents of EPI in the conjugate were evaluated as reported in the section 4.4. The purity of PSA-EPI conjugate was evaluated by GPC using an Agilent Zorbax GF-250 (4.6 x 250 mm; 5 µm) column, $NaH_2PO_4$ buffer 20mM + NaCl 130 mM + 20% $CH_3CN$ as buffer running and the UV settled at 480 nm.

## 4.4 DETERMINATION OF FREE AND TOTAL EPI CONTENTS IN THE CONJUGATES

The amount of free Epi in the conjugate was evaluated by reverse phase HPLC, using an Agilent 300-Extend C18 (4.6 x 250 mm; 5 µm) column, with the UV detector settled at 480 nm. The eluent A and B were $H_2O$ and $CH_3CN$, respectively, both of them with 0.05% TFA. The elution was performed by the following gradient: from 25%B to 30%B in 10 min., from 30%B to 80%B in 5 min., and from 80%B to 25%B in 5 min., at flow rate of 1 ml/min.
The total drug content was evaluated by RP-HPLC after incubation of the conjugate in HCL 2N at 50°C for 2h, freeing the aglycone moiety. The elution was performed as above reported.

## 4.5 CONJUGATES STUDIES

### 4.5.1 Conjugates stability in buffer solution at different pH value

Conjugates (1.5 x $10^{-4}$ mmol Epi/ml) were incubated at 37°C for 48h in PBS 0.1M at pH 5 and 7.4 to evaluate the drug release. Samples of 50 µl were withdrawn at predetermined times and analysed by RP-HPLC using the same condition reported at section

### 4.5.2 Conjugates stability in plasma

Conjugates (1.5 x $10^{-4}$ mmol Epi/ml) were incubated for 48h at 37°C in mouse plasma, obtained after centrifugation of blood at 2000 x g for 10 min. Samples of 60 µl were withdrawn at predetermined times and 60 µl of $CH_3CN$ were added to achieve plasma protein precipitation. Samples were centrifuged at 15,000 x g and the supernatant was withdrawn and analysed by RP-HPLC using the same condition reported at section 4.4.

### 4.5.3 Degradation in presence of Tritosomes

The biodegradation of conjugates was investigated using tritosomes. conjugates (3.8 × 10-2 mM Epi equiv.) were incubated for 72 h at 37°C in 100 mM sodium acetate buffer (pH 5) containing 10 mM cysteine, 2 mM EDTA and 0.45 mg protein/ml of rat liver lysosomes. Lysosomes were isolated from an adult Wistar rat liver homogenate by differential centrifugation as described elsewhere [95]. Lysosomal proteins content was estimated by the bicinchoninic acid procedure using bovine serum albumin as standard protein. In control experiments, conjugates were incubated under the same conditions in the absence of lysosomal proteins. Samples of 60 µl were withdrawn at predetermined times, added with 60 µl of $CH_3CN$ and centrifuged at 15,000 × g for 3 min. Epi was quantified in the supernatant by RP-HPLC using the same method above reported. Detection was performed by a spectrofluorometric detector: exc. 488 nm and em. 555 nm.

## 4.6 CELLS STUDIES

### 4.6.1 General cell line maintenance

MCF-7 and MCF-7/DX were cultured in RPMI 1640 medium supplemented with 5% FBS and kept in standard tissue culture conditions (37°C, in humidified atmosphere with 5% $CO_2$). To maintain the resistance to anthracyclins, MCF-7/DX were cultured in Dox supplemented medium (1 µM) once every two passages.

### 4.6.2 Cell viability assay

Conjugates cytotoxicity was evaluated using the MTT cell viability assay (72 h cell exposure time). MCF-7 and MCF-7/DX cell, suspended in WRPMI + 5% FBS ($2 \times 10^4$ cells/mL), were seeded into sterile 96-well plates (100 µL) and incubated overnight. Solutions of the conjugates in medium (100 µL) were then added to obtain final concentrations in the range 1-1000 nM (Epi-equiv.). After a 67 h incubation, MTT (20 µL of a 5 mg/mL solution in PBS) was added to each well, and the cells were incubated for 5 h. The medium was then removed and replaced with DMSO. After a 30 min incubation at 37°C, the plates were read spectrophotometrically at 540 nm. Cell viability was expressed as a percentage viability of untreated control cells.

### 4.6.3 Uptake studies

Uptake studies were conducted for all the polymer-Epi conjugates in presence and absence of endocytosis inhibitors, namely (a) Cytochalasin B (25 µM), (b) methyl-β-cyclodextrin (10 mM) + Lovastatin (1 µM) and (c) Chlorpromazine (15 µM). RPMI 1640 medium supplemented with 5% FBS and with each inhibitor was prepared from stock solutions of the inhibitors (2.4 mg/mL in DMSO, 100 mg/mL in water + 5 mg/mL in ethanol, 10 mg/mL in water respectively). MCF-7 and MCF-7/DX cells were seeded in 6-well plates at a density of $5 \times 10^5$ cells/mL in WRPMI and allowed to adhere for 24 h. At time zero, the medium was removed from the plates and all wells were washed with PBS. 900 µL of complete medium (containing the appropriate inhibitor where necessary) were then added and the cells were incubated for 1 hour either at 37°C. 100 µL of polymer-Epi solution (50 µM Epi equiv.) were added and the plates were incubated for a further hour. All the plates were placed on ice, the medium was removed and each well was washed with ice chilled PBS (3 × 1 mL). Cells were then harvested and the suspension centrifuged (1400 rpm for 5 min). The supernatant was removed, the pellet re-suspended in ice cold PBS (200 µL) and immediately analysed by FACS (20,000 events counted for each sample). The experiment was performed in triplicate.

## 4.7 *IN VIVO* STUDIES

### 4.7.1 Pharmacokinetic in mice

Pharmacokinetics of Epi, mPEG-Epi, HPMA-GG-Epi, PGAEpi and PSA-Epi were determined in adult female Balb/C mice (23–25 g). 40 mice were randomly divided in five groups of 8 animals. 150 µL of Epi or one of the Epi conjugates, in PBS pH 7.4 (dose: 10 mg/Kg Epi equiv.), were administered *via* tail vein to mice anaesthetized with 5% isoflurane gas (mixed with O2 in enclosed cages). At predetermined times, blood samples (150 µL) were withdrawn from the retro-orbital plexus/sinus of animals, with a heparinized capillary. The samples were centrifuged at 1,500 × *g* for 15 min. In the case of Epi, PEG-Epi and HPMA-GG-Epi, 50 µL of the plasma were mixed with 350 µL of $CH_3CN$, the mixture was centrifuged at 20,000 × *g* for 5 min. 300 µL of the supernatant was collected and freeze-dried. The residue was dissolved in 50 µL of water and analyzed by RP-HPLC using the method above reported. In the case of PGA-Epi and PSA-Epi, 50 µl of the plasma were diluted with 450 µl of PBS and directly detected by spectrofluorometer settled with exc. at 488 nm and em. at 555 nm.

## 4.8 SYNTHESIS AND CHARACTERIZATION OF PTX-PEG, PEG-ALN AND PTX-PEG-ALN CONJUGATES

### 4.8.1 Synthesis of 2'-succinyl-paclitaxel

Paclitaxel was derivatized by succinic anhydride, in pyridine, to 2'-succinyl-paclitaxel, as reported in reaction scheme 4.7.

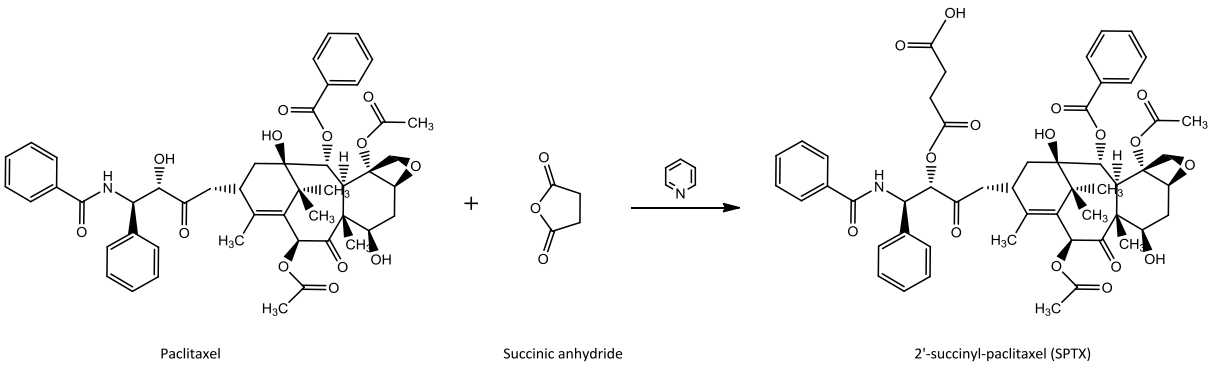


**Scheme 4.7:** Synthesis of 2'-succinyl-paclitaxel.

To 1 g (1.17 mmol) of paclitaxel (MW 853.9 Da) , dissolved in 30 ml of an anhydrous pyridine, 585 mg (5.85 mmol) of succinic anhydride (MW 100.08 Da; 5 equivalent in excess respect to hydroxyl groups of PTX) were added. The reaction was stirred at room temperature for 48 h. The SPTX was purified by chromatography on a $SiO_2$ column (30 x 2.5 cm) eluted with a chloroform-methanol mixture (97:3 to 90:10) and determined by TLC (Rf 0.5 in chloroform-methanol 90:10). The fractions containing SPTX were combined ad dried under vacuum. The purified product was characterized via UV-VIS spectroscopy, RP-HPLC and $^{1}$H-NMR.

## 4.8.2 Synthesis of PEG-dendrimer

### 4.8.2.1 Synthesis of Boc-NH-PEG-β-Glu-$(COOH)_2$ (**1**)

Boc-NH-PEG-β-Glu-$(COOH)_2$ (**1**) was obtained by forming an amide bond between the activated carboxyl group of PEG and the amino group of β-glutamic acid as reported in the reaction scheme 4.8.

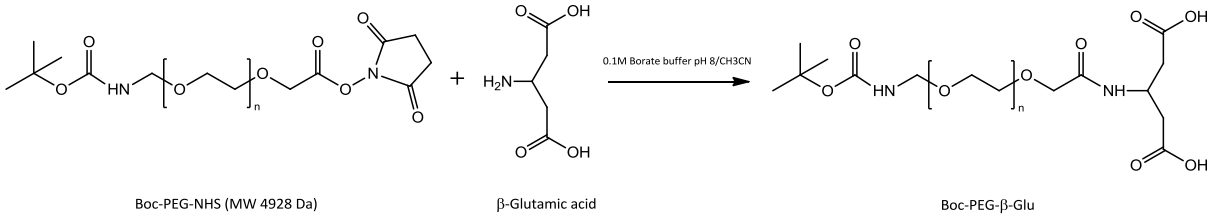


**Scheme 4.8**: Synthesis of Boc-NH-PEG-β-Glu-$(COOH)_2$

3.5 g (0.71 mmol) of Boc-NH-PEG-NHS (MW 4928 Da; 87% of activated carboxylic groups) was added to 313 mg (2.13 mmol) of β-glutamic acid (βGlu) (MW 147.1 Da; 3 equivalent in excess to activated -COOH groups of PEG), dissolved in 150 mL of 0.1 M borate buffer/$CH_3CN$ (3:2) mixture pH 8.0. The reaction was let to proceed for 5 h under stirring. Then, the pH was adjusted to about 4.5 with HCl 0.2 N and product **1** was purified from the excess of βGlu by extractions with $CHCl_3$ (6 × 300 mL). The organic phase, dried over anhydrous $Na_2SO_4$, was concentrated under vacuum and dropped into 1 L of cold diethyl ether under stirring. After 1 h at -20°C, the precipitate of **1** was filtered and dried under vacuum (yield: 3.345 g, 95 %). The absence of free βGlu in the conjugate was verified by TNBS test (see table 4.1 section 4.8.2.2) according to Snyder and Sabocinsky assay [96].

### 4.8.2.2 Activation of carboxylic groups of Boc-NH-PEG-β-Glu-$(COOH)_2$ via NHS/DCC (**2**)

The carboxylic groups of product **1** were activated to succinimide ester with NHS/DCC as reported in reaction scheme 4.9:

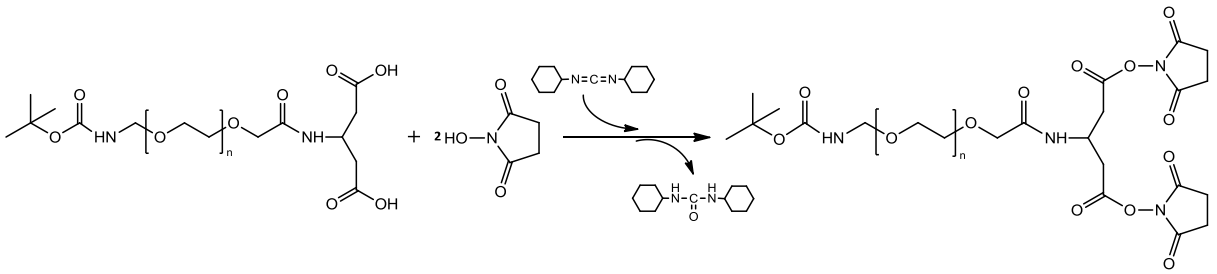


**Scheme 4.9**: Activation of carboxyl groups of Boc-NH-PEG-β-Glu-$(COOH)_2$

To 3.33 g (0.67 mmol) of **1** (MW 4942 Da), dissolved in 100 mL of anhydrous $CH_2Cl_2$, 469 mg (4.07 mmol) of NHS (MW 115.09 Da; 3 equivalent in excess for each carboxyl groups of **1**) and 1.114 g (5.4 mmol) of DCC (MW 206.33 Da; 4 equivalent in excess for each carboxyl groups of **1**) were added. The reaction was stirred at room temperature overnight. Then the mixture was filtered and dropped into 1 L of cold diethyl ether. After 1 h at -20°C, the precipitate of Boc-NH-PEG-(β-Glu)-$(NHS)_2$ (**2**) was recovered by filtration and dried under vacuum (yield: 3.1 mg, 89.5%). The degree of activation was 91%, determined on the basis of the amino group modification of an equimolar solution of Gly-Gly as follows reported.

*Snyder-Sobocinski Assay*

The degree of activation of the product **2** is determined by a colorimetric assay with 2,4,6-Trinitrobenzenesulfonic acid (TNBS) [97] which reacts stoichiometrically with primary amino group in alkaline medium to give a trinitrophenyl derivative absorbing at 420 nm (see reaction scheme 4.10).

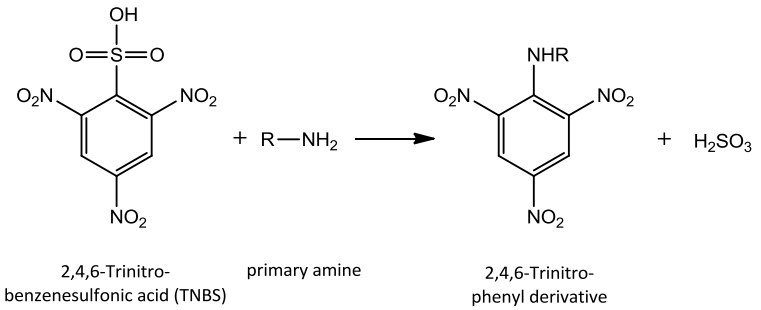


**Scheme 4.10**: Reaction between 2,4,6-Trinitrobenzenesulfonic acid and primary amine

To 1 ml of Gly-Gly solution (0.00216 mmol/mL; MW 132.12 Da) in 0.1 M borate buffer pH 8, 5.5 mg (0.0011 mmol; MW 5132 Da) of **2** were added, and the reaction was let to proceed for 30 minutes under stirring. TNBS assay was performed in duplicate at room temperature as reported in table 4.1.

| ***Blank*** | ***PEG reaction mixture*** | ***Gly-Gly standard solution*** |
|---|---|---|
| 20 µL of TNBS | 20 µL of TNBS | 20 µL of TNBS |
| 980 µL of 0.1 M borate | 955 µL of 0.1 M borate | 955 µL of 0.1 M borate |
| buffer pH 9.3 | buffer pH 9.3 | buffer pH 9.3 |
| | 25 µL of sample reaction | 25 µL of Gly-Gly solution |
| | mixture (polymer + Gly-Gly) | (0.285 mg/ml) |

**Table 4.1**: Preparation of test solution for the TNBS assay

The reactions were incubated for 30 minutes and then the absorbance at 420 nm were read by UV-VIS spectrophotometer.

### 4.8.2.3 Synthesis of Boc-NH-PEG-β-Glu-(β-Glu)$_2$-(COOH)$_4$ (**3**)

Boc-NH-PEG-β-Glu-(β-Glu)$_2$-(COOH)$_4$ (reaction scheme 4.11) was obtained in the same manner of Boc-NH-PEG-β-Glu-(COOH)$_2$ (see section 4.8.2.1).

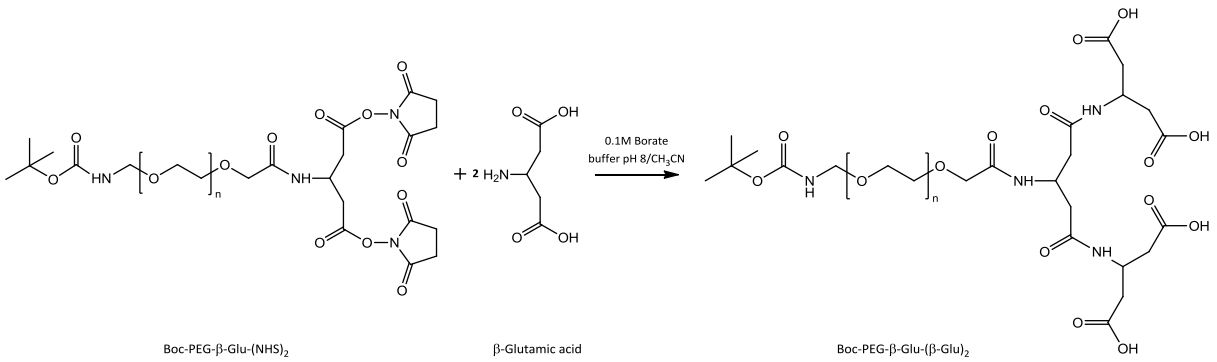


**Scheme 4.11**: Synthesis of Boc-NH-PEG-β-Glu-$(β\text{-Glu})_2$-$(COOH)_4$

To 532 mg (3.6 mmol) of βGlu (MW 147.1; 3 equivalent in excess for each activated carboxyl groups of **2**), previously dissolved into 200 mL of 0.1 M borate buffer/$CH_3CN$ (3:2) mixture at pH 8.0, 3.09 g (0.6 mmol) of **2** (MW 5132 Da) were added. The reaction was conducted as for **1** and the product was purified by the same method (yield: 2.9 g, 92%). 1.2 g of **3** was preserved for PTX conjugation (section 4.8.3)

### 4.8.2.4 Activation of carboxylic groups of Boc-NH-PEG-β-Glu-$(β\text{-Glu})_2$-$(COOH)_4$ via NHS/DCC (**4**)

The carboxylic groups of product **3** were activated to succinimide ester with NHS/DCC as reported in reaction scheme 4.12.

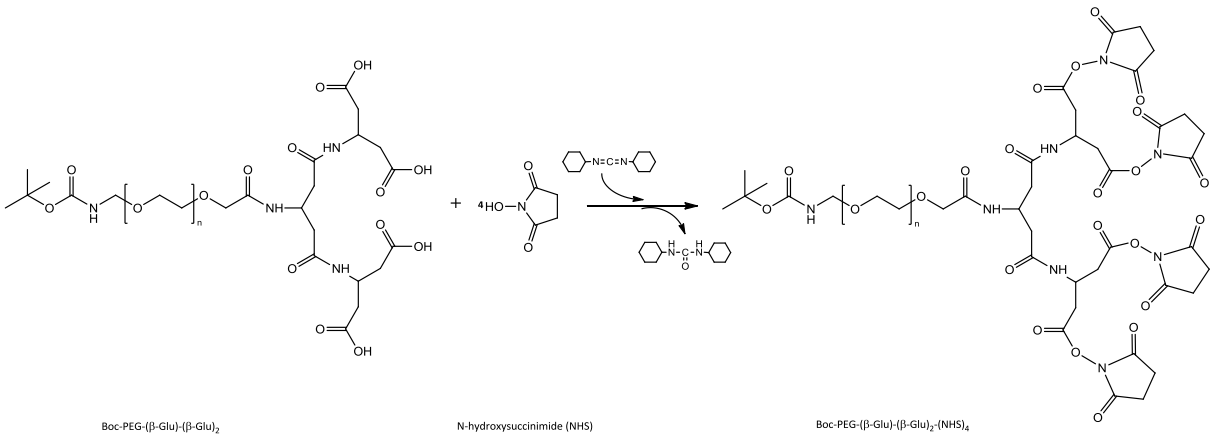


**Scheme 4.12**: Activation of carboxyl groups of Boc-NH-PEG-β-Glu-$(β\text{-Glu})_2$-$(COOH)_4$

1.7 g (0.32 mmol) of **3** were activated with NHS and DCC as reported in the section 4.8.2.2. The degree of activation was 81% (yield: 1.52 g, 89%).

### 4.8.2.5 Synthesis of Boc-NH-PEG-β-Glu-(β-Glu)$_2$-(ALN)$_4$ (**5**)

Boc-NH-PEG-β-Glu-(β-Glu)$_2$-(ALN)$_4$ (**5**) was obtained by forming an amide bond between the four activated carboxyl groups of PEG dendrone and the amino group of alendronate as reported in the reaction scheme 4.13.

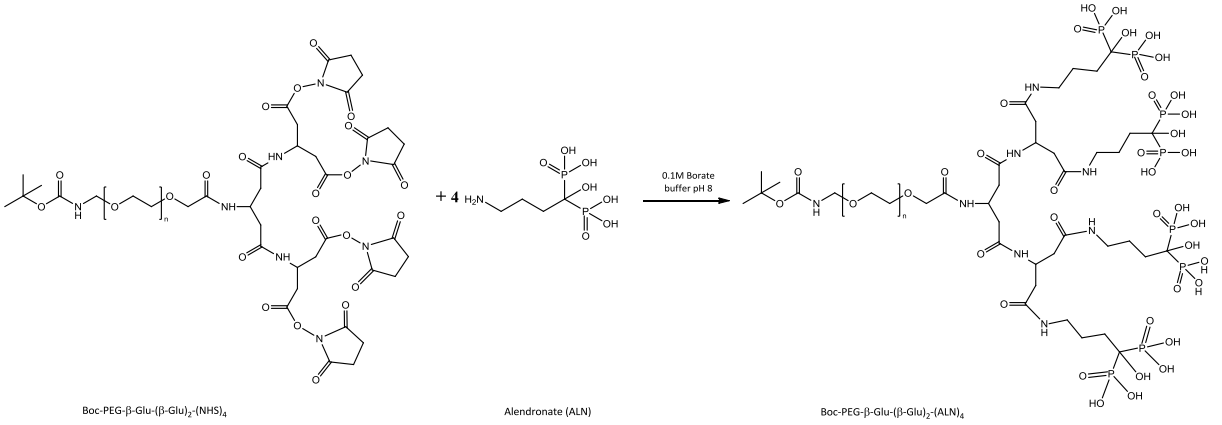


**Scheme 4.13:** Synthesis of Boc-NH-PEG-β-Glu-(β-Glu)$_2$-(ALN)$_4$

To 802 mg (2.46 mmol) of ALN (MW 325.12 Da; 3 equivalent in excess for each activated carboxyl groups of **4**) dissolved in 0.1 M borate buffer at pH 8.0, 1.45 g (0.25 mmol) of **4** (MW 5592 Da) were added and the reaction proceeded for 5 h under stirring. Then, the pH was adjusted to about 4.5 with HCl 0.2 N and product **5** was purified from the excess of ALN by extractions with $CHCl_3$ (6 × 300 mL). The organic phase, dried over anhydrous $Na_2SO_4$, was concentrated under vacuum and dropped into 500 mL of cold diethyl ether under stirring. After 1 h at -20°C, the precipitate of **5** was filtered and dried under vacuum (yield: 1.3g, 83%). The absence of free ALN in the conjugate was verified by TNBS test according to Snyder and Sabocinsky assay [96]. The ALN content in the conjugate was determined as reported in section 4.11.

#### 4.8.2.6 Removal of protecting group t-Boc from Boc-NH-PEG-β-Glu-(β-Glu)$_2$-(ALN)$_4$ and Boc-NH-PEG-β-Glu-(β-Glu)$_2$-(COOH)$_4$

1.2 g of product **3** or 1.3 g of **5** were dissolved in 4 ml of $CH_2CH_2/CF_3COOH/H_2O$ (55.4:45.4:0.1 percent) mixture for 3 h to remove the protecting group t-Boc. The reaction mixture was evaporated to remove the TFA and the obtained oil was solubilised in $CH_2Cl_2$ and dropped into 400 mL of diethyl ether. The product was recovered by filtration and dried under vacuum (yield: 1.17 g, 97% for $H_2N$-PEG-β-Glu-(β-Glu)$_2$-(COOH)$_4$ (**6**) 1.1 g, 91% for and $H_2N$-PEG-β-Glu-(β-Glu)$_2$-(ALN)$_4$ (**7**)).

### 4.8.3 Synthesis of PTX-PEG-β-Glu-(β-Glu)$_2$-(COOH)$_4$ (*PTX-PEG*) and PTX-PEG-β-Glu-(β-Glu)$_2$-(ALN)$_4$ (*PTX-PEG-ALN*)

PTX-PEG and PTX-PEG-ALN were obtained by forming an amide bond between carboxylic groups of 2'-succinyl-paclitaxel and the amino groups of PEG dendrimer via EDC/HOBT (reaction scheme 4.13). The two PTX conjugates were obtained with the same synthetic route, so, below, will be reported the procedure for PTX-PEG-ALN.

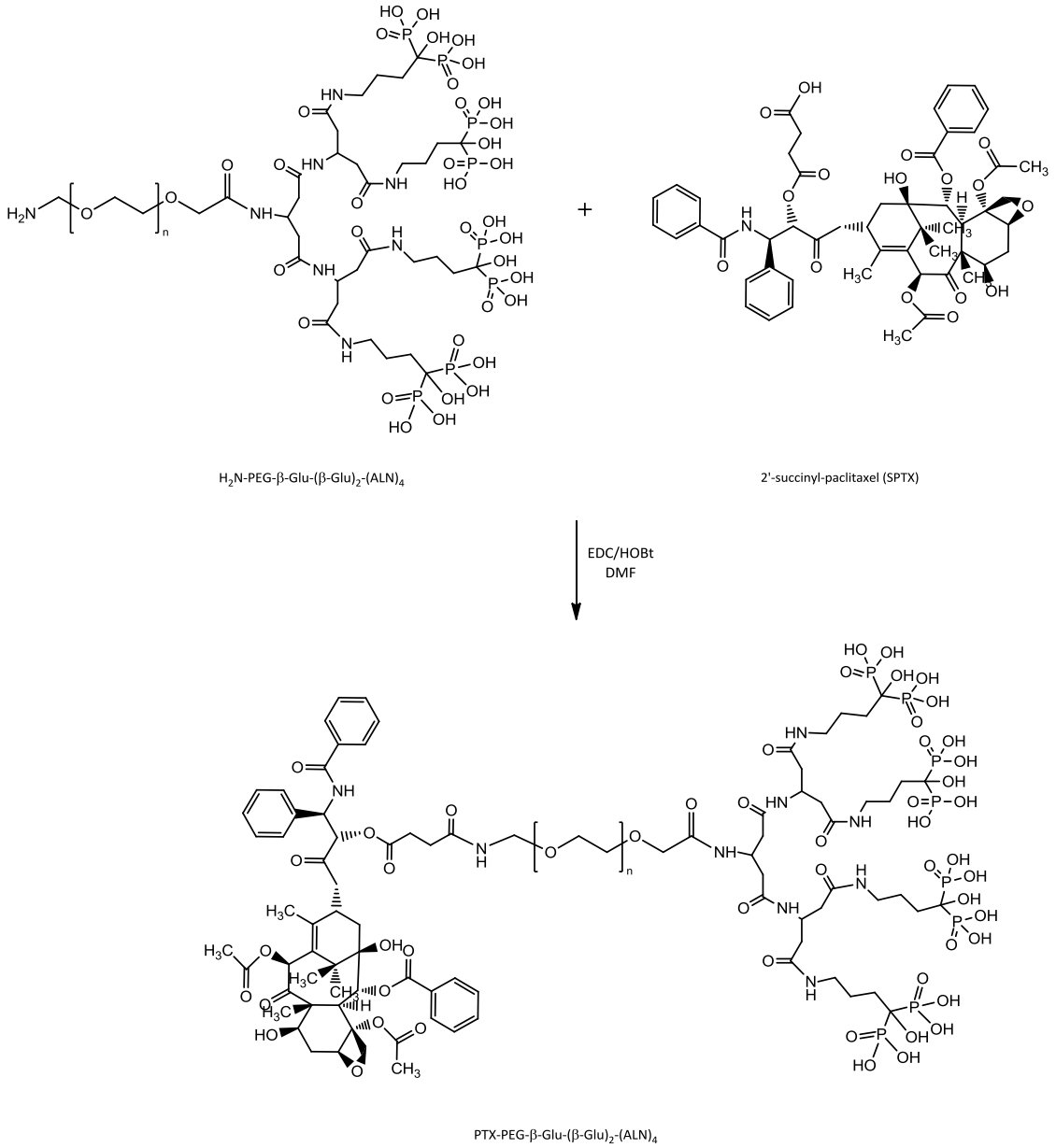


**Scheme 4.13**: Synthesis of PTX-PEG-β-Glu-(β-Glu)$_2$-(ALN)$_4$

To 190 mg (0.2 mmol) of SPTX (MW 953.9 Da), dissolved in anhydrous DMF, 40.5 mg (0.3 mmol) of HOBT (MW 135.12 Da) and 40.2 mg (0.22 mmol) of EDC (MW 191.7 Da), already dissolved in anhydrous DMF, were added. The reaction was stirred for 5 h at room temperature and then 650 mg of product **7** (MW 6328.3 Da), previously dissolved in DMF, was added and let to react for 24 h. The product was purified from the excess of SPTX by gel-filtration chromatography using Sephadex LH-20 resin eluted with DMF. The fractions containing PTX-PEG-ALN were collected in a round bottom flask and DMF was evaporated under vacuum. The product was dissolved in anhydrous $CH_2Cl_2$ and dropped into 500 mL of cold diethyl ether under stirring. After 1 h at -20°C, the precipitate was filtered and dried

under vacuum. The amounts of free and total contents of PTX in PTX-PEG-ALN conjugate were evaluated as reported in the section 4.8.

## 4.9 SYNTHESIS AND CHARACTERIZATION OF FITC LABELLED PTX-PEG, PEG-ALN AND PTX-PEG-ALN CONJUGATES

Synthesis of FITC labelled conjugates was performed exploiting the same chemical strategy for the preparation of non-labelled conjugates reported previously. The new steps are following briefly reported.

### 4.9.1 Synthesis of FITC labelled PEG-dendrimer

#### 4.9.1.1 Synthesis of Boc-NH-PEG-L-Lys(εFmoc)-OH (**8**)

Boc-NH-PEG-L-Lys(εFmoc)-OH (**8**) was obtained by forming an amide bond between the activated carboxyl group of PEG and the amino group of L-Lys(εFmoc)-OH as reported in the reaction scheme 4.14.

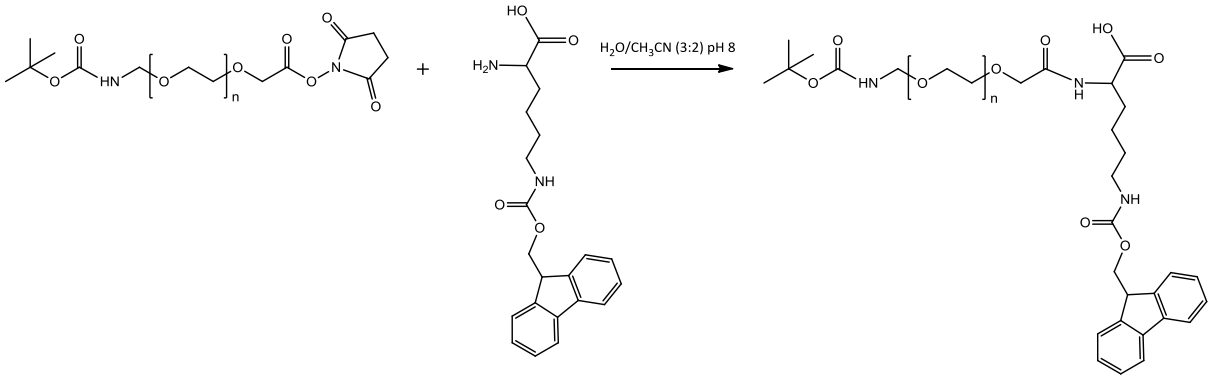


**Scheme 4.14:** Synthesis of Boc-NH-PEG-L-Lys(εFmoc)-OH

To 313 mg ( 0.67 mmol) of L-Lys(εFmoc)-OH (MW 468.54 Da; 3 equivalent in excess to activated -COOH groups of PEG), previously dissolved in 50 mL of $H_2O/CH_3CN$ (3:2) mixture pH 8, 1.1 g (0.2 mmol) of Boc-NH-PEG-NHS (MW 4928 Da) was added and the reaction was let to proceed for 5 h under stirring. Then the pH was adjusted to about 4.5 with HCl 0.2 N and product **8** was purified from the excess of L-Lys(εFmoc)-OH by extractions with $CHCl_3$ (5 x 80 ml) (yield: 911 mg; 88%). The conjugate was characterized by the Snaider Sobociski assay, as reported elsewhere (section 4.8.2.2), to verify the absence of free L-Lys(εFmoc)-OH.

#### 4.9.1.2 Activation of carboxylic groups of Boc-NH-PEG-L-Lys(εFmoc)-OH via NHS/DCC (**9**) and synthesis of Boc-NH-PEG-L-Lys(εFmoc)-β-Glu-$(COOH)_2$ (**10**)

The carboxylic groups of product **8** were activated to succinimide ester with NHS/DCC. After, Boc-NH-PEG-L-Lys(εFmoc)-β-Glu-$(COOH)_2$ (**10**) was obtained by forming an amide bond between the carboxyl group of PEG previously activated and the amino group of β-glutamic acid as reported in the reaction scheme 4.15.

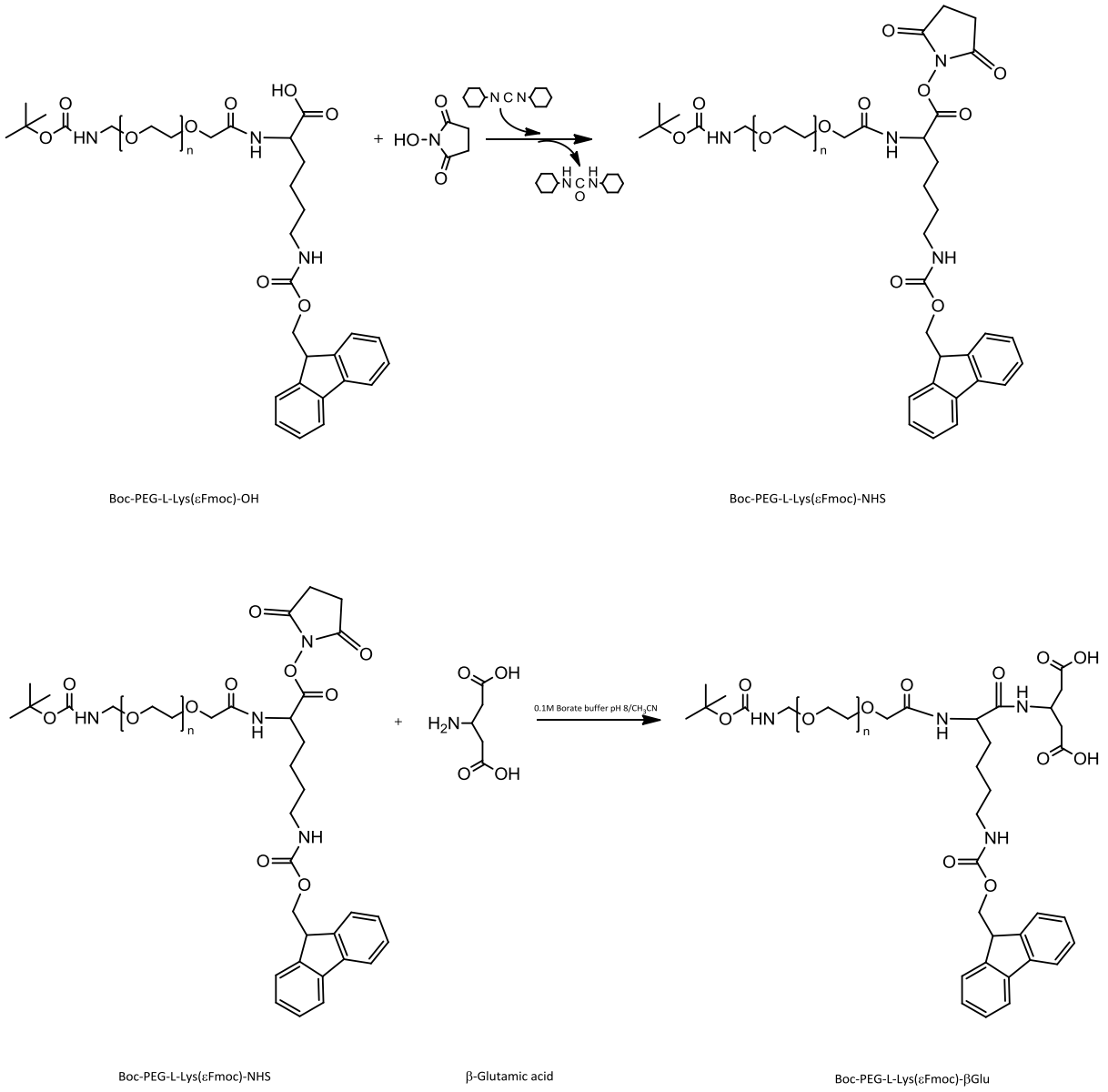


**Scheme 4.15**: Activation of carboxyl groups of Boc-NH-PEG-L-Lys(εFmoc)-OH and synthesis of Boc-NH-PEG-L-Lys(εFmoc)-β-Glu

800 mg (0.152 mmol) of **8** (MW 5263.5 Da) were activated with NHS and DCC as reported in the section 4.2.2.2. The degree of activation was 76% (yield: 766 mg, 94%). After, 750 mg (0.14 mmol) of Boc-NH-PEG-L-Lys(εFmoc)-β-Glu-$(NHS)_2$ (**9)** (MW 5360.5 Da) was added to 53.3 mg (0.36 mmol) of β-Glu (MW 147.1 Da; 3 equivalent in excess to activated -COOH groups of PEG), dissolved in 25 mL of 0.1 M borate buffer/$CH_3CN$ (3:2) mixture pH 8.0. The reaction was let to proceed for 5 h under stirring and then purified as previously reported (section 4.8.2.1).

### 4.9.1.3 Activation of carboxylic groups of Boc-NH-PEG-L-Lys(εFmoc)-β-Glu-$(COOH)_2$ via NHS/DCC (**11**) and synthesis of Boc-NH-PEG-L-Lys(εFmoc)-β-Glu-$(\beta\text{-Glu})_2$-$(COOH)_4$ (**12**)

As for product **10**, the carboxylic groups of Boc-NH-PEG-L-Lys(εFmoc)-β-Glu were first activated with NHS and DCC (product **11**) and then conjugated to other 2 β-glutamic acid to obtained Boc-NH-PEG-L-Lys(εFmoc)-β-Glu-$(\beta\text{-Glu})_2$ (**12**) as reported in reaction scheme 4.16.

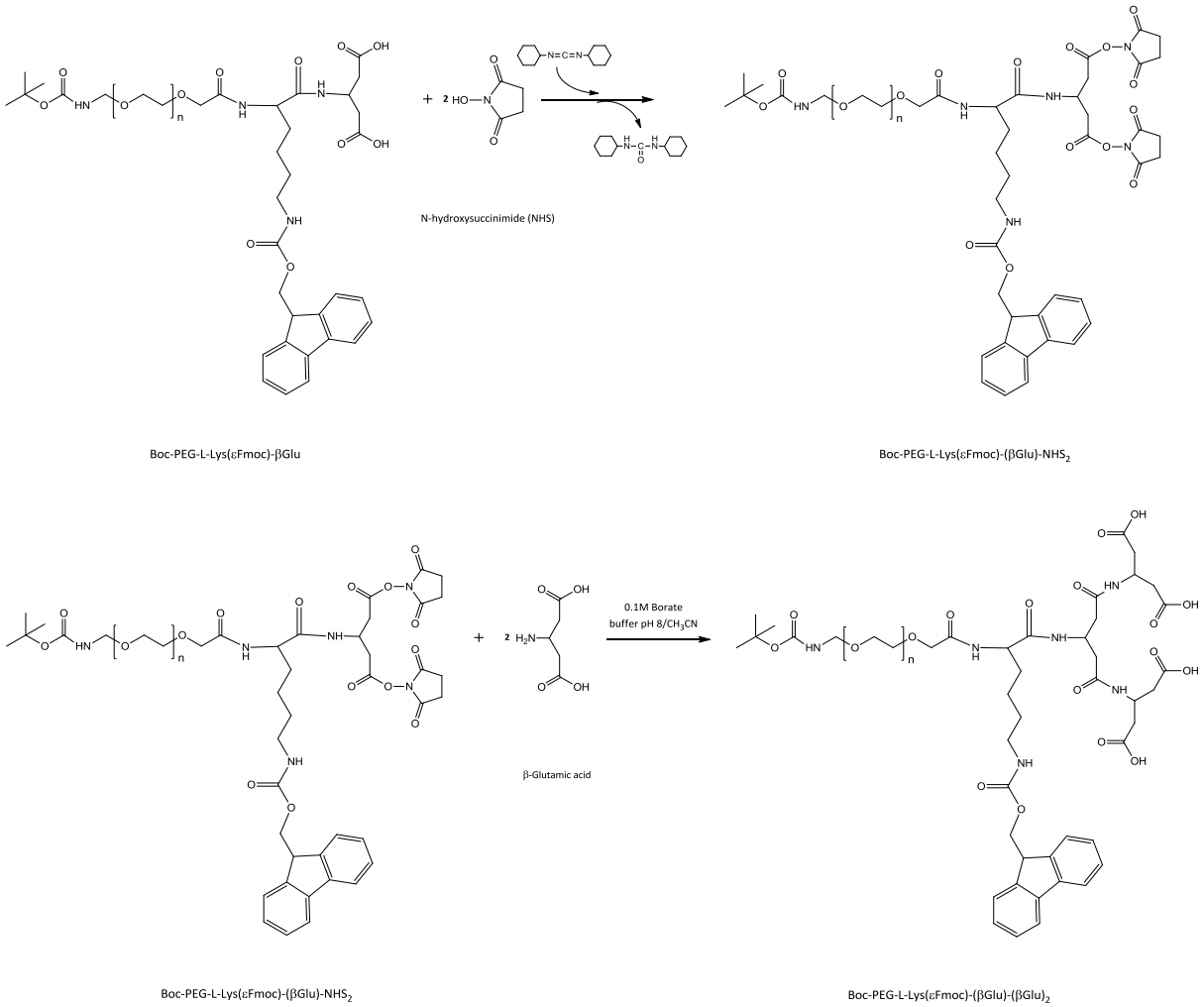


**Scheme 4.16**: Activation of carboxylic groups of Boc-NH-PEG-L-Lys(εFmoc)-β-Glu and synthesis of Boc-NH-PEG-L-Lys(εFmoc)-β-Glu-$(\beta\text{-Glu})_2$

700 mg (0.13 mmol) of **10** (MW 5392.6 Da) were activated with NHS and DCC as reported in the section 4.2.2.2. The degree of activation was 75% (yield: 560 mg, 77%). After, 550 mg (0.098 mmol) of **11** (MW 5586.6 Da) was added to 86 mg (0.588 mmol) of β-Glu (MW 147.1 Da; 3 equivalent in excess to each activated -COOH groups of PEG), dissolved in

25 mL of 0.1 M borate buffer/$CH_3CN$ (3:2) mixture pH 8.0. The reaction was let to proceed for 5 h under stirring and then purified as previously reported (section 4.8.2.1).

### 4.9.1.4 Removal of protecting group Fmoc from Boc-NH-PEG-L-Lys(εFmoc)-β-Glu-(β-Glu)$_2$-(COOH)$_4$

530 mg of Boc-NH-PEG-L-Lys(εFmoc)-β-Glu-(β-Glu)$_2$ (**12**) were dissolved in 10 ml of DMF with 20% of piperidine for 15 min. to remove the protecting group Fmoc. The reaction mixture was evaporated to remove the solvent and the residues was solubilized in $CH_2Cl_2$ and dropped into 300 mL of diethyl ether. The product was recovered by filtration and dried under vacuum (yield: 483 mg, 93%).

### 4.9.1.5 Synthesis of Boc-NH-PEG-L-Lys(εFITC)-β-Glu-(β-Glu)$_2$-(COOH)$_4$ (**13**)

Boc-NH-PEG-L-Lys(εFITC)-β-Glu-(β-Glu)$_2$-(COOH)$_4$ was obtained by reaction between fluorescein isothiocyanate and the amino group of lysine conjugated to PEG as reported in the reaction scheme 4.17.

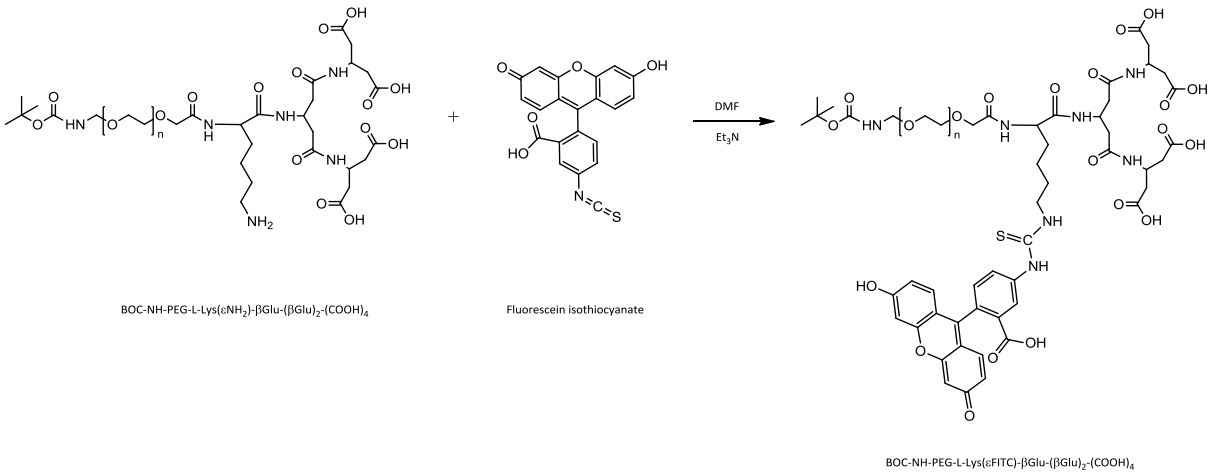


**Scheme 4.17**: Synthesis of Boc-NH-PEG-L-Lys(εFITC)-β-Glu-(β-Glu)$_2$-(COOH)$_4$

32.4 mg (0.08 mmol) of FITC (MW 389.4 Da) and 11 µL (0.14 mmol) of $Et_3N$ were added to 470 mg (0.08 mmol) of Boc-NH-PEG-L-Lys(ε$NH_2$)-β-Glu-(β-Glu)$_2$-$(COOH)_4$ (MW 5292.45 Da), previously dissolved in 10mL of DMF. The mixture was let to react for 5 h and then the product was purified from excess of FITC by extensive dialysis vs 0.1 M phosphate buffer pH 8.0 using a membrane with cut-off 3500 Da. The last step of dialysis was performed overnight with $H_2O$ mQ to eliminate the phosphate salts and then the product was lyophilized (yield: 394 mg, 83%). The conjugate was characterized by RP-HPLC to verify the absence of free FITC using an Agilent 300-Extend C18 (4.6 x 250 mm; 5 µm) column, with the UV detector settled at 494 nm. The eluent A and B were $H_2O$ and $CH_3CN$ with 0.05% TFA respectively. The elution was performed by the following gradient: from 10%B to 70%B in 25 min, from 70%B to 90%B in 2 min, from 70%B to 10%B in 2 min, at flow rate of 1 ml/min.

#### 4.9.1.6 Activation of carboxylic groups of Boc-NH-PEG-L-Lys(εFITC)-β-Glu-(β-Glu)$_2$-$(COOH)_4$ via NHS/DCC (**14**) and synthesis of Boc-NH-PEG-L-Lys(εFITC)-β-Glu-(β-Glu)$_2$-$(ALN)_4$ (**15**)

As for product **10**, the carboxylic groups of Boc-NH-PEG-L-Lys(εFITC)-β-Glu-(β-Glu)$_2$-$(COOH)_4$ were first activated with NHS and DCC (product **14**) and then conjugated to other alendronate to obtained Boc-NH-PEG-L-Lys(εFITC)-β-Glu-(β-Glu)$_2$-$(ALN)_4$ (**15**) as reported in reaction scheme 4.18.

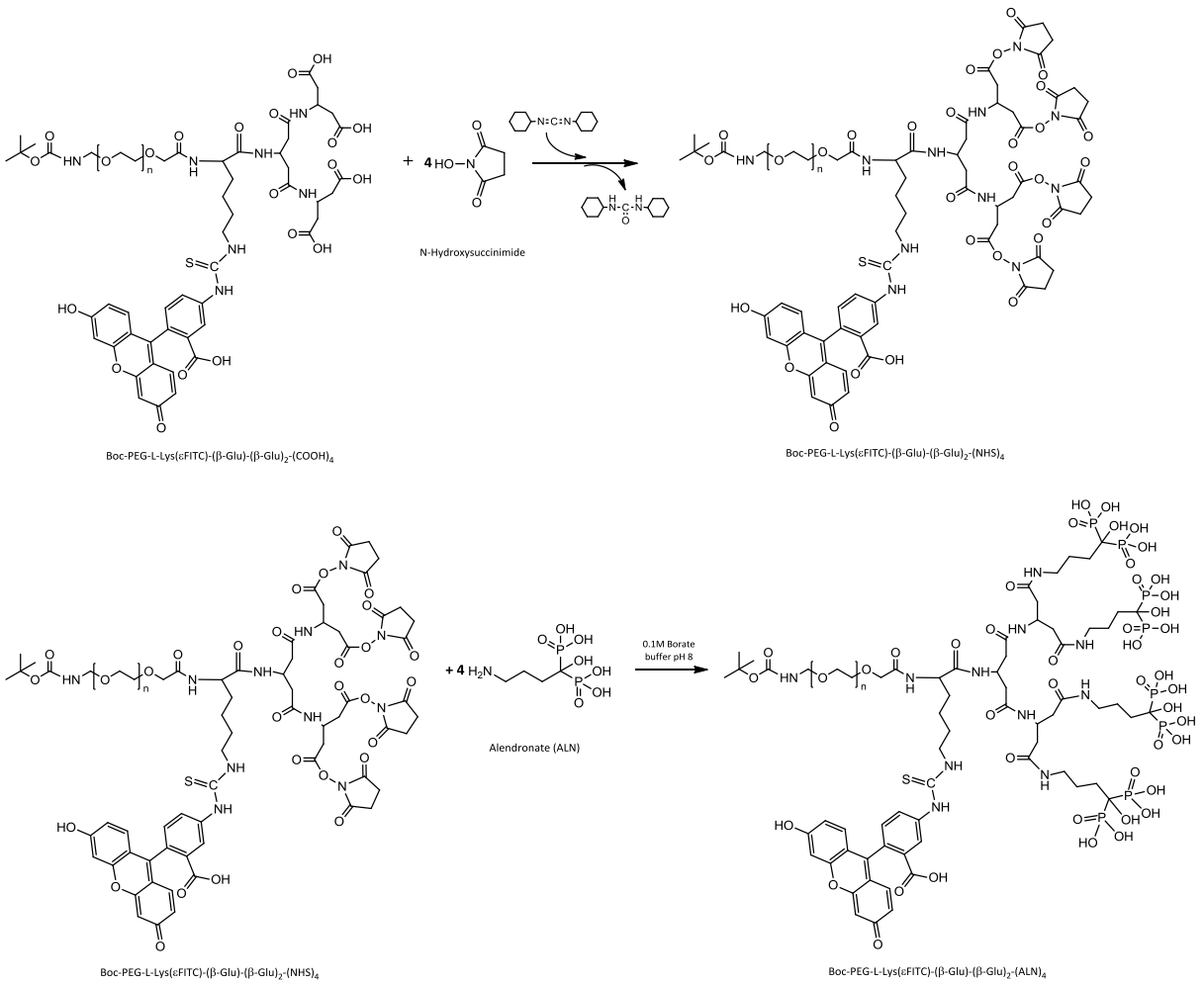


**Scheme 4.18**: Activation of carboxylic groups of Boc-NH-PEG-L-Lys(εFITC)-β-Glu-$(β\text{-Glu})_2$-$(COOH)_4$ and synthesis of Boc-NH-PEG-L-Lys(εFITC)-β-Glu-$(β\text{-Glu})_2$-$(ALN)_4$

244 mg (0.043 mmol) of **13** (MW 5664 Da) were activated with NHS and DCC as reported in the section 4.8.2.2. The degree of activation was 68% (yield: 197 mg, 75%). After, 185 mg (0.03 mmol) of **14** (MW 6052 Da) was added to 78 mg (0.24 mmol) of alendronate (MW 325.12 Da; 3 equivalent in excess to each activated -COOH groups of PEG), dissolved in 15 mL of 0.1 M borate buffer pH 8.0. The reaction was let to proceed for 5 h under stirring and then purified as previously reported (section 4.8.2.6) (yield: 156 mg, 82%).

#### 4.9.1.7 Removal of protecting group *t*-Boc from Boc-NH-PEG-L-Lys(εFITC)-β-Glu-(β-Glu)$_2$-(COOH)$_4$ (**13**) and Boc-NH-PEG-L-Lys(εFITC)-β-Glu-(β-Glu)$_2$-(ALN)$_4$ (**15**)

150 mg of product **13** or 140 mg of **15** were dissolved in 2 ml of $CH_2CH_2$/$CF_3COOH$/$H_2O$ (55.4%:45.4%:0.1%) mixture for 3 h to remove the protecting group *t*-Boc as reported for product **6** and **7** in the section 4.8.2.7.

### 4.9.2 Synthesis of PTX-PEG-L-Lys(εFITC)-β-Glu-(β-Glu)$_2$-(COOH)$_4$ (*PTX-PEG-FITC*) and PTX-PEG-L-Lys(εFITC)-β-Glu-(β-Glu)$_2$-(ALN)$_4$ (*PTX-PEG-ALN-FITC*)

PTX-PEG-FITC and PTX-PEG-ALN-FITC were obtained by forming an amide bond between carboxylic groups of 2'-succinyl-paclitaxel and the amino groups of PEG dendrimer via EDC/HOBT (reaction scheme 4.19) as already reported in section 4.8.3. The two PTX conjugates were obtained with the same synthetic route, so, below, will be reported the procedure for PTX-PEG-ALN-FITC.

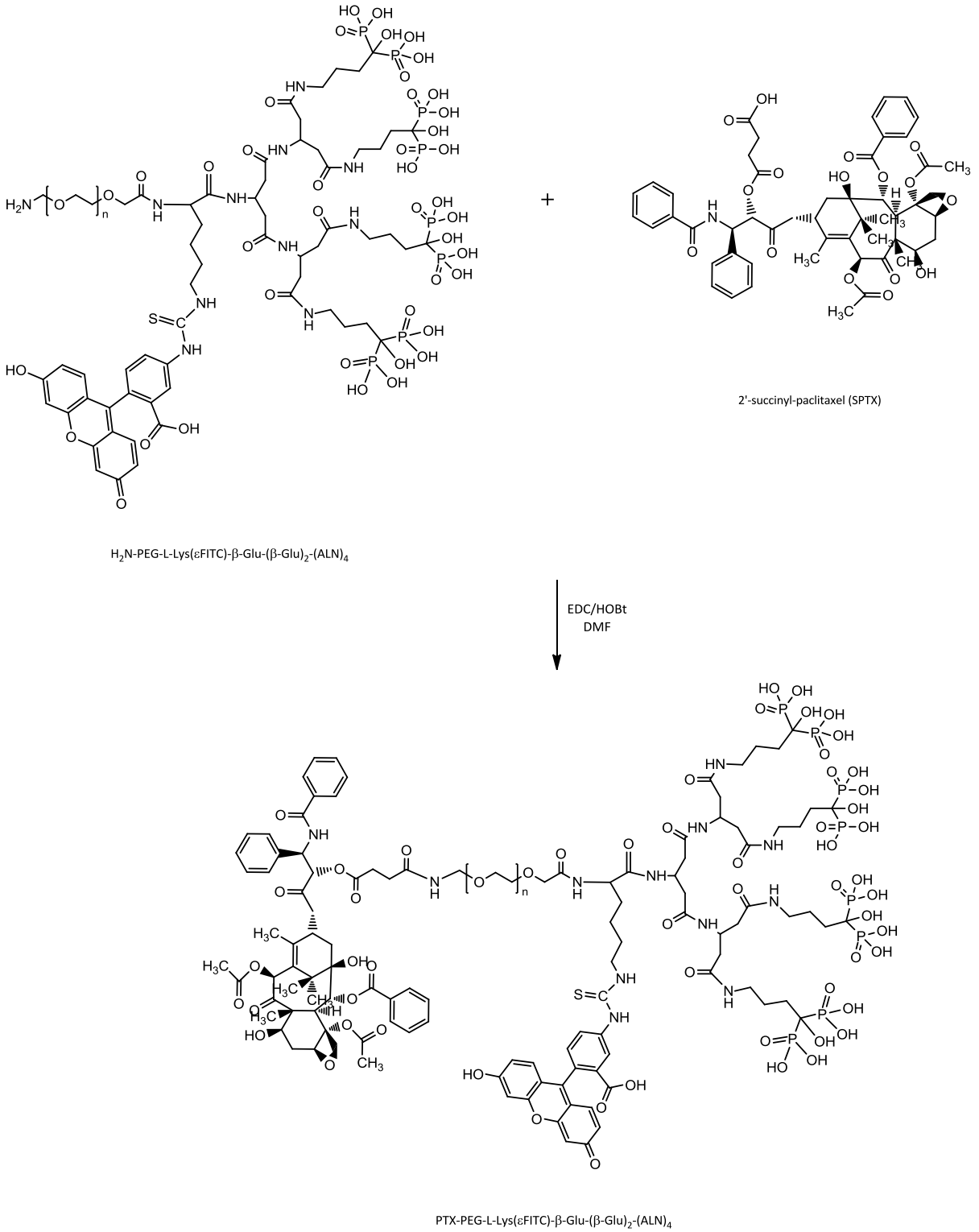


**Scheme 4.19**: Synthesis of PTX-PEG-ALN-FITC

To 190 mg (0.2 mmol) of SPTX (MW 953.9 Da), dissolved in anhydrous DMF, 40.5 mg (0.3 mmol) of HOBT (MW 135.12 Da) and 40.2 mg (0.22 mmol) of EDC (MW 191.7 Da), already dissolved in anhydrous DMF, were added. The reaction was stirred for 5 h at room temperature and then 100 mg of $H_2N$-PEG-L-Lys(εFITC)-βGlu-$(\beta Glu)_2$-$(ALN)_4$ (MW 7180 Da),

previously dissolved in DMF, was added and let to react for 24 h. The product was purified from the excess of SPTX as reported in the section 4.8.3. The amounts of free and total contents of PTX in PTX-PEG-ALN conjugate were evaluated as reported in the section 4.10.

## 4.10 DETERMINATION OF FREE AND TOTAL PTX CONTENTS IN THE CONJUGATES

The amount of PTX in the conjugates was evaluated by reverse phase HPLC using an Agilent 300-Extend C18 (4.6 × 250 mm; 5 µm) column, with the UV detector settled at 227 nm. The eluents A and B were $H_2O$ and $CH_3OH$, respectively. The elution was performed by the following gradient: from 5%B to 50%B in 5 min, from 50%B to 80%B in 14 min, from 80%B to 100%B in 5 min, and from 100%B to 5%B in 5 min at a flow rate of 1 mL/min.

The total drug content was evaluated by RP-HPLC following the release of PTX from the conjugates. 3 mg of conjugate were dissolved in 1 mL of MeOH. Following the addition of 2% (v/v) of NaOH 0.2 N, the solution was incubated at 50°C for 2 h. The drug was then extracted by ethyl acetate. The organic phase was evaporated and the residue was solubilized in methanol. The elution was performed as reported above. The amount of PTX was calculated using PTX calibration curve obtained using the same method.

## 4.11 DETERMINATION OF ALN CONTENT BOUND TO PEG

The formation of chromophoric complex between ALN and $Fe^{3+}$ ions in perchloric acid solution was used to determine the ALN content by spectrophotometry [98].

Conjugates (2.5, 5 and 10 mg) were dissolved in a mixture of 0.1 mL 4 mM $FeCl_3$ and 0.8 ml 0.2 M perchloric acid ($HClO_4$). The content of ALN in the conjugates was determined against a calibration graph of serial dilutions of 0-3 mM ALN. Sample absorbance was measured spectrophotometrically at λ=300 nm.

## 4.12 DETERMINATION OF FITC CONTENT

The content of FITC was measured spectrophotometrically using ε 64185 $M^{-1}$ $cm^{-1}$ in PBS pH 8.

## 4.13 CONJUGATES STUDIES

### 4.13.1 Conjugates stability in buffer solution at different pH values and in plasma

PTX-PEG and PTX-PEG-ALN (3 mg/mL) were incubated at 37°C for 48 h in PBS at pH 5 and 7.4 to evaluate the drug release. Samples of 50 µL were withdrawn at predetermined times and analyzed by RP-HPLC using the same conditions reported in section 4.4, evaluating the decrease of the conjugate peak in the chromatographic profile.

The conjugates were also incubated at 37°C for 48 h in mouse plasma, obtained after centrifugation of blood sample at 2000 × g for 10 min. Samples of 60 µL were withdrawn at predetermined times and 60 µL of $CH_3CN$ were added to achieve plasma protein precipitation. Samples were centrifuged at 15000 × g and the supernatant was withdrawn and analyzed by RP-HPLC using the same conditions reported above.

### 4.13.2 Stability of polymeric structures in buffer solutions at different pH values

The stability of the conjugates was also evaluated by dynamic light scattering. Solution of each conjugate (7 mg/mL) was obtained by solubilization in PBS pH 5 and 7.4. These solutions were immediately extruded with manual extruder (Liposofast Avestin) at 200 nm and analyzed using a light scattering instrument (Malvern Nano-S, Worcestershire, United Kingdom). The instrument was settled at 37°C, the detector position was at 173° and the analysis was performed every 20 min (the first measurement was performed after 5 min of

equilibration) for 4 h and, after storage in similar conditions, the sample was analyzed at 24 h.

### 4.13.3 Hydroxyapatite binding assay

PEG, PEG-ALN and PTX-PEG-ALN conjugates were dissolved in phosphate buffered saline (PBS), pH 7.4 (5 mg/mL). The conjugate solution (600 µL) was incubated with HA powder (30 mg), in 600 µL PBS, pH 7.4. $NH_2$-PEG-$COOH_4$ was used as control. Incubated samples were centrifuged at 7000 RPM for 3 min and a sample from the upper layer (100 µL) was collected after 0, 2, 5, 10 and 60 min. Fast protein liquid chromatography (FPLC, AKTA™ Purifier®, Amersham Biosciences) analysis using HiTrap™ desalting column (Amersham®) was used for detection of unbound conjugates in the samples (FPLC conditions: AKTA™ Purifier®, mobile phase 100% DDW, 2 mL/min, λ=215 nm). HA-binding kinetic analysis of the conjugates was performed using the Unicorn® AKTA™ software. Areas under the curve (AUC) were calculated from chromatographs at each time point. AUC of each HA-incubated conjugate chromatogram was normalized to percent AUC of conjugate sample in the absence of HA.

### 4.13.4 Red blood cells (RBC) lysis assay

Rat RBC solution (2% w/w) was incubated with serial dilutions of the combination of PTX plus ALN, PEG, and PTX-PEG-ALN conjugate at equivalent PTX and ALN concentrations, for 1 h at 37$^{o}$C. Negative controls were PBS and Dextran (MW ~70000 Da) while positive controls were 1% w/v solution of Triton X100 (100% lysis) and poly(ethylenimine) (PEI). Following centrifugation, the supernatant was drawn off and its absorbance measured at 550 nm using a microplate reader (Genios, TECAN). The results were expressed as percent of hemoglobin released relative to the positive control (Triton X100).

## 4.14 CELL STUDIES

### 4.14.1 Cell culture

PC3 human prostate adenocarcinoma cell line, MDA-MB-231 human mammary adenocarcinoma and 4T1 murine mammary adenocancinoma cell lines were purchased from the American Type Culture Collection (ATCC). PC3 and MDA-MB-231 cells were cultured in DMEM supplemented with 10% FBS, 100 µg/ml Penicillin, 100 U/ml Streptomycin ,12.5 U/ml Nystatin and 2 mM L-glutamin. 4T1 cells were cultured in RPMI 1640 supplemented with 10% FBS, 100 µg/ml Penicillin, 100 U/ml Streptomycin ,12.5 U/ml Nystatin, 2 mM L-glutamin, 10 mM Hepes buffer, and 1 mM sodium pyruvate. Human umbilical vein endothelial cells (HUVEC) were obtained from Cambrex (Walkersville, MD, U.S.A) and grown according to the manufacturer's protocol in EGM-2 medium (Cambrex). Cells were grown at 37°C; 5% $CO_2$.

### 4.14.2 Cell toxicity assay

HUVEC were plated onto 24-well plate (1.5 x $10^4$ cells/well) in growth factors reduced media, (EBM-2, Cambrex, USA) supplemented with 5% FBS. Following 24 h of incubation (37°C; 5% $CO_2$), medium was replaced with EGM-2 (Cambrex, USA). PC3, 4T1 and MDA-MB-231 cells were plated onto 96 well plate (5 x $10^3$ cells/well) in DMEM supplemented with 5% FBS and incubated for 24 h (37°C; 5% $CO_2$). Following 24 h of incubation, medium was replaced with DMEM containing 10% FBS. Cells were challenged with the combination of free PTX plus ALN, each free drug alone, and with PEG, PEG-ALN, PTX-PEG, PTX-PEG-ALN conjugates at serial concentrations for up to 72 h. After incubation HUVEC and the cancer cell lines (PC3, 4T1, MDA-MB-231) were counted by Coulter Counter or by MTT (Sigma), respectively.

### 4.14.3 Migration assay

Cell migration assay was performed using modified 8 µm Boyden chambers Transwells® (Costar Inc., USA) coated with 10 µg/mL fibronectin (Biological industries, Beit Haemek, Israel). PC3 and HUVEC (15 x $10^4$ cells/100 µL) were challenged with the combination of free PTX (10 nM) and ALN (46 nM), each free drug alone, and with PEG, PEG-ALN, PTX-PEG, PTX-PEG-ALN conjugates at equivalent PTX and ALN concentrations, and were added to the upper chamber of the transwells for 2 h incubation prior to migration towards DMEM containing 10% FBS for PC3 and prior to migration to vascular endothelial growth factor (VEGF) for HUVEC. Following incubation, cells were allowed to migrate to the underside of the chamber for 4 h in the presence or absence of 10% FBS o VEGF (20 mg/mL) in the lower chamber. Cells were then fixed and stained (Hema 3 Stain System; Fisher Diagnostics, USA). The stained migrated cells were imaged using Nikon TE2000E inverted microscope integrated with Nikon DS5 cooled CCD camera by 10X objective, brightfield illumination. Migrated cells from the captured images per membrane were counted using NIH image software. Migration was normalized to percent migration, with 100% representing migration to medium containing FBS for PC3 cell or VEGF for HUVEC.

### 4.14.4 Capillary-like tube formation assay

The surface of 24-well plates was coated with Matrigel matrix (50 µL/well) (BD Biosciences, USA) on ice and was then allowed to polymerize at 37°C for 30 min. HUVEC (3 x $10^4$) were challenged with the combination of free PTX (5 nM) plus ALN (23 nM), each free drug alone, and with PEG, PEG-ALN, PTX-PEG and PTX-PEG-ALN conjugates at equivalent concentrations, and were seeded on coated plates in the presence of complete EGM-2 medium. After 8 h of incubation (37°C; 5% $CO_2$), wells were imaged using Nikon TE2000E inverted microscope integrated with Nikon DS5 cooled CCD camera by 4X objective, brightfield technique.

## 4.15 *IN VIVO* STUDIES

### 4.15.1 Body distribution of FITC labeled PEG, PTX-PEG, PEG-ALN and PTX-PEG-ALN conjugates

SCID mice bearing MDA-MB-231 tumors in the tibia were injected *i.v.* with FITC labeled PEG, PTX-PEG, PEG-ALN and PTX-PEG-ALN conjugates. FITC labeled conjugates accumulation in the tumor was assessed at different time points (0, 2, 4, 6, and 8 h). At termination (after 8 h) tumors, organs and bones were excised and imaged.

Both organs and FITC labeled conjugates accumulation in tumors in live animals were imaged using noninvasive imaging system (CRI Maestro™). Fluorescence was determined using defined regions of interest (ROI) measurements on tumors and other tissues. Time dependent tumor contrast profile was determined by the ratio between fluorescence intensities of tumors and those of normal skin. Data were expressed as mean ± standard deviation (SD) (n=3).

### 4.15.2 Pharmacokinetic studies in mice

Pharmacokinetics of PTX, PTX-PEG and PTX-PEG-ALN were determined in female Balb/C mice (23–25 g). The 30 mice were randomly divided in three groups of 10 animals. 150 µL of PTX in 1:1:8 Ethanol:Cremophor EL:Saline, PTX-PEG in PBS pH 6 or PTX-PEG-ALN in PBS pH 6 (dose: 10 mg/Kg PTX equiv.) were administered *via* tail vein to mice anaesthetized with 5% isoflurane gas (mixed with $O_2$ in enclosed cages). At predetermined times, two blood samples (150 µL) were withdrawn from the retro-orbital plexus/sinus of two animals, with a heparinized capillary, and then centrifuged at 1,500 *g* for 15 min. To 50 µL of plasma, 350 µL of $CH_3CN$ was added for protein precipitation and the resulting mixture was centrifuged at 20,000 *g* for 5 min. 300 µL of the supernatant was collected and freeze-dried. The residue was dissolved in 50 µL of $CH_3OH$ and analyzed by RP-HPLC under condition reported above. For PTX-PEG and PTX-PEG-ALN the residues after freeze-drying were also hydrolyzed with 2% NaOH 0.2N as reported above.

### 4.15.3 Evaluation of antitumor activity of PTX-PEG-ALN conjugate

A syngeneic mouse model of breast cancer was established by injecting Balb/c female mice 100 µl of $4\times10^5$ mCherry-labeled 4T1 cells intra-tibia. Therapy was initiated one day after tumor cells inoculation. Mice were randomly divided into 9 groups (n = 6 mice/group) and intravenously *(i.v.)* injected with 100 µl of PTX (15 mg/kg), ALN (35 mg/kg), the combination of free PTX plus ALN, PTX vehicle (1:1:8 Ethanol:Cremophor EL:Saline), saline, PEG, PTX-PEG, PEG-ALN or PTX-PEG-ALN conjugates. A xenograft mouse model was established by injecting SCID female mice 100 µl of $1\times10^5$ mCherry-labeled MDA-MB-231 cells intra-tibia. Therapy was initiated 10 days after tumor inoculation, when most mice had fluorescent signals indicating tumors uptake. Mice were divided into 5 groups (n=4-5 mice/group) and the mean fluorescence intensity was approximately equivalent for all groups. These groups were randomly assigned and received *i.v.* injections of 100 µl PTX (15 mg/kg) plus ALN (35 mg/kg), PTX (7.5 mg/kg) plus ALN (17.5 mg/kg), PTX vehicle, saline, and PTX-PEG-ALN conjugate. All treatments for both mouse models were injected intravenously (i.v.) via the tail vain, every other day from initial therapy, 5 injections. Tumor progression was monitored by CRI™ Maestro non-invasive intravital imaging system. At termination, tibias were removed and analyzed. Data is expressed as mean± s.e.m.

### 4.15.4 White Blood Cell (WBC) counts

Blood was obtained from anaesthetized mice by retro-orbital sinus bleeding. Twenty four hours after treatment, blood was collected in tubes containing 0.1M EDTA to avoid clotting. Samples were counted no longer than five minutes after blood was drawn from mice. Ten µl of blood samples were mixed with 90 µl of track solution (1 % acetic acid in DDW), and cells were counted by a Z1 Coulter® Particle Counter (Beckman Coulter™). Data is expressed as mean ± s.e.m.

# RESULTS

*Studies on polymer conjugation as versatile tool for drug delivery*

## 5.1 POLYMERIC CARRIERS-BASED EPIRUBICIN

### 5.1.1 SYNTHESIS AND CHARACTERIZATION OF EPIRUBICIN CONJUGATES

Five EPI conjugates (Fig. 5.1) were obtained by forming an amide bond between carboxylic groups of polymer and the amino group of EPI. All conjugates were purified (by extractions, precipitation or GPC) in order to remove residual free EPI, and characterized by HPLC (Fig. 5.2), UV-VIS and fluorescence spectrometry (Fig. 5.3) and by 1H-NMR (Fig. 5.4-5.7). In all cases we obtained a pure products with a free EPI content below to 1% wt/wt total drug (Table 5.1).

***Non-Biodegradable***

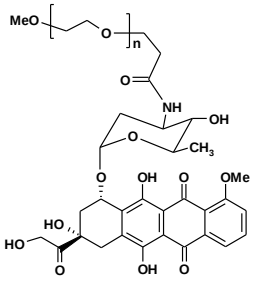

**PEG-EPI**

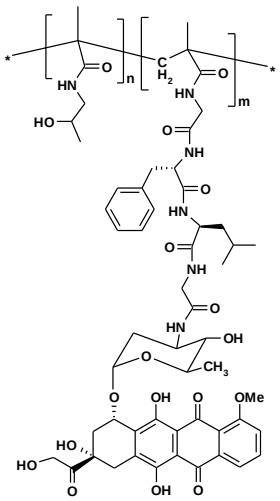

**HPMA-GPLG-EPI**

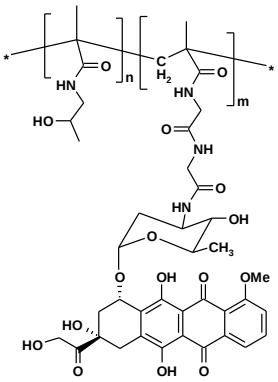

**HPMA-GG-EPI**

***Biodegradable***

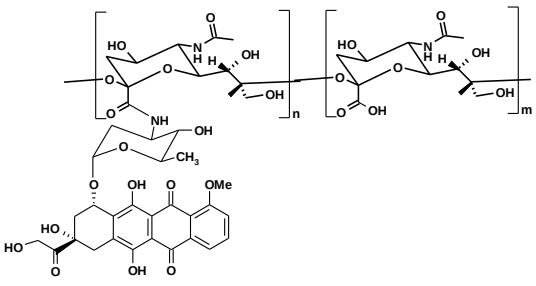

**PSA-Epi**

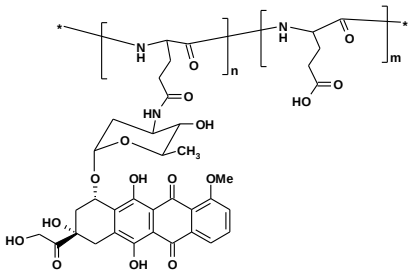

**PGA-Epi**

**Figure 5.1:** Schematic representation of the five conjugates

*HPLC characterization:*

n figure 5.2, a EPI conjugates chromatography spectrum are showed. For PEG, HPMA and PGA the elution were performed in RP-HPLC. The conjugates retention time ($t_R$ about 16 min) were different from free EPI ($t_R$= 8.7 min). In case of PSA-EPI, the elution was performed in GPC because the polymer does not elute in reverse phase. AS for the other conjugates, PSA-EPI eluted with a retention time ($t_R$=7 min) completely different to the free EPI ($t_R$=14 min).

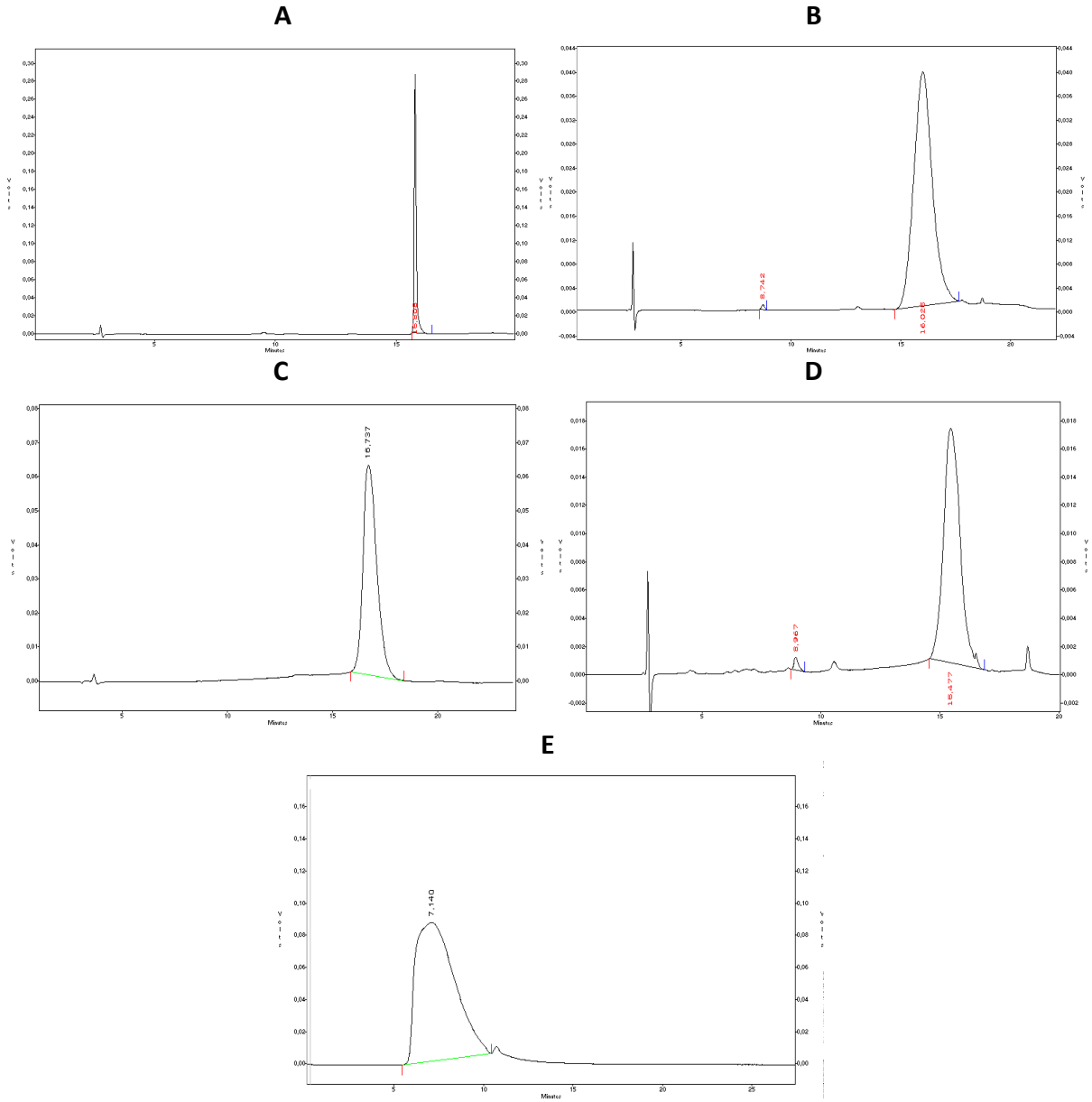


**Figure 5.2**: Cromatography characterization of mPEG-EPI (**A**), HPMA-GFLG-EPI (**B**), HPMA-GG-EPI (**C**), PGA-EPI (D) and PSA-EPI (**E**). The analysis were performed by RP-HPLC (experimental condition reported in section 4.9) for **A**, **B**, **C**, **D**, and by GPC for **E** (experimental condition reported in section 4.8.5).

The total drug amount (free and bond) was determinated after acid hydrolysis of a conjugate solutions (Table 5.1).

**Table 5.1:** Total and free EPI content in the polymer conjugates

| Conjugates | Total EPI content (%wt/wt) | Free EPI content (%wt/wt total drug) |
|---|---|---|
| mPEG-EPI | 3.8 | - |
| HPMA-GPLG-EPI | 6.6 | 0.12 |
| HPMA-GG-EPI | 6 | 0.2 |
| PGA-EPI | 4.82 | 0.16 |
| PSA-EPI | 1.58 | 0.6 |

*UV-VIS and fluorescence characterization:*

All EPI conjugates were characterized and compared to free EPI by UV-VIS spectrometry and by fluorometer (Fig. 5.3). These studies were performed because it is known that polymer conjugation can affect the extinction coefficient and the fluorescence emission of a drug [99].

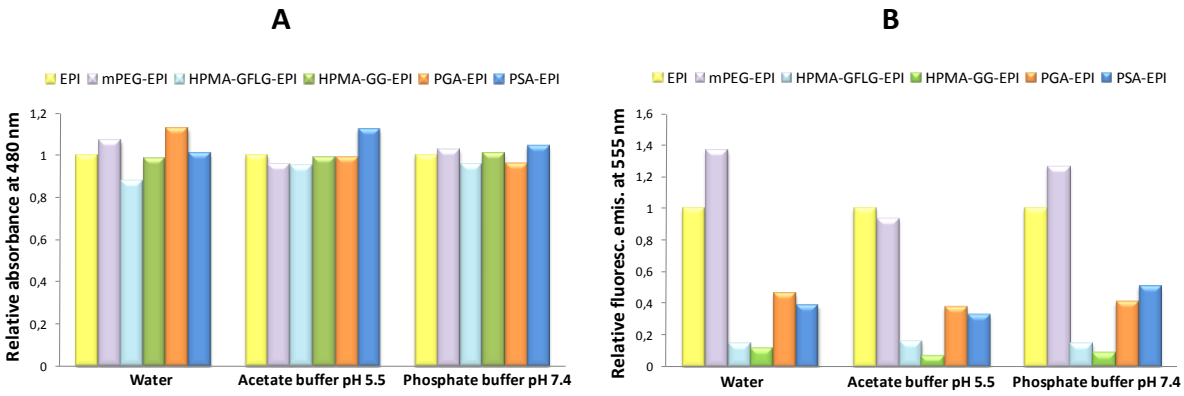


**Figure 5.3:** Relative UV absorbance at 480 nm (**A**) or fluorescence emission at 555 nm (**B**) of conjugates with EPI set at 1

All conjugates showed similar UV-Vis absorption at 480 nm, while significant differences were noticed in fluorescence emission. In particular, the fluorescence output of HPMA copolymers-EPI was approximately 6-10 times smaller than that of free EPI. This data were taken into consideration for the next studies that rely on fluorescence (e.g FACS).

*[1]H-NMR spectroscopy characterization*

*mPEG-EPI*

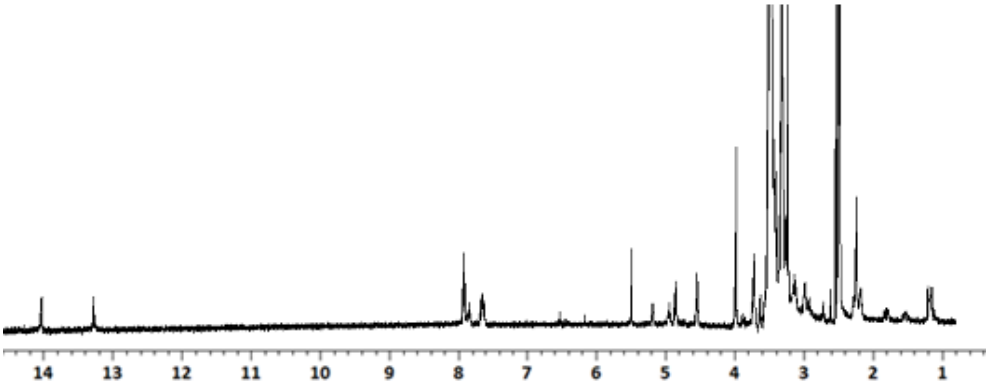


**Figure 5.4:** [1]H-NMR spectroscopy of mPEG-EPI in $d_6$-DMSO

**Table 5.2:** principal signal [1]H-NMR of mPEG-EPI in $d_6$-DMSO

| δ(ppm) | Multiplicity | Assignment |
|---|---|---|
| 1.43 | d | 3H, $C^{5'}$-$CH_3$ EPI |
| 3.3 | s | 3H, $CH_3$-O PEG |
| 3.3-3.8 | s | -$CH_2$-$CH_2$-O PEG |
| 4.96 | t | 1H, $C^{10}$-H EPI |
| 7.4 | d | 1H, $C^{4}$-H EPI |
| 7.8 | t | 1H, $C^{3}$-H EPI |
| 13.2 | s | 1H, $C^{6}$-OH EPI |
| 14 | s | 1H, $C^{11}$-OH EPI |

*HPMA-GPLG-EPI*

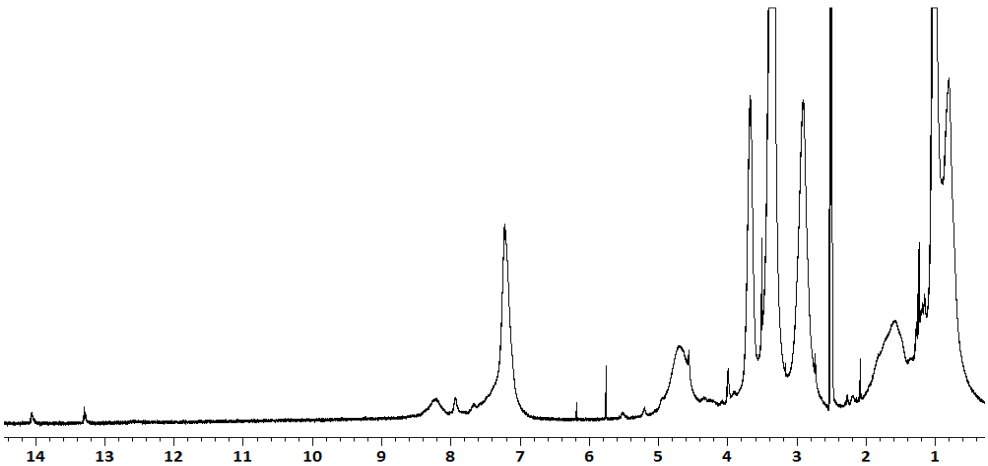


**Figure 5.5:** [1]H-NMR spectroscopy of HPMA-GPLG-EPI in $d_6$-DMSO

**Table 5.3:** principal signal $^{1}$H-NMR of HPMA-GPLG-EPI in $d_6$-DMSO

| δ(ppm) | Multiplicity | Assignment |
|---|---|---|
| 0,8-1 | d<br>q | 3H, $CH_3$-CH(R)-OH HPMA<br>1H, CH-$(CH_3)_2$ Leu HPMA |
| 1.45 | d | 2H, $CH_2$ Phe HPMA |
| 3.4 | s | 3H, $CH_3$-C(R')(R'')-$CH_2$- HPMA |
| 4.5-4.8 | m | 1H, $CH_3$-CH(R)-OH HPMA |
| 7.2 | s | 1H, $CH_3$-CH(R)-OH HPMA |
| 13.2 | s | 1H, $C^6$-OH EPI |
| 14 | s | 1H, $C^{11}$-OH EPI |

*HPMA-GG-EPI*

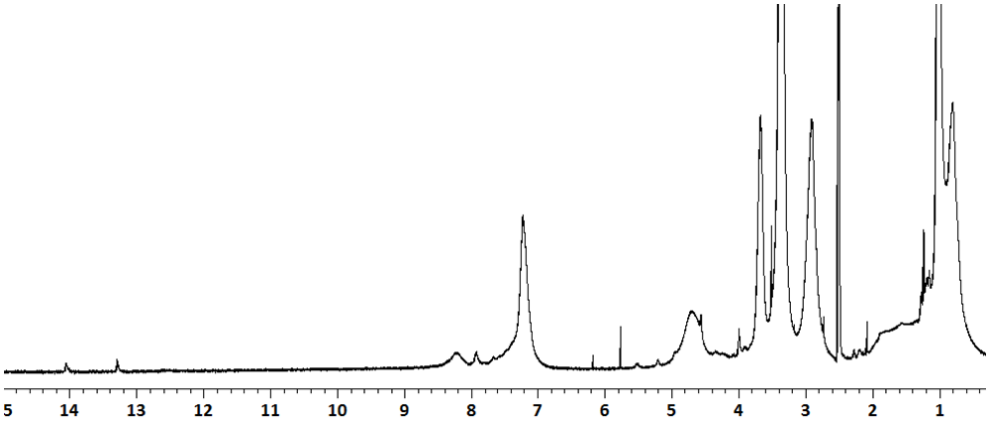


**Figure 5.6:** $^{1}$H-NMR spectroscopy of HPMA-GG-EPI in $d_6$-DMSO

**Table 5.4:** principal signal $^{1}$H-NMR of HPMA-GG-EPI in $d_6$-DMSO

| δ(ppm) | Multiplicity | Assignment |
|---|---|---|
| 0,8-1 | d | 3H, $CH_3$-CH(R)-OH HPMA |
| 3.4 | s | 3H, $CH_3$-C(R')(R'')-$CH_2$- HPMA |
| 4.5-4.8 | m | 1H, $CH_3$-CH(R)-OH HPMA |
| 7.2 | s | 1H, $CH_3$-CH(R)-OH HPMA |
| 13.2 | s | 1H, $C^6$-OH EPI |
| 14 | s | 1H, $C^{11}$-OH EPI |

$^{1}$H-NMR of PSA-EPI and PGA-EPI are not included as the conjugates were not soluble in DMSO while in water the signal of Epi are shielded.

## 5.1.2 CONJUGATES STUDIES

### 5.1.2.1 Conjugates *in vitro* stability in buffer, plasma and tritosomes

The stability of conjugates was measured in different conditions: buffers at pH 5 (to mimic lysosomal environment) and 7.4 (to mimic extracellular environment), mouse plasma and tritosome. All conjugates were stable at different pH and in plasma, with less than 2% (w/w) of EPI released after 48 h (Table 5.6). This confirmed that the chosen linkage ensured stability of the conjugate and was an appropriate choice to investigate the role of carrier in cell internalization.

**Table 5.6**: Conjugates stability in buffer solutions (pH 5 and 7.4) and il mause plasma after 48h

| Conjugates | EPI release (% total) | | |
|---|---|---|---|
| | pH 7.4 | pH 5 | Plasma |
| mPEG-EPI | 0.8 | 1.3 | 0.09 |
| HPMA-GPLG-EPI | 0.28 | 0.35 | 0.02 |
| HPMA-GG-EPI | 0.56 | 0.65 | 0.53 |
| PGA-EPI | 0.72 | 1.06 | 1.4 |
| PSA-EPI | 1.02 | 1.9 | 0.8 |

To complete the investigation on the stability of the conjugates, EPI release in presence of lysosomes extracts was explored. In this case, different behaviours were observed: HPMA-GPLG-EPI, as expected, and PSA-EPI displayed a time-dependent drug release (Fig. 5.8 **A**) with about 40% of EPI released in the first 5 hours and 80% and 45% EPI release within 48 h, respectively. Conversely, no or limited drug release was observed from PEG-EPI and HPMA-GG-EPI conjugates. A different pattern was observed for PGA-EPI. About 50% of the starting conjugate was degraded within 48 h (Fig. 5.8 **B**) but free EPI was not released during this incubation time. The lysosomal enzymes cleaved the PGA polymeric backbone, thus forming a range of PGA-EPI oligomers.

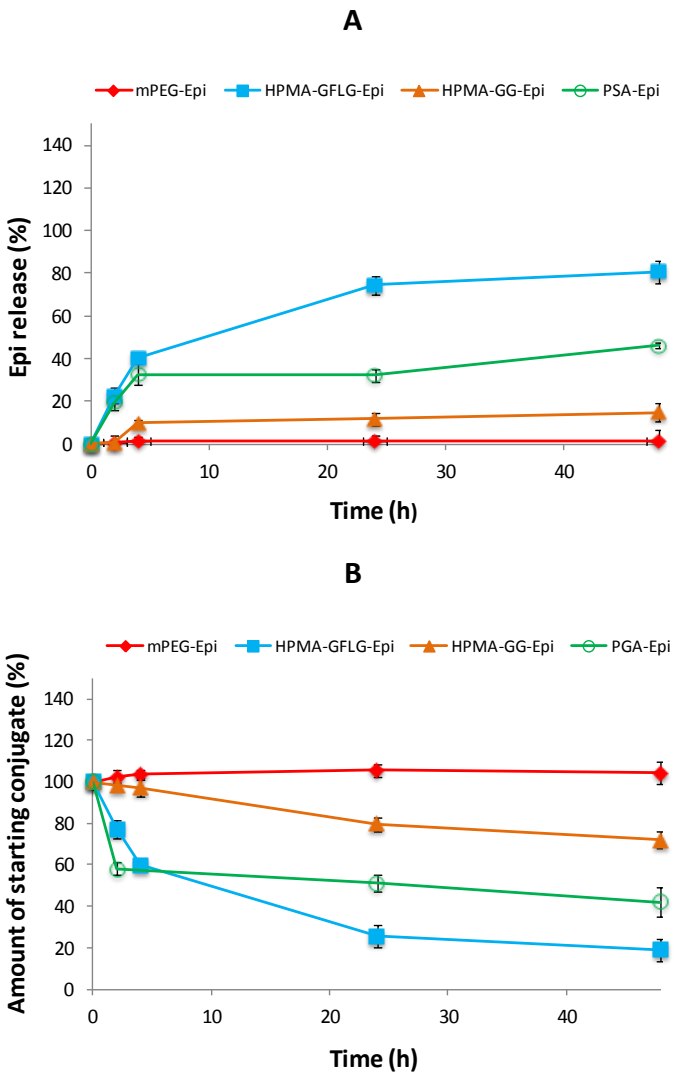


**Figure 5.8:** Drug release and conjugates stability after incubation with lysosomes. Percentages of free EPI release (**A**) and of starting conjugate remaining (**B**) are reported after incubation with lysosomes for up to 48 h. The profile for PGA-EPI is not reported in panel a as free EPI was always below the limit of detection. The profile for PSA-EPI is not reported in panel b, because the conjugate did not elute in RP-HPLC. Data represent mean ± SD, n=3.

## 5.1.3 CELLS STUDIES

### 5.1.3.1 Conjugates in vitro cytotoxicity in MCF-7 and MCF-7/DX cells

The cytotoxicity studies were conducted in MCF-7 and MCF-7/DX cells, where, MCF-7/DX cell line was characterized for the P-glycoprotein overexpression. It has been previously reported, in fact, that polymer-drug conjugates are able to by-pass certain

mechanisms of drug resistance in cancer chemotherapy [100] such as MDR1 (P-glycoprotein)-mediated multidrug-resistance.

In figure 5.9 a cell viability curve of EPI conjugates were reported.

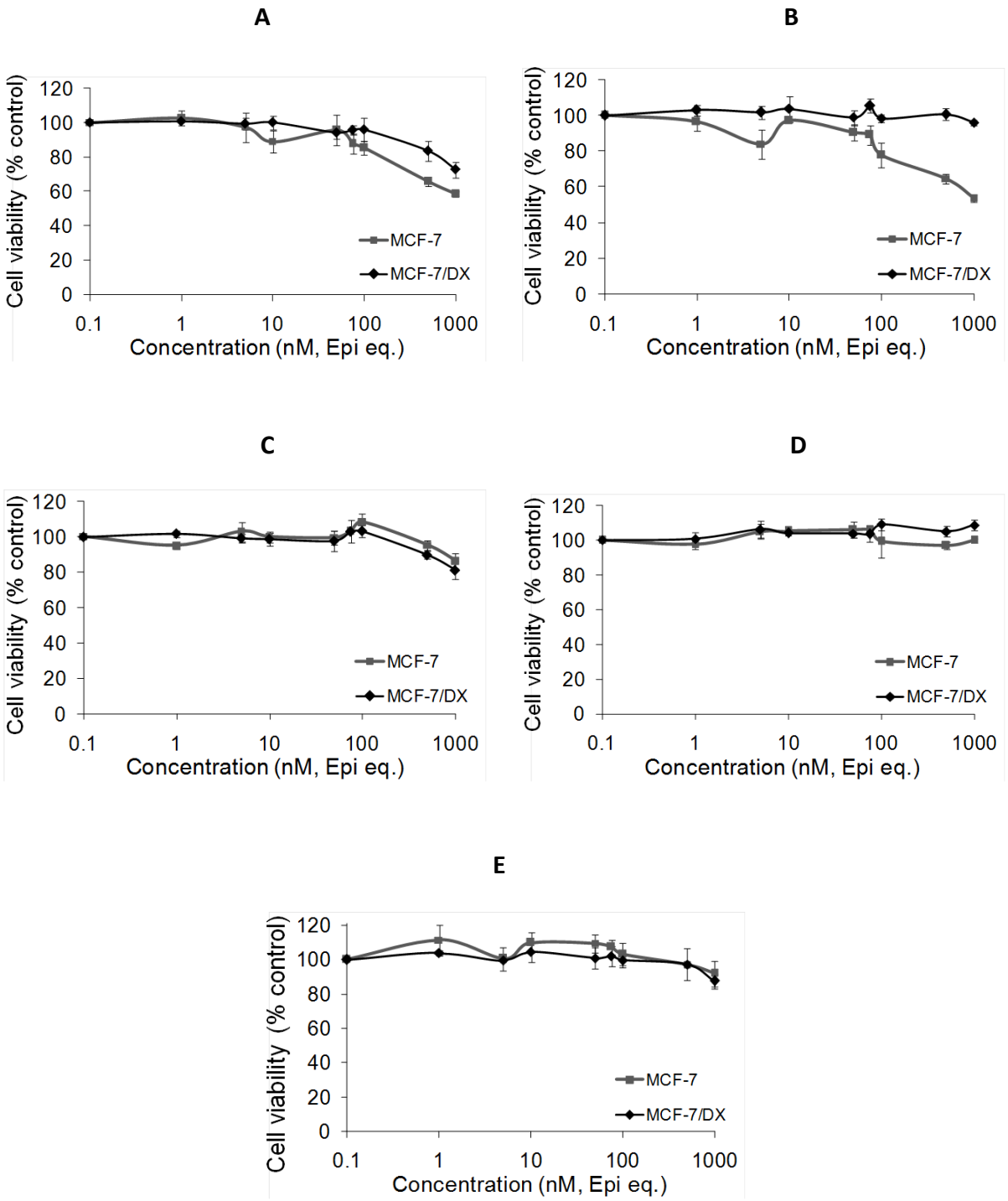


**Figure 5.9** : In vitro cytotoxicity of PSA-EPI (**A**), PGA-EPI (**B**), PEG-EPI (**C**), HPMA-GLPG-EPI (**D**) and HPMA-GG-EPI (**E**) in MCF-7 and MCF-7/Dx cells.

As can be seen from the figure reported above, all conjugates were relatively non-cytotoxic ($IC_{50}$ > 1μM), as expected for *in vitro* studies for this type of drug delivery technology [100] and for the chosen type of drug-polymer linkage. However, in the case of PGA and PSA, the two biodegradable polymers, a certain degree of cytotoxicity was observed (approx 40% reduction of viability at 1μM).

In MCF-7/DX cell, as expected, PEG-EPI, HPMA-GG-EPI, and HPMA-GPLG-EPI were inactive also against this cell line. Of the two conjugate based on biodegradable polymers, PGA-EPI was inactive, while PSA-EPI retained some activity (approx 30% reduction of viability at 1 μM). This is an important finding as it showed that the latter conjugate was still active in anthracycline-resistant cells. It also indirectly suggests that the cytotoxicity observed for this conjugates against MCF-7 cells cannot simply be attributed to the free EPI.

### 5.1.3.2 Cell uptake experiments

To investigate if the different toxicity profiles were due also to a different internalization mechanism, uptake studies were carried out in MCF-7 and MCF-7/DX cells. The experiment was conducted in both cell lines used for cytotoxicity studies, at 37°C and in presence or absence of endocytosis inhibitors (methyl-β-10 cyclodextrin for cholesterol-dependent, chlorpromazine for clathrin-dependent endocytosis and cytochalasin for macropinocytosis). The internalization was evaluated by flow cytometry exploiting the fluorescence characteristic of EPI. This was an advantage as fluorophores can affect cellular uptake and produce artefacts. In figure 5.10 the cell uptake graphics of all conjugates were reported.

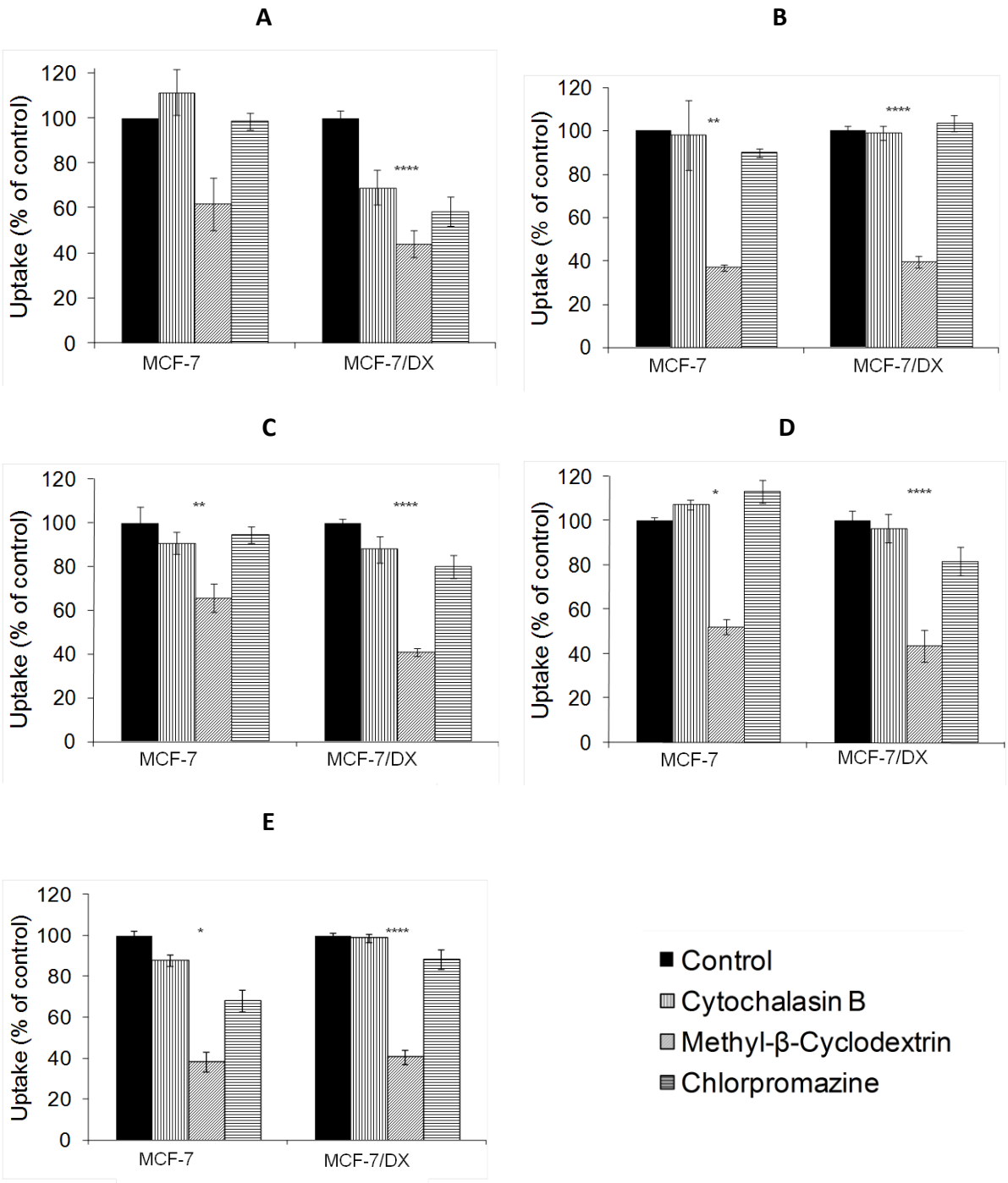


**Figure 5.10:** Uptake of PSA-EPI (**A**), PGA-EPI (**B**), mPEG-EPI (**C**), HPMA-GPLG-EPI (**D**) and HPMA-GG-EPI (**E**) by MCF-7 and MCF-7/Dx cell in presence of inhibitors of different endocytic pathway. Data rapresent mean ± SEM, n=3 (* $p<0.05$, ** $p<0.01$, **** $p<0.0001$).

As shown in figure 5.10, in both MCF-7 and MCF-7/DX cells the uptake of all conjugates was decreased by the presence of methyl-β-cyclodextrin, indicating that they all relied on cholesterol for uptake. By contrast, cytochalasin B and chlorpromazine did not affect in conjugates cell uptake. Taken together, these results suggest that all conjugates enter in the cells via a cholesterol-dependent, clathrin-independent endocytic route. As no differences in

the uptake mechanism were detected, it was considered unlikely that the mechanism of uptake was responsible for the different cytotoxicity observed. As reported in section 5.1.1, the polymers quenching the EPI fluorescence, so the direct comparison between the different conjugates fluorescence was inappropriate, as a comparison of normalised data. Here the assessment was restrict to series of each conjugates.

### 5.1.4 *IN VIVO* STUDIES

All animal procedures were approved by the Ethic Committee of University of Padua and communicated to the Italian Health Ministry. All animals received care according to the DLGS 116/92 and in compliance with the "Guide for the Care and Use of Laboratory Animals"

#### 5.1.4.1 Pharmacokinetics in mice

Pharmacokinetics studies have been conducted in 40 adult female Balb/c mice by injecting into tail vein a EPI or a EPI conjugates physiological solution. At predetermined time blood samples were withdrawn from the retro-orbital plexus/sinus of anesthetized animals. In figure 5.11, pharmacokinetic profiles of EPI and EPI conjugates are reported.

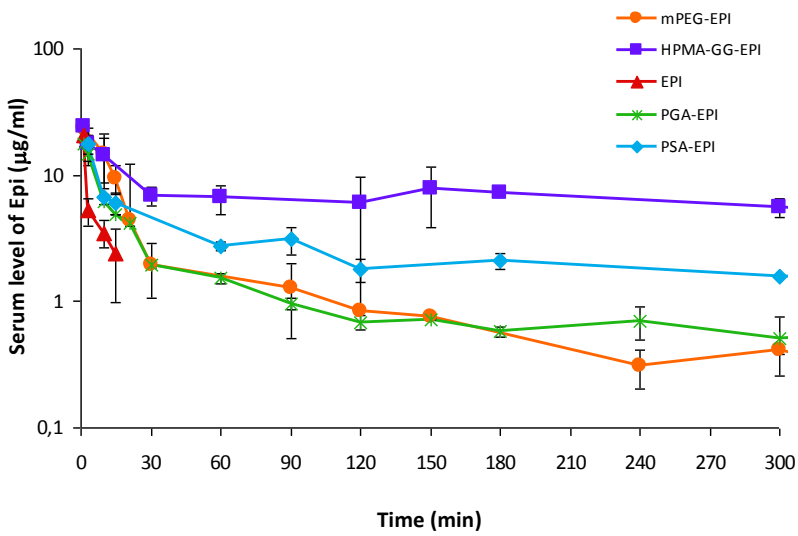


**Figure 5.11**: Pharmacokinetic profiles of EPI ad EPI conjugates in mice. Data represent mean ± SD, n=3

As expected, the plasma concentration of free EPI after injection of the free drug (control), decreased dramatically after 3 min, and at 30 min post injection the drug was not detectable. Conversely, all conjugates were detectable in serum at 5h, showing a marked prolongation of the drug pharmacokinetic.

The pharmacokinetics curves were describe as:

$$y = Ae^{-\alpha t} + Be^{-\beta t}$$

where:

- **A** represents the plasmatic concentration at $t_0$, obtained in presence of only distribution,
- **B** represents the plasmatic concentration at $t_0$, obtained in presence of only elimination,
- **(A+B)** represents the plasmatic concentration at the time where distribution and elimination were presents,
- **t** represents the time in minutes,
- **α** and **β** represents, respectively, the slopes of distribution and elimination line obtained from pharmacokinetics profiles.

With these elements, a pharmacokinetics parameter were calculated:

- **t½α** (half life of distribution) and **t½β** (half life of elimination), were calculated with the slope of distribution and elimination line with following formulas:

$$t½\alpha = -0.693/\alpha \qquad t½\beta = -0.693/\beta$$

- The area under concentration curve *versus* time (**AUC**) measures the unchanged drug amount that reaches the systemic circulation after administration of dose. This is calculated using the following equations:

$$AUC_{(0\rightarrow t)} = {}_0\int^t C_{(t)}\,dt = {}_0\int^t C_{(0)E} \cdot e^{-KE\cdot t}\,dt = {}_0\int^t B \cdot e^{\beta t}\,dt$$

$$AUC_{(t\rightarrow\infty)} = C_{(t)}/K_E = C_{(t)}/-\beta$$

$$AUC_{(0\rightarrow\infty)} = AUC_{(0\rightarrow t)} + AUC_{(t\rightarrow\infty)}$$

- The clearence (**Cl**) indicates the plasma volume that is purified from drug over time. It is a parameter that describe the patient's ability to eliminate the drug. Is calculates as the ratio of administered drug and the AUC with the equation:

$$\mathbf{Cl = D / AUC \quad or \quad Cl = 0.693\ V_d / t½ = K_E \cdot V_d}$$

- The distribution volume ($\mathbf{V_d}$), finally, describes the drug amount in the body respect to the plasma concentration. Is useful to describe the distribution. The $V_d$ is high for drug with a high tissue concentration respect to plasma concentration and vice versa. Is calculated as following:

$$\mathbf{V_d = D / C_{(0)E} \quad or \quad V_d = Cl / -\beta = Cl / K_E}$$

The principal pharmacokinetic parameter for EPI and EPI conjugates were reported in table 5.7.

**Table 5.7:** Pharmacokinetic parameters of EPI ad EPI conjugates

| Conjugates | T½α (min) | T½β (min) | $V_d$ (mL) | $AUC_{0-\infty}$ (μg·min/ml) | Clereance (mL/min) |
|---|---|---|---|---|---|
| EPI | 1.1 | 8.4 | 33.6 | 83.3 | 2.8 |
| mPEG-EPI | 13.3 | 102.5 | 99.6 | 340.9 | 0.7 |
| HPMA-GG-EPI | 9.8 | 288.9 | 51.8 | 1852.4 | 0.1 |
| PGA-EPI | 10 | 169.9 | 147.2 | 385.8 | 0.6 |
| PSA-EPI | 7.7 | 283.9 | 71.4 | 1317.3 | 0.2 |

## 5.2 POLY(ETHYLENE GLYCOL)-BASED CONJUGATE OF PACLITAXEL AND ALENDRONATE

### 5.2.1 SYNTHESIS AND CHARACTERIZATION OF PTX-PEG, PEG-ALN AND PTX-PEG-ALN CONJUGATES

The synthesis of PTX-PEG conjugates was performed in 3 steps:

- Synthesis of 2'-succinyl-paclitaxel (SPTX);
- Synthesis of PEG-dendrimer;
- Binding of SPTX to PEG-dendrimer.

#### 5.2.1.1 Synthesis of 2'-succinyl-paclitaxel (SPTX)

PTX was derivatized by succinic anhydride in order to obtained 2'-succinyl-paclitaxel (SPTX). SPTX was purified by silica gel and then characterized by RP-HPLC (Fig. 5.12), UV-VIS spectrometry (Fig. 5.13) and $^{1}$H-NMR (Fig. 5.14 and Table 5.8), to determine purify and the success of reaction (the coupling reaction conversion was 58%).

*RP-HPLC characterization:*

SPTX was characterized by reverse phase chromatography to determine its purify. As showed in figure 5.12, the SPTX retention time ($t_R$= 19.4 min) was different from free PTX ($t_R$=20.2 min), indicating a good purification of product (free PTX is not detectable).

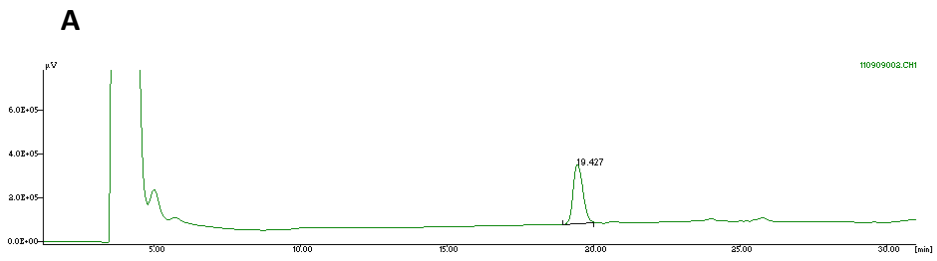

**B**

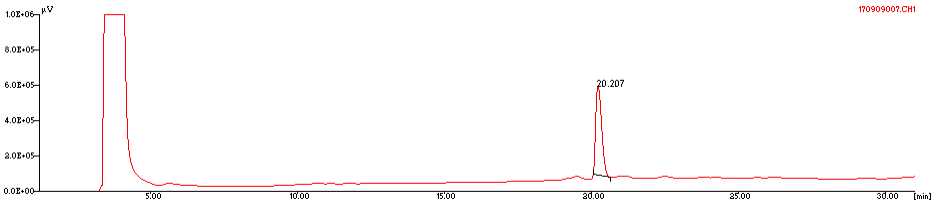


**Figure 5.12:** Cromatography characterization of SPTX (a) and PTX (b). The analysis were performed by RP-HPLC (experimental condition reported in section 4.4).

*UV-VIS spectrometry characterization:*

SPTX was characterized and compared with PTX by UV-VIS spectroscopy.

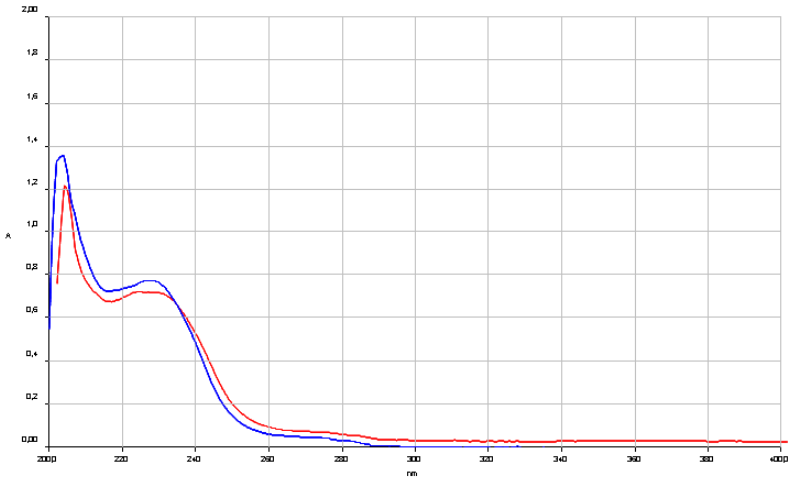


**Figure 5.13 :** UV-VIS spectrum of PTX (—) and SPTX (—) performed in $CH_3OH$.

As showed in figure 5.13 , SPTX spectrum (blue) is superimposable to PTX spectrum (red), indicating that the PTX modification with a spacer did not compromise the physic-chemical characteristic of the drug.

*[1]H-NMR spectroscopy characterization:*

The [1]H-NMR spectroscopy characterization allowed the confirmation to confirm that the reaction between PTX and succinic anhydride occurred in the experimental condition used.

In figure 5.14, PTX (**A**) and SPTX (**B**) spectra were reported, while in table 5.8 , the principal [1]H signals of SPTX were reported.

SPTX spectrum showed the presence of a signal at 2.5-2.7 ppm relative to the -$CH_2$-$CH_2$- of succinic spacer and the characteristic signals of PTX.

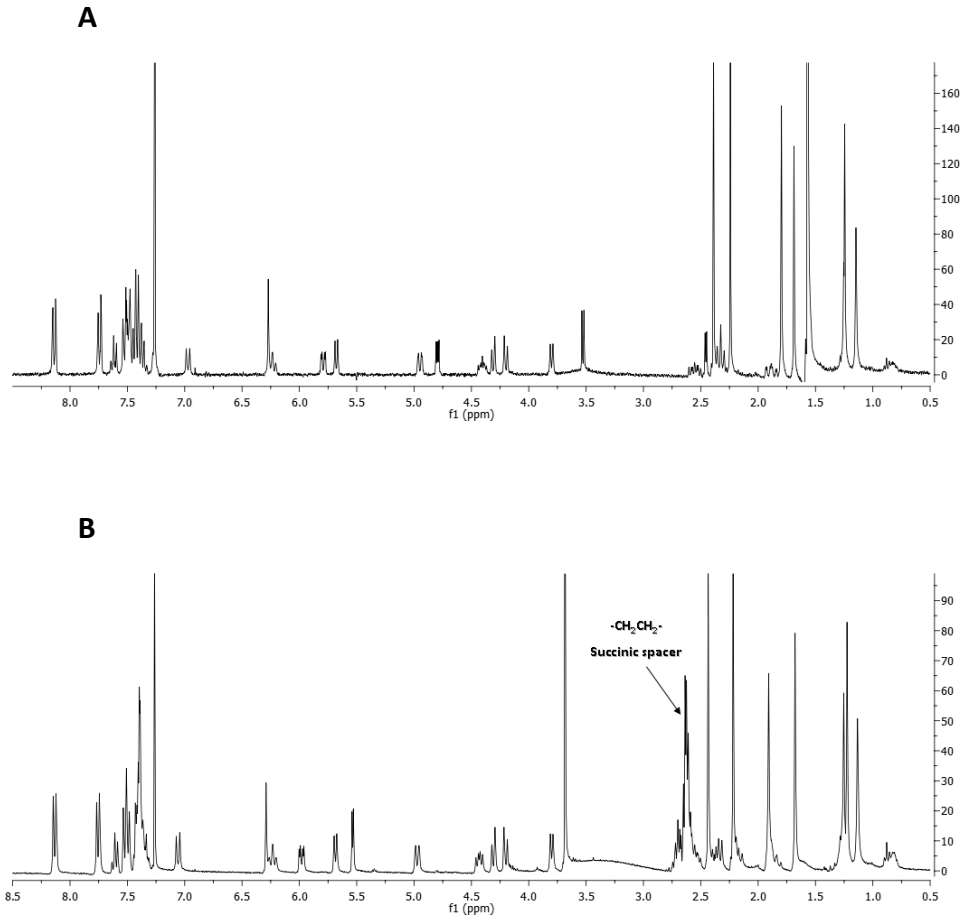


**Figure 5.14** : [1]H-NMR spectroscopy of PTX (**A**) and 2'-succinyl-paclitaxel (**B**) in $CDCl_3$

**Table 5.8:** principal signal $^{1}$H-NMR of 2'-succinyl-paclitaxel

| δ(ppm) | Multiplicity | Assignment |
|---|---|---|
| 1.15 | s | 3H, $C^{16}$ |
| 1.24 | s | 3H, $C^{17}$ |
| 1.68 | s | 3H, $C^{18}$ |
| 1.79 | s | 3H, $C^{19}$ |
| 2.24 | s | 3H, $C^{31}$ |
| 2.38 | s | 3H, $C^{29}$ |
| 2.5-2.7 | m | 4H, $-CH_2-CH_2-$ succinic anhydride |
| 4.9 | d | 1H, $C^{5}$ |
| 5.66 | d | 1H, $C^{2'}$ |
| 6.27 | s | 1H, $C^{10}$ |
| 7.25 | s | 3'-Ph |
| 7.4 | m | 3'-NBz |
| 7.5 | m | 2-OBz |
| 7.75 | d | 3'NBz |
| 8.1 | d | 2-OBz |

### 5.2.1.2 Synthesis of PEG-dendrimer

The PEG-dendrimer (Boc-PEG-β-Glu-$(β\text{-Glu})_2$-$(COOH)_4$) was built starting from commercial Boc-PEG-NHS (MW 5000 Da), using β-Glutamic acid as symmetric bicarboxylic branching unit. To the PEG dendrimer with four carboxylic groups at the end chain, alendronate, used as targeting residues, was coupled yielding Boc-PEG-β-Glu-$(β\text{-Glu})_2$-$(ALN)_4$. The loading of ALN in the conjugate was 11.9% w/w.

### 5.2.1.3 Binding of SPTX to PEG-dendrimer

The SPTX coupling to PEG-dendrimer (with and without ALN) occurred by formation of an amide bond between the activated carboxylic group of SPTX and the amino group of PEG-dendrimer, after boc removed. The final products, PTX-PEG-β-Glu-$(β\text{-Glu})_2$-$(COOH)_4$ (PTX-PEG) and PTX-PEG-β-Glu-$(β\text{-Glu})_2$-$(ALN)_4$ (PTX-PEG-ALN), were purified from excess of SPTX

by gel filtration and then characterized in RP-HPLC (Fig. 5.15), UV-VIS spectrometry (Fig. 5.16) and $^{1}$H-NMR (Fig. 5.17 and Table 5.9).

The total drug amount (free and bond) was determinate after basic hydrolysis of a solution of the conjugates (Table 5.11 section 5.2.3).

*RP-HPLC characterization:*

PTX-PEG-β-Glu-(β-Glu)$_2$-(COOH)$_4$ and PTX-PEG-β-Glu-(β-Glu)$_2$-(ALN)$_4$ were characterized by reverse phase chromatography to determine their purity. As showed in figure 5.15, the conjugates retention times ($t_R$= 22.4 min for PTX-PEG and $t_R$= 18.3 min for PTX-PEG-ALN) were different from free PTX ($t_R$= 20 min), indicating a good purification of product (free PTX < 0.6% w/w).

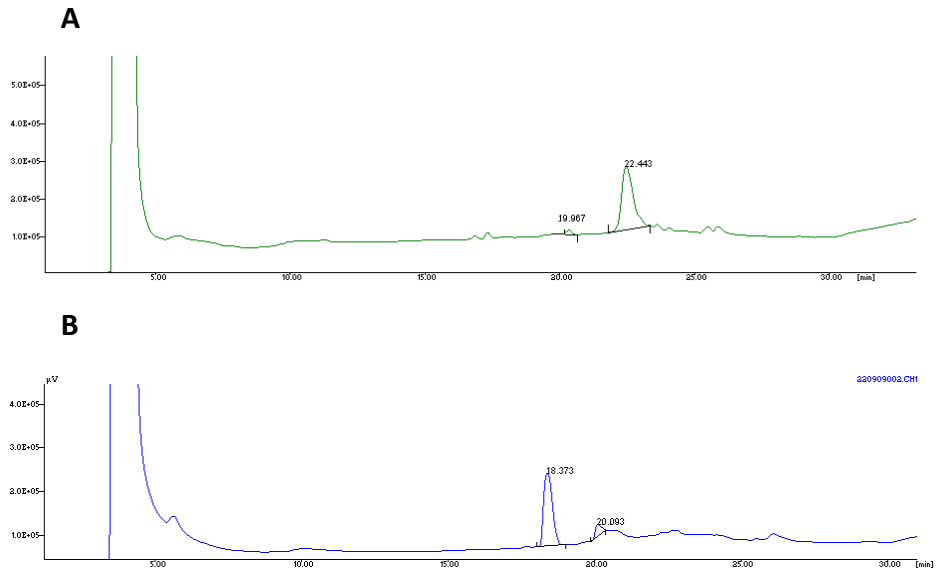


**Figure 5.15:** Cromatography characterization of PTX-PEG (**A**) and PTX-PEG-ALN (**B**). The analysis were performed by RP-HPLC (experimental condition reported in section 4.4).

*UV-VIS spectrometry characterization:*

PTX-PEG and PTX-PEG-ALN were characterized and compared to PTX by UV-VIS spectroscopy.

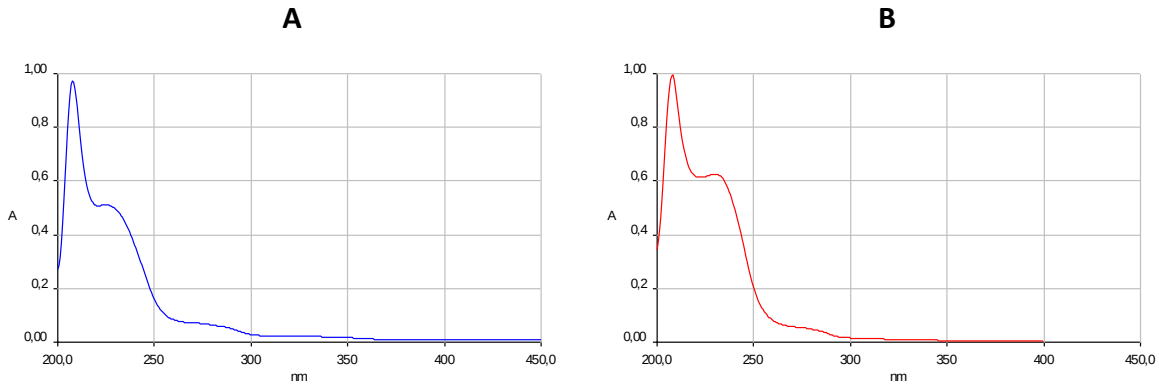


**Figure 5.16** : UV-VIS spectrum of PTX-PEG (**A**) and PTX-PEG-ALN (**B**) performed in $CH_3OH$.

As showed in figure 5.16 , PTX conjugates (PTX-PEG panel A and PTX-PEG-ALN panel B) presented the same characteristic spectrum of free drug (already reported in figure 5.13).

*$^1$H-NMR spectroscopy characterization:*

The $^1$H-NMR spectroscopy characterization allowed the confirmation that the reaction between SPTX and PEG-dendrimer occurred in the experimental conditions used.

As example, in figure 5.17 a PTX-PEG-ALN spectrum was reported, while in table 5.9, the principal $^1$H signals of PTX-PEG-ALN were reported.

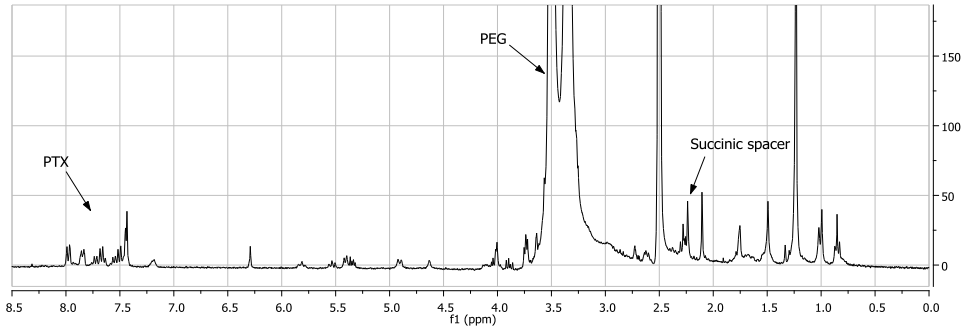


**Figure 5.17** : $^1$H-NMR spectroscopy of PTX-PEG-ALN in $d_6$-DMSO

**Table 5.9:** principal signal $^{1}$H-NMR of PTX-PEG-ALN

| δ(ppm) | Multiplicity | Assignment |
|---|---|---|
| 2.1 | s | 3H, $C^{29}$ PTX |
| 2.2-2.3 | m | 4H, -$CH_2$-$CH_2$- succinic anhydride |
| 3.4-3.6 | s | -$CH_2$-$CH_2$-O PEG |
| 4.9 | d | 1H, $C^{5}$ PTX |
| 6.27 | s | 1H, $C^{10}$ PTX |
| 7.25 | s | 3'-Ph PTX |
| 7.4 | m | 3'-NBz PTX |
| 7.5 | m | 2-OBz PTX |
| 7.75 | d | 3'NBz PTX |
| 8.1 | d | 2-OBz PTX |

As showed in figure reported above, in the PTX-PEG-ALN spectrum there are signals of both PEG-dendrimer and SPTX.

## 5.2.2 SYNTHESIS AND CHARACTERIZATION OF FITC LABELED PTX-PEG, PEG-ALN AND PTX-PEG-ALN CONJUGATES

For the synthesis of FITC labelled conjugates, BOC-NH-PEG-L-Lys(εFMOC)-OH was synthesized and used as starting polymer. The ε amino group of lysine was exploited for the coupling with FITC.

BOC-NH-PEG-L-Lys(εFMOC)-OH was obtained by forming an amide bond between activated carboxylic group of PEG and amino group of L-Lys(εFMOC)-OH. The occurred reaction was confirmed by $^{1}$H-NMR spectroscopy (Fig. 5.18 and table 5.10).

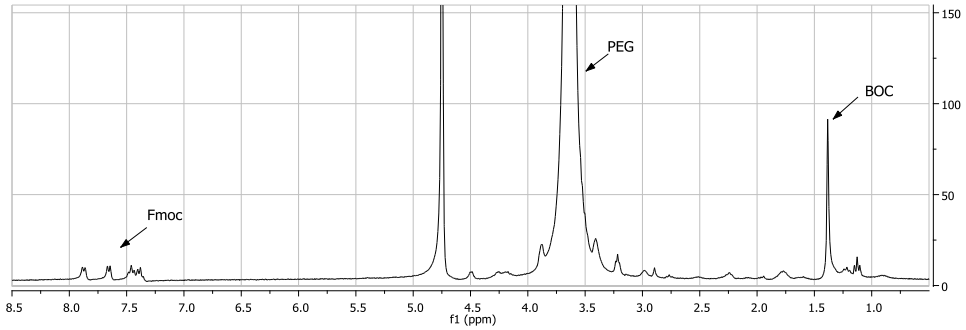


**Figure 5.18**: $^{1}$H-NMR spectroscopy of BOC-NH-PEG-L-Lys(εFMOC)-OH in $d_6$-DMSO

**Table 5.10:** principal signal $^{1}$H-NMR of BOC-NH-PEG-L-Lys(εFMOC)-OH

| δ(ppm) | Multiplicity | Assignment |
|---|---|---|
| 1.3 | s | 9H, -$(CH_3)_3$ BOC |
| 3.4-3.6 | s | 422H, -$CH_2$-$CH_2$-O PEG |
| 7.2-7.5 | m | 8H, FMOC group |
| 7.7 | d | 4H, FMOC group |
| 7.9 | d | 4H, FMOC group |

The yield of linkage of L-Lys to the PEG was calculated attributing to the peak at δ= 1.2 ppm, relative to the Boc group of PEG, the value of 9. The integral value of peaks at δ=7.2-7.5, 7.7 and 7.9, relative to the FMOC group of Lys, were respectively of 4.2, 1.7 and 1.9 indicating a yield of 49%.

Subsequently, starting from Boc-NH-PEG-L-Lys(εFMOC)-OH, a PEG-dendrimer was built as above reported. When Boc-NH-PEG-L-Lys(εFMOC)-β-Glu-$(β\text{-Glu})_2$-$(COOH)_4$ was obtained, the FMOC group was removed in basic environment, and then the FITC was coupled. Boc-NH-PEG-L-Lys(εFITC)-β-Glu-$(β\text{-Glu})_2$-$(COOH)_4$ was obtained by reaction between fluorescein isothiocyanate and the amino group of Lys conjugated to PEG. The product was purified by dialysis and then characterized in RP-HPLC and in UV-VIS spectrometry to determine the FITC amount in the conjugate.

*RP-HPLC characterization*

Boc-NH-PEG-L-Lys(εFITC)-β-Glu-$(β\text{-Glu})_2$-$(COOH)_4$ was characterized by reverse phase chromatography to determine its purify. As showed in figure 5.19, the conjugates retention time ($t_R$= 18 min) was different from free FITC ($t_R$= 23 min), indicating a good purification of the product.

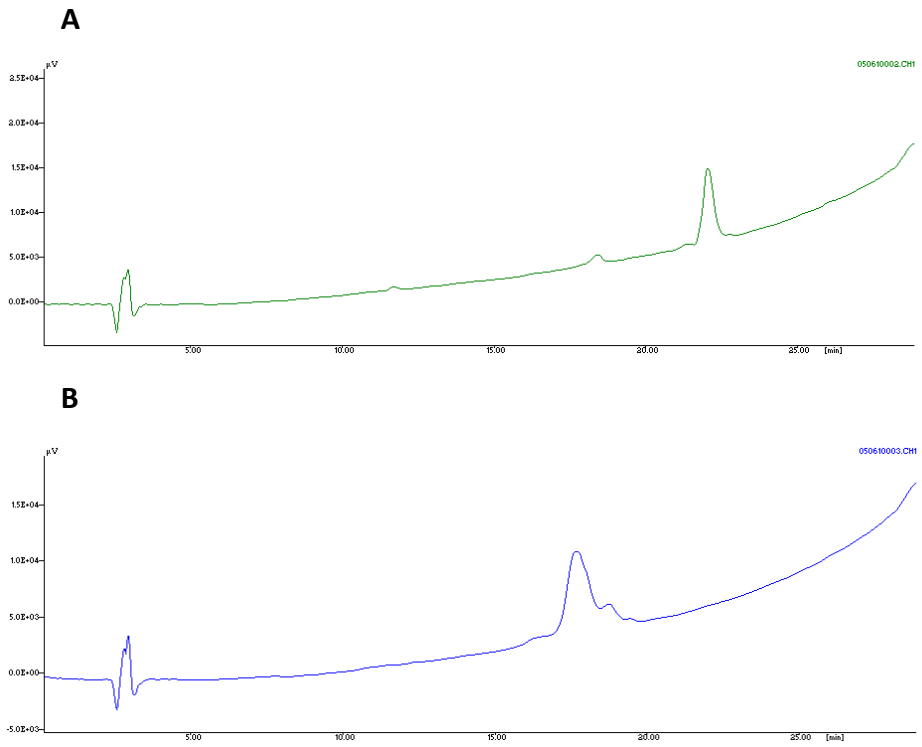


**Figure 5.19:** Cromatography characterization of FITC (**A**) and Boc-NH-PEG-L-Lys(εFITC)-β-Glu-$(β\text{-Glu})_2$-$(COOH)_4$ (**B**). The analysis were performed by RP-HPLC (experimental condition reported in section 4.3.1.4).

*UV-VIS spectrometry characterization*

The content of FITC in the conjugate was measured spectrophotometrically using ε 64185 $M^{-1}$ $cm^{-1}$ in PBS pH 8 (Fig. 5.20). The amount of FITC was of 3.3% w/w (yield of linkage: 51%, corresponding to the % of Lys linked to PEG).

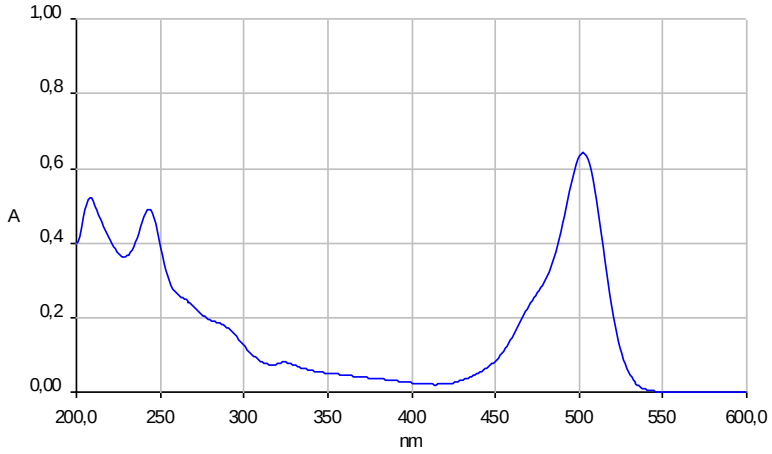


**Figure 5.20:** UV-VIS spectrum of BOC-NH-PEG-L-Lys(εFITC)-β-Glu-(β-Glu)$_2$-(COOH)$_4$ performed in PBS pH 8.

After FITC conjugation, the synthesis of PEG-dendrimer was completed with the addition of ALN to the four carboxylic groups of PEG, as already reported for non-labelled conjugates. Subsequently, t-Boc was removed and PTX was conjugate with the same procedure showed for non-labelled conjugates.

The total drug amount (free and bond) was determinate after basic hydrolysis of a solution of conjugates (Table 5.11 section 5.2.3).

## 5.2.3 DETERMINATION OF FREE AND TOTAL PTX CONTENT IN THE CONJUGATES

The total drug amount (free and bond) was determinate in RP-HPLC after basic hydrolysis of a solution of conjugates. The summary table of PTX content in the conjugates was beloved reported.

**Table 5.11:** Total and free PTX content in the polymer conjugates

| Conjugates | Total PTX content (%wt/wt) | Free PTX content (%wt/wt total drug) |
|---|---|---|
| PTX-PEG | 7.29 | 0.42 |
| PTX-PEG-ALN | 5.95 | 0.6 |
| PTX-PEG-FITC | 3.6 | 0.39 |
| PTX-PEG-ALN-FITC | 4.26 | 0.65 |

## 5.2.4 CONJUGATES STUDIES

### 5.2.4.1 Conjugates stability in buffer solution at different pH values and in plasma

The stability of PTX-PEG and PTX-PEG-ALN were evaluated in buffer solutions at physiological pH (7.4), at lysosomal pH (pH 5), and in mice plasma (Fig. 5.22). Samples were taken at the indicated time points and analyzed by RP-HPLC.

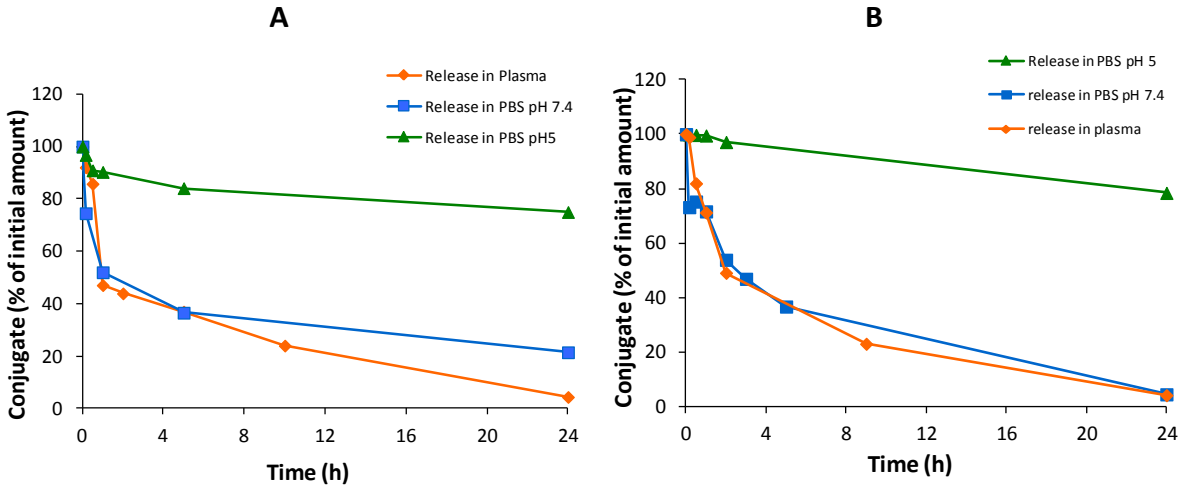


**Figure 5.22**: Stability of PTX-PEG-ALN (**A**) and PTX-PEG (B) in PBS pH 5, 7.4 and in plasma.

As showed in figure 5.22, at pH 7.4 and in plasma, about 50% of the PTX-PEG-ALN conjugate was degraded within the first 1 h, the remaining conjugate was degraded within 24 h. At pH 5, instead, the conjugate result more stable; after 24 h only 20% of conjugate was degraded. Similar results were found with PTX-PEG.

### 5.2.4.2 Dynamic light scattering of conjugates

The hydrodynamic diameter and size distribution of PTX-PEG-ALN and of PTX-PEG conjugates were evaluated using laser light scattering microscopy with nanoparticle tracking analysis (NTA) technology (NanoSight LM20, Salisbury, UK).

The mean hydrodynamic diameter of both PTX-PEG-ALN and of PTX-PEG conjugates in PBS pH 7.4 was ~190 nm (Fig. 5.21).

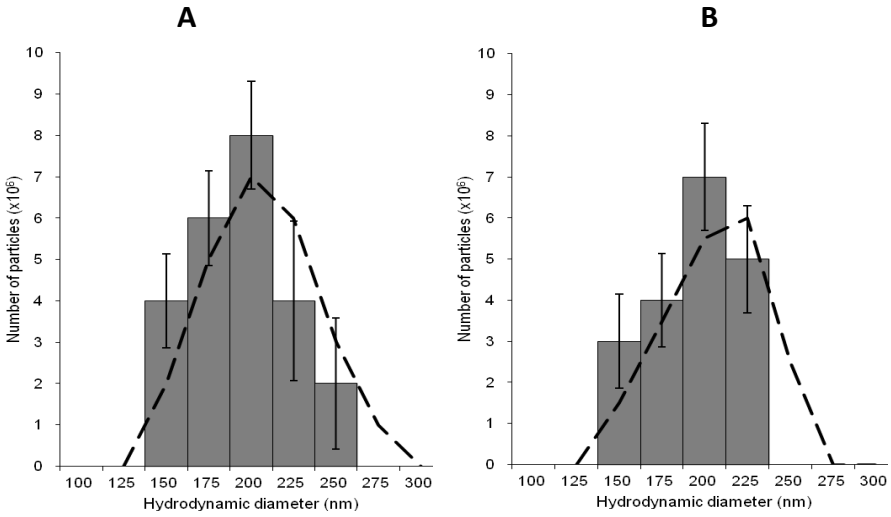


**Figure 5.21:** Mean hydrodynamic diameter and size distribution of PTX-PEG (**A**) and PTX-PEG-ALN (**B**)

### 5.2.4.3 Stability of polymeric structures in buffer solutions at different pH values

Conjugates were incubated in buffers at pH 5 and pH 7.4 at 37°C, immediately extruded at 200 nm and analyzed using DLS (Malvern Nano-S). The size of the micelles was monitored over time (Fig. 5.23).

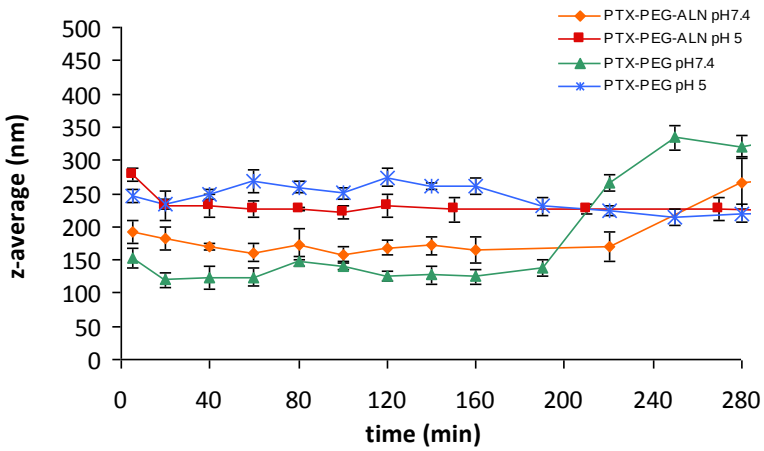


**Figure 5.23:** PTX-PEG and PTX-PEG-ALN structure stability in buffer solution at pH 5 and 7.4 at 37°C.

As showed in figure reported above, the stability of the conjugates micelles, monitored at 37 °C for 24 h by DLS, was in line with the kinetics of PTX release. At acidic pH the micelles

were stable for up to 24 h, whereas after 3 h at pH 7.4 the size of the samples start to increase owing to the release of PTX from the conjugates, which is insoluble in the aqueous buffer and precipitates, forming a suspension and destabilising the system.

### 5.2.4.4 Hydroxyapatite binding assay

The binding capacity of PTX-PEG-ALN and PEG-ALN conjugates to bone mineral through ALN was evaluated. Hydroxyapatite (HA) was used as a model mineral mimicking bone tissue. The conjugates were incubated with the bone mineral HA for 0, 2, 5, 10 and 60 min. Samples were taken at the indicated time points and analyzed. An *in vitro* HA binding assay and FPLC analysis using a HiTrap desalting column was performed. Following 5 min of incubation, 80% or 90% of PTX-PEG-ALN or PEG-ALN conjugates, respectively, were bound to HA and reached a plateau (Fig. 5.24).

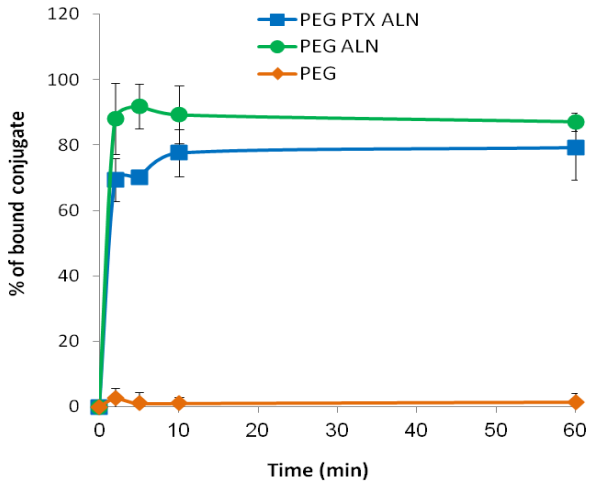


**Figure 5.24:** Binding Kinetics of PEG-ALN and PTX-PEG-ALN conjugates to the bone mineral HA

### 5.2.4.5 Red blood cell (RBC) lysis assay

The biocompatibility of PTX-PEG-ALN was evaluated using rat red blood cell (RBC) hemolysis assay [102]. Rat RBC solution was incubated with serial concentrations of the combination of PTX and ALN, PEG, or PTX-PEG-ALN conjugate at equivalent PTX and ALN

concentrations, PTX vehicle (1:1:8 ethanol/Cremophor EL/saline), and poly(ethylene imine) (PEI) which served as control for hemolysis [103].

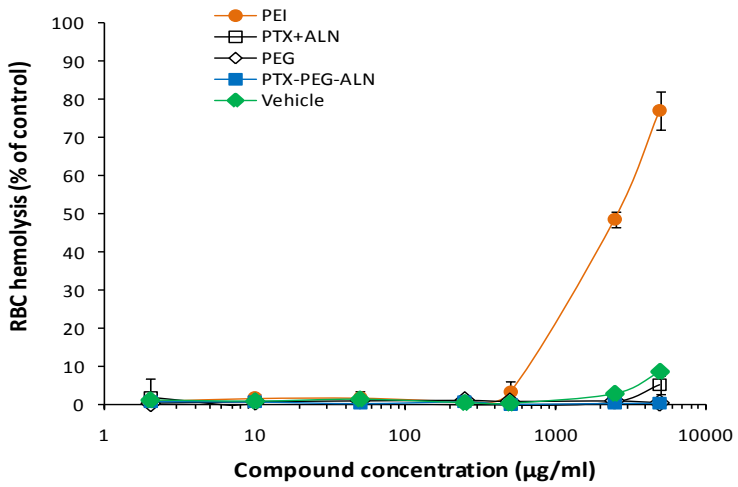


**Figure 5.25:** Biocompatibility of PTX, ALN, PTX-PEG-ALN, PEG, PEI and PTX Vehicle in RBC. Results are presented as % of haemoglobin release produced by different compounds ± SEM.

As shown in figure 5.25, PTX-PEG-ALN conjugate did not exhibit detectable RBC hemolysis at all concentrations up to 5 mg/mL (the estimated blood concentration after *in vivo* administrations is about 0.5 mg/mL). PTX vehicle cytotoxicity is known on normal nonproliferating cells [101] and indeed, a slight RBC hemolysis of ~8% was observed in RBCs incubated with PTX vehicle. About 5% hemolysis was observed in RBCs incubated with the combination of PTX plus ALN at the highest equivalent to the conjugate concentration of 5 mg/mL. This hemolysis observed is probably caused by the Cremophor EL vehicle in which these drugs were dissolved.

## 5.2.5 CELL STUDIES

### 5.2.5.1 Cell toxicity assay

To evaluate whether PTX retained its cytotoxic activity following conjugation with PEG polymer, a proliferation assay of 4T1, MDA-MB-231 and PC3 cells was performer. In figure 5.26 cells viability curves were reported.

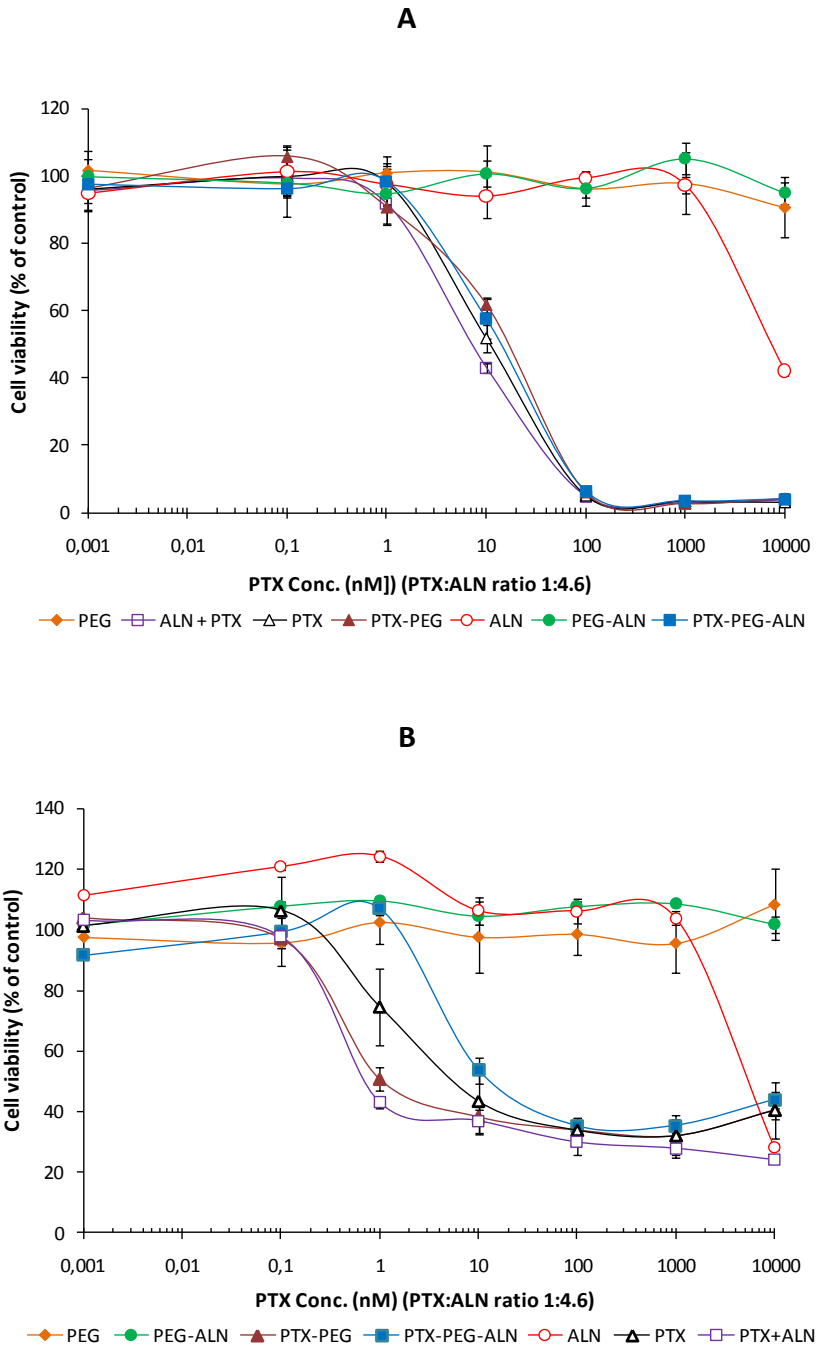

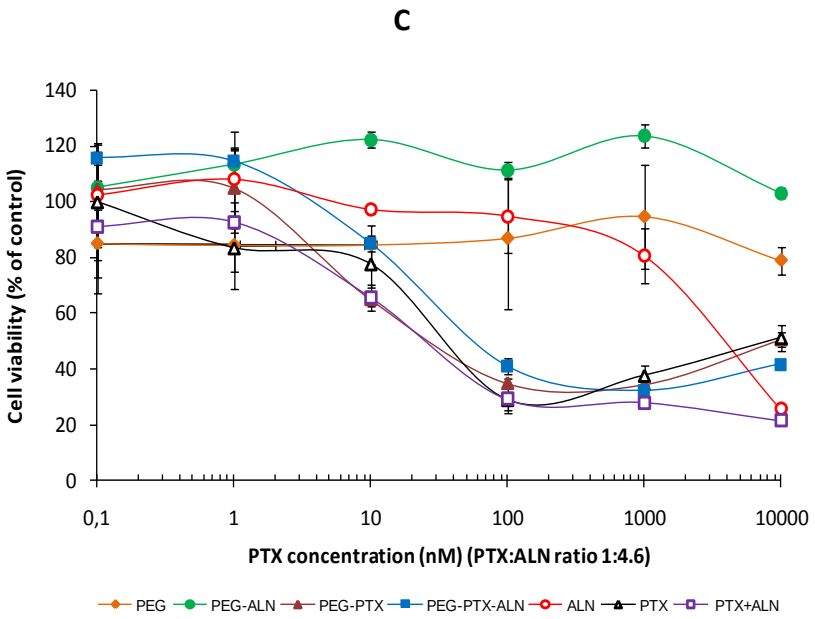


**Figure 5.26:** Cell toxycity assay in murine 4T1 mammary adenocarcinoma cells (A), human MDA-MB-231 mammary adenocarcinoma cells (**B**) and human PC3 prostate adenocarcinoma cells (**C**). Cells were incubated with PTX-PEG-ALN, PTX-PEG, and PEG-ALN conjugates, PEG, free PTX or ALN, and the combination of free PTX plus ALN at equivalent concentrations for 72 h. Data represent the mean ± SD (standard deviation). The X-axis is presented at a logarithmic scale

Cells proliferation was inhibited similarly by both PTX-PEG and PTX-PEG-ALN conjugates and by PTX and combination of free PTX plus ALN, exhibiting in 4T1 an $IC_{50}$ of ~25nM (Fig. 5.26 **A**), in MDA-MB-231 an $IC_{50}$ of 1-10nM (Fig. 5.26 **B**) and in PC3 an $IC_{50}$ of 25-60 nM (Fig. 5.26 **C**). In all cases, PEG-dendrimer served as the control and was nontoxic at any of the concentrations tested. ALN alone was found to be toxic only at the highest concentration tested of 10 µM; however, ALN bound to PEG at equivalent concentration was not toxic at any of the concentrations tested.

### 5.2.5.2 Inhibition of angiogenic cascade

In order to assess whether, similarly to PTX, PTX-PEG-ALN possesses anti-angiogenic properties, endothelial cell proliferation, capillary-like tube formation and migration assays were carried out using the conjugates. HUVEC were incubated with PEG, PTX-PEG, PEG-ALN, PTX-PEG-ALN conjugates, and with free PTX and ALN alone and combined. The proliferation of HUVEC was inhibited similarly by the combination of free PTX plus ALN and by PTX-PEG

and PTX-PEG-ALN conjugates at PTX-ALN-equivalent concentrations exhibiting an $IC_{50}$ of ~3 nM (Fig. 5.27).

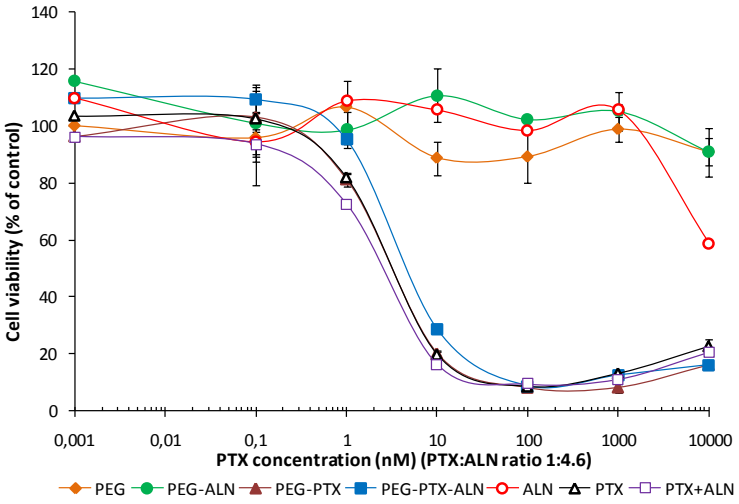


**Figure 5.27:** Cell toxicity assay in human umbilical vein endothelial cell (HUVEC). HUVEC cells were incubated with PTX-PEG-ALN, PTX-PEG, and PEG-ALN conjugates, PEG, free PTX or ALN, and the combination of free PTX plus ALN at equivalent concentrations for 72 h. Data represent the mean ± SD (standard deviation). The X-axis is presented at a logarithmic scale.

Next, the effect of PTX-PEG and PTX-PEG-ALN on the ability of HUVEC to migrate towards VEGF was tested. HUVEC were incubated with each free PTX (100 nM) or ALN (460 nM), the combination of the free drugs, and with PEG conjugates at equivalent concentrations for 6 h. The migration of HUVEC incubated with both PTX-PEG and PTX-PEG-ALN conjugates and the combination of free PTX plus ALN towards VEGF was inhibited by ~80% (Fig. 5.28).

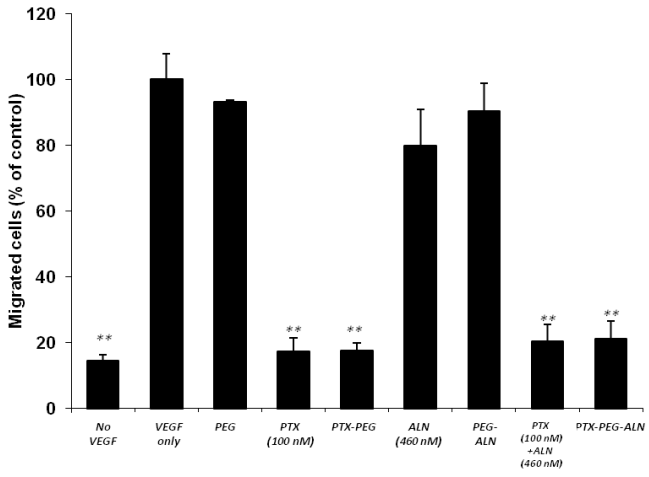


**Figure 5.28:** Migration assay in HUVEC. PTX-PEG-ALN and PTX-PEG conjugates inhibit the migration of HUVEC towards the chemoattractant VEGF. Migration was normalized to percent migration with 100% representing migration to VEGF alone.

As shown, free and conjugated PTX-ALN possess anti-angiogenic potential by inhibiting the proliferation and migration of HUVEC. The effect of these drugs on the ability of HUVEC to form capillary-like tube structures on Matrigel was examined (Fig. 5.29). Following 8 h incubation, the combination of 5 nM PTX plus 23 nM ALN inhibited the formation of tubular structures of HUVEC by ~50%. Both PTX-PEG and PTX-PEG-ALN conjugates at equivalent concentrations inhibited the formation of tubular structures of HUVEC by ~60%. (Fig. 29 **B**). The indicated treatments concentrations of both migration and capillary tube formation assays on HUVEC were tested and found as non-cytotoxic at the indicated incubation times, but rather specifically inhibited the ability to migrate and form capillary-like tubes.

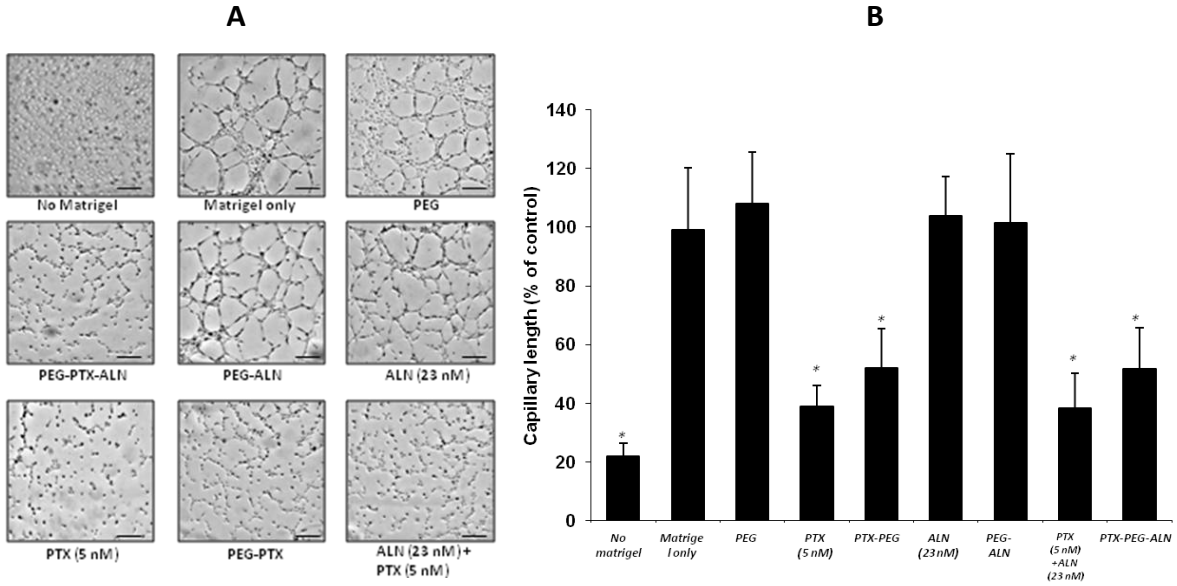


**Figure 5.29**: Capillary like-tube formation assay. PTX-PEG-ALN and PTX-PEG conjugates inhibit the ability of HUVEC to form capillary-like tube structures. (**A**) Representative images of capillary-like tube structures of HUVEC seeded on Matrigel following treatment (scale bar represents 100 µm). (**B**) Quantitative analysis of the mean length of the tubes. Data represents mean ± SD.

## 5.2.6 *IN VIVO* STUDIES

### 5.2.6.1 Tumor accumulation and body distribution

Noninvasive fluorescence imaging technology was utilized to monitor the real-time distribution, excretion, and tumor accumulation of FITC-labeled PEG, PTX-PEG, PEG-ALN and PTX-PEG-ALN conjugates. Mice bearing MDA-MB-231-mCherry breast cancer tumors in the tibia were injected *i.v.* with FITC-labeled conjugates. Immediately following conjugates administration, mice became entirely fluorescent. A semi-quantitative time-dependent tumor/background contrast profile was derived from the average fluorescence intensities of equal areas within tumor and normal skin regions. FITC labeled conjugates accumulated gradually and preferentially at tumor sites (Fig. 5.30 **A**). This preferred tumor accumulation of the conjugates is likely due to prolonged circulation and EPR effect. Interestingly, PTX-PEG-ALN conjugate had the highest tumor to background ratio, that could be explain by the fact that this conjugate possess dual targeting, a molecule targeting moiety ALN and targeting mediated by the EPR effect. At 8 h. post injection, tumors and major organs were excised for *ex vivo* imaging to determine tissue distribution (Fig. 5.30 **B**). In all conjugates, apart for tumors, uptake was predominant in kidney tissues due to renal excretion. Preferred accumulation in bones was obvious only in PEG-ALN and PTX-PEG-ALN conjugates, indicating that ALN in the conjugated form remained its binding capacity to bone mineral.

**A**

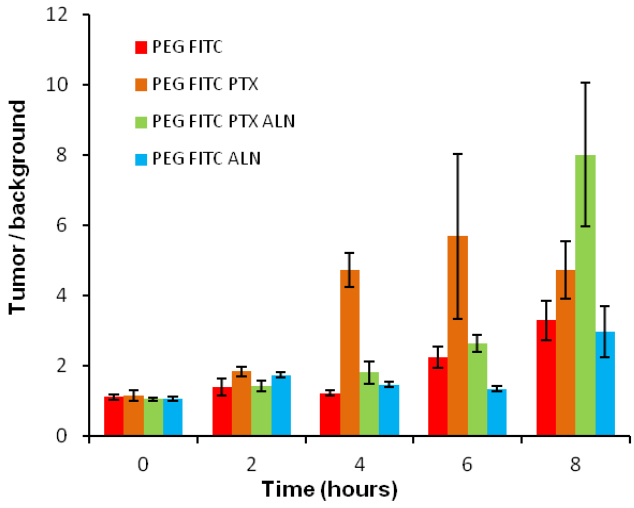

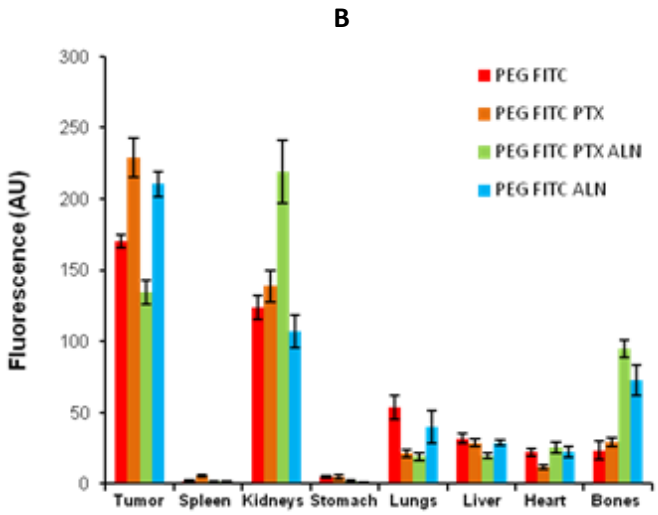


**Figure 5.32 :** *In vivo* and *ex vivo* biodistribution of FITC labeled PEG (red), PTX-PEG (orange), PEG-ALN (blue) and PTX-PEG-ALN (green), conjugates. Mice were imaged by the Maestro system for 8 h. (**A**) Semi-quantitative time dependent tumor accumulation profile of FITC labeled conjugates. Accumulations were assesses as tumor to background (normal skin) ratios of florescence intensities of representative regions of interest. (**B**) *Ex vivo* Fluorescence intensities of tumors and organs dissected after 8 h incubation post FITC labeled injections.

### 5.2.6.2 Pharmacokinetics in mice

Pharmacokinetics studies have been conducted in 30 adult female Balb/c mice by injecting into tail vein a PTX ( in 1:1:8 ethanol:cremophor EL:saline) or PTX conjugates (in PBS pH 6) solution, and withdrawn samples from the retro-orbital plexus/sinus of animals. The serum levels of PTX were evaluated by RP-HPLC. In figure 5.31 a pharmacokinetic profiles of PTX and PTX conjugates were reported.

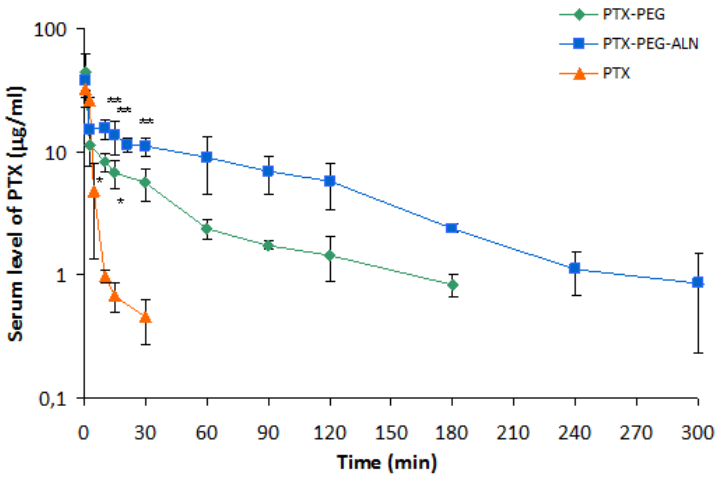


**Figure 5.31:** Pharmacokinetic profiles of PTX ad PTX conjugates in mice (dose 10 mg/Kg PTX equiv., n = 10 animals per group). Each point is the mean of PTX serum leavel in animals (* = p <0.05 of PTX-PEG vs PTX; ** = p < 0.05 of PTX-PEG-ALN vs PTX). Y-axis is presented at a logarithmic scale.

As shown in figure 5.31, after administration of free PTX, high levels of the drug were recorded, however at 5 min postinjection, the PTX concentration decreased dramatically, and it was not detectable at 60 min. On the contrary, the two conjugates showed a marked half-life prolongation, with detectable levels of PTX after 3 h for PTX-PEG and after 24 h for PTX-PEG-ALN.

The pharmacokinetics curves were describe as reported in section 5.1.4.1. The principal pharmacokinetic parameter for PTX and PTX conjugates were reported in table 5.12.

**Table 5.12:** Pharmacokinetic parameters of PTX ad PTX conjugates

| Conjugates | T½α (min) | T½β (min) | $V_d$ (mL) | $AUC_{0-\infty}$ (μg·min/ml) | Clereance (mL/min) |
|---|---|---|---|---|---|
| PTX | 1.3 ± 0.3 | 15.1 ± 4.8 | 160.9 ± 2.1 | 31.2 ± 9.2 | 7.4 ± 1.5 |
| PTX-PEG | 7.5 ± 0.6 | 77.9 ± 4.0 | 63.4 ± 6.2 | 407.3 ± 70.7 | 0.56 ± 0.08 |
| PTX-PEG-ALN | 18.9 ± 0.8 | 85.5 ± 19.8 | 29.9 ± 5.5 | 948.4 ± 119.2 | 0.24 ± 0.03 |

The elimination half-life (T½β) of PTX-PEG and PTX-PEG-ALN were 77.9 and 85.5 min respectively, which is a marker prolongation with respect to the 15.1 min of free PTX. Consequently, also, the area under curve (AUC) of conjugates were increased, in particular it was 13- and 30-times bigger than the AUC of free PTX, respectively (table 5.12)

### 5.2.6.3 *In vivo* antitumor-activity of PTX-PEG-ALN

#### 5.2.6.3.1 Anti-tumor efficacy and toxicity PTX-PEG-ALN conjugates on 4T1-mCherry murine mammary adenocarcinomas inoculated in the tibia

The antitumor effect of PTX-PEG-ALN conjugate following *i.v.* injection was evaluated on mCherry labeled 4T1 murine mammary adenocarcinomas in the tibia. Saline, Vehicle, PTX (15 mg/kg), ALN (35 mg/kg), the combination of free PTX and ALN, PEG-ALN, PTX-PEG, and PTX-PEG-ALN conjugates at equivalent concentrations to free PTX and ALN, were injected on days 1, 4, 6, 8, and 11. Tumor growth was monitored using noninvasive intravital imaging system (CRI™ Maestro). Although tumor progression was noted in all treatment groups, it

was inhibited in mice treated with all PTX formulations with PTX-PEG-ALN conjugate being the most effective. On day 15, when mice were euthanized, PTX-PEG-ALN conjugate inhibited tumor growth by 47% compared with 37% of free PTX (n = 6 mice per group; Fig. 5.32 **A** and **B**). Treatment with ALN was very toxic and caused severe body weight loss and mortality within 2 injections both in free ALN and in the combination of free ALN plus PTX, mice treated groups. Therefore, in these groups, tumor progression could not be determined. In contrast to free ALN, mice treated with PEG-ALN conjugate did not lose weight, suggesting that the conjugation with PEG polymer contributes to specific targeting in tumor tissue through leaky blood vessels rather than non-specific diffusion through normal vasculature. Further body weight loss was not recorded in any of the other treatment groups (Fig. 5.32 **C**). On day 11, blood samples were collected and WBC were counted. WBC counts in mice treated with PEG conjugates or with PTX vehicle were all at the normal range and similar to those of control mice injected with saline. Only in mice treated with free PTX a significant decrease in the WBC counts was recorded (Fig. 5.32 **D**). Due to the severe toxicity effect of free ALN and the combination of free ALN plus PTX, that caused mortality prior to day 11, there is no data concerning the WBC counts from these mice groups.

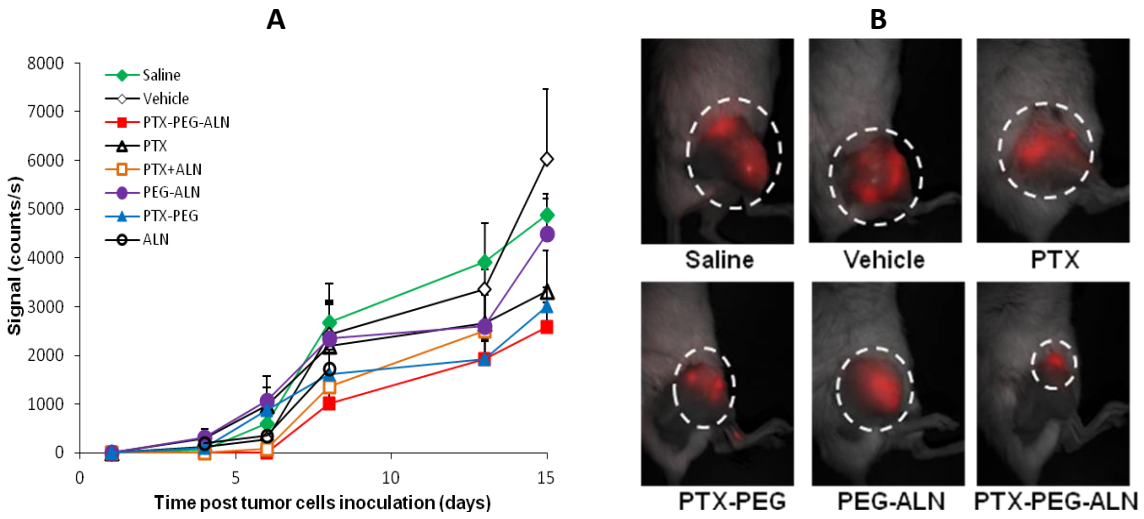

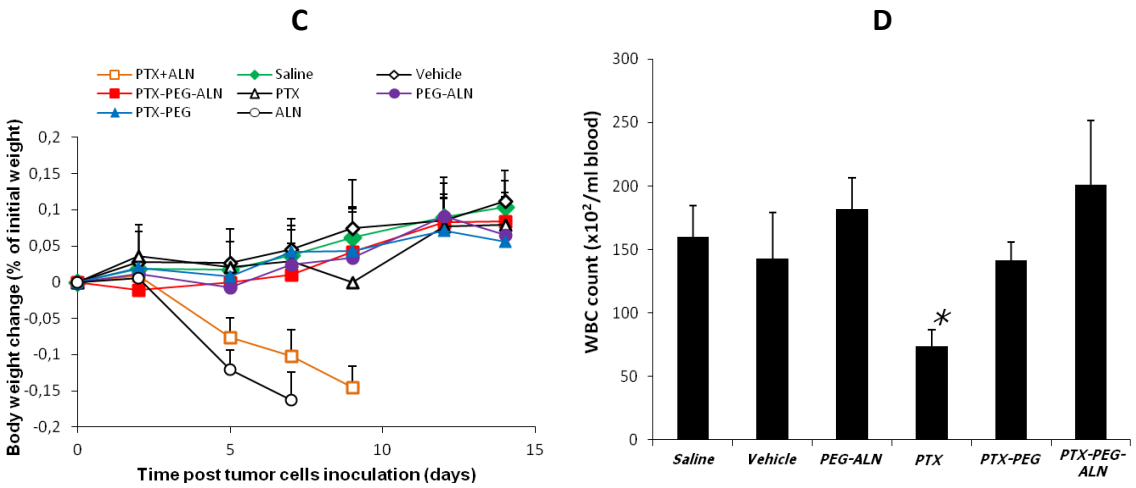


**Figure 5.34:** Mice bearing 4T1-mCherry tumors inoculated in the tibia were administered *i.v.* every other day with 15 mg/kg PTX (open triangles), 35 mg/kg ALN (open circles), the combination of free ALN plus PTX (open orange squares), PTX-PEG (blu triangles), PEG-ALN (porpore circles), PTX-PEG-ALN (red squares) conjugates at equivalent concentrations and with saline (green diamonds) and vehicle (open diamonds) as controls. (**A**) Antitumor efficacy measured by intravital non-invasive fluorescence imaging of 4T1-mCherry tumors in the tibia. (**B**) Fluorescence images of 4T1-mCherry tumors in the tibia. (**C**) Percent body weight change from day one. (**D**) WBC counts from blood samples collected on day 11.

### 5.2.6.3.2 Anti-tumor efficacy and toxicity of PTX-PEG-ALN conjugate on a xenograft model of MDA-MB-231-mCherry mammary adenocarcinomas in the tibia

The antitumor effect of PTX-PEG-ALN conjugate following *i.v.* injections was evaluated on mCherry labeled MDA-MB-231 human mammary adenocarcinomas in the tibia. Saline, Vehicle, the combination of free PTX (15 mg/kg) plus ALN (35 mg/kg), combination of free PTX (7.5 mg/kg) plus ALN (17.5 mg/kg), and PTX-PEG-ALN conjugate at equivalent concentrations to free 15mg/kg PTX and 35mg/kg ALN, were injected *i.v.*, every other day. Tumor growth was monitored using non-invasive intravital imaging system (CRI™ Maestro). On day 30, when mice were euthanized, tumor growth was inhibited only in mice treated with PTX-PEG-ALN conjugate, exhibiting 50% inhibition as compared to control mice (n = 4 mice per group; Fig. 5.33 **A** and **B**). In addition, the conjugate did not induce body weight loss (Fig. 5.33 **C**). However, the combination of free PTX (15 mg/kg) plus ALN (35 mg/kg) was very toxic and induced mortality within one treatment. Also, treatment with free PTX (7.5 mg/kg) plus ALN (17.5 mg/kg) was very toxic and caused severe body weight loss. On day 20, blood

samples were collected, no decrease in WBC counts was recorded in mice treated with PTX-PEG-ALN conjugate (Fig. 5.33 **D**). Since the toxic effect of free PTX on both Balb/c and SCID mice was shown previously and in this study on Balb/c mice inoculated with 4T1 cells, these results indicate that the conjugation of PTX with PEG polymer and ALN is able to rescue the bone marrow from the toxic effect of free PTX (49).

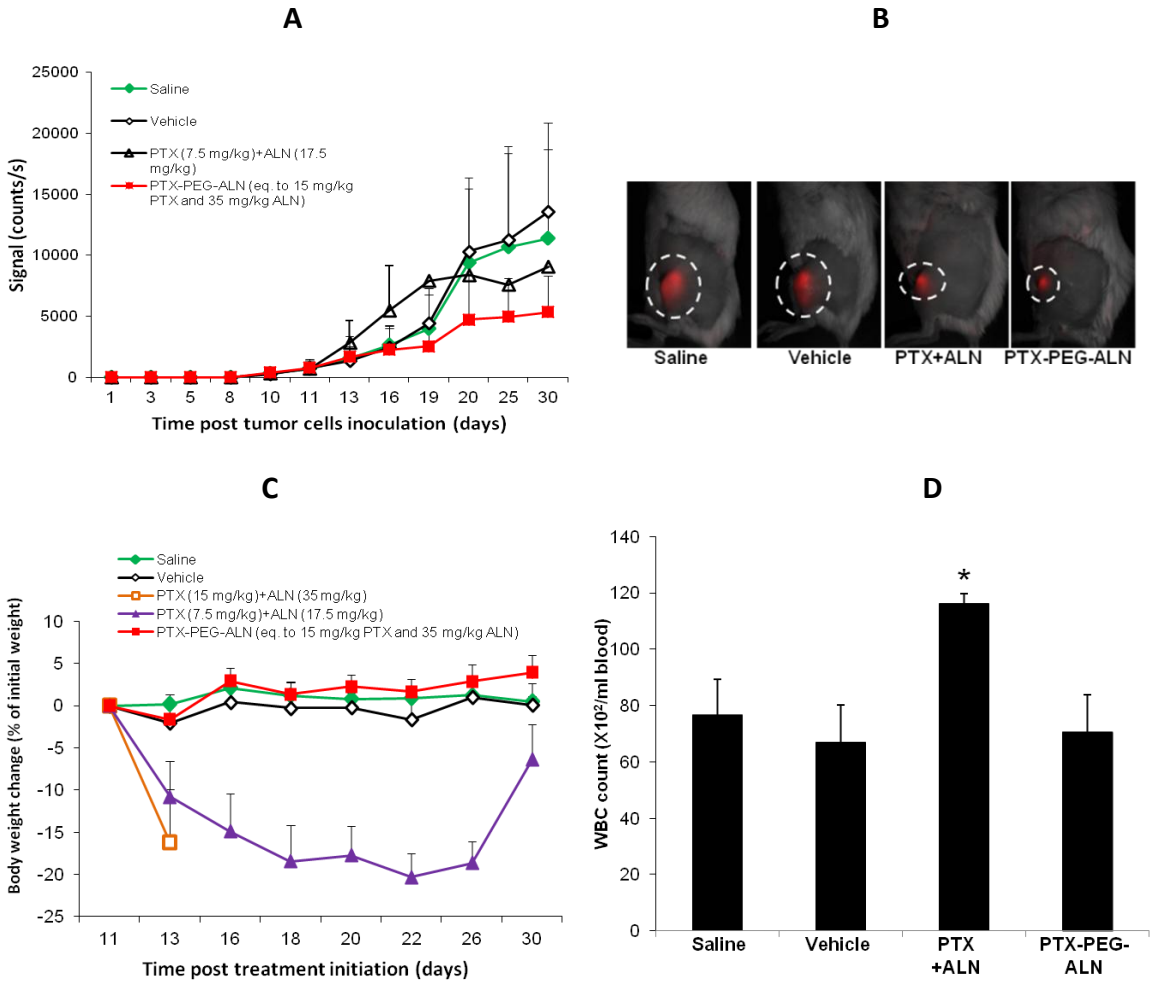


**Figure 5.33:** Mice bearing MDA-MB-231-mCherry tumors in the tibia were administered *i.v.* every other day with the combination of free 35 mg/kg ALN plus 15 mg/kg PTX (open orange squares), the combination of free 17.5 mg/kg ALN plus 7.5 mg/kg PTX (porpore triangles), PTX-PEG-ALN conjugate (red squares) at equivalent concentrations to the high dose of PTX plus ALN, and with saline (green diamonds) and vehicle (open diamonds) as controls. (**A**) Antitumor efficacy measured by intravital non-invasive fluorescence imaging of MDA-MB-231-mCherry tumors in the tibia. (**B**) Fluorescence images of MDA-MB-231-mCherry tumors in the tibia. (**C**) Percent body weight change from day one. (**D**) WBC counts from blood samples collected on day 20. Data represent mean ± s.e.m. of six mice per group.

# DISCUSSION

*Studies on polymer conjugation as versatile tool for drug delivery*

Drug delivery is a rapidly evolving field that is increasingly used to maximize the potential of therapeutic agents.

The work reported in this thesis focuses on the design and preparation of drug delivery systems (*DDSs*),based on polymeric carriers. These systems have been studied for the obtainment of targeted drug carrier and for the optimization of the polymeric carrier. The firs investigated application of this *DDS* is in the field of cancer therapeutics but hopefully its exploitation can be expanded in other field like tissue engineering where the same issues are important for the delivery of growth factors.

Polymer-anticancer drug conjugates have been investigated for decades, as improved therapies against cancer aimed to address the relevant limitations of current protocols using low molecular weight drugs. It is well known that most of the chemotherapeutics are potent drugs. On the other hand, they lack a mandatory selectivity to direct the cytotoxicity to tumor cells, thus causing severe and dramatic adverse effects to normal healthy cells. The coupling of these agents with water-soluble polymers has been demonstrated to strongly improve both the safety profile and antitumor efficacy by acting on several aspects, such as: i) increasing the solubility; many antineoplastic drugs are almost insoluble in biological fluids requiring a oil formulation for clinical administration, ii) improving the biodistribution; conjugates have restricted distribution, due to their large sizes, thus reducing the concentration in sites of dose-limiting toxicity, iii) providing passive targeting to solid tumors; the enhanced permeability and retention (EPR) effect promotes the extravasation of macromolecules into tumors due to the abnormally leaky blood vessels in cancers with respect to healthy tissues, iv) by-passing P-glycoprotein-mediated drug resistance; due to alternative cellular entry and trafficking, and v) preventing drug inactivation and degradation.

This work was divided into two studies. The first study focused on the comparison of the biological behavior (*in vitro* cytotoxicity, cellular uptake and pharmacokinetic properties *in vivo*) of five polymer-drug conjugates differing in the polymeric carrier and containing Epirubicin as a model anticancer drug, conjugated via amide bond.

Very few studies have looked at the role played by the type of polymeric carrier on the biological activity of polymer-drug conjugates and such few have largely focused on the impact of the carrier on endocytic uptake, but it does not assess the effect of the carrier on

the biological activity, so we decided to compare, within the same experimental setting, five different conjugates.

The carriers considered are distinguished on: non-biodegradable polymers such as N-(2-hydroxypropyl) metacrylamide (HPMA) with either the enzymatic cleavable linker GPLG or the stable GG and poly(ethylene glicol) (PEG) and biodegradable polymers such as polyglutamic acid (PGA) and polysialic acid (PSA). HPMA copolymers, PEG and PGA were chosen as many previous studies have indicated their suitability within the context of polymer-drug conjugates [104-106]. PSA has been previously reported in the context of protein delivery [61-62], and as targeting moiety [107]. One study showed the feasibility of PSA as carrier of low molecular weight drugs, using fluorescein as model compound [108] but, to date, such application had remained unexplored. Thus, a PSA-EPI conjugate was synthesized to complete the series, but also to probe the suitability of this carrier for drug delivery and compare it against established drug carriers.

Conjugates was synthesized through a simple chemistry which provided the initial carboxylic groups activation and the subsequent EPI conjugation leading to formation of a stable amide bound. In all cases, was obtained a pure products with a free EPI content below 1% wt/wt total drug therefore compatible for cellular studies. In order to explain the difference in the cytotoxicity profiles observed, the stability of the conjugates under different condition was evaluated. In particular, EPI release was measured in mouse plasma, buffers at pH 5 (to mimic acidic compartments of endosomes) and pH 7.4 (to mimic the extracellular environment). The conjugates were stable in all conditions, with less than 2% EPI being released from each conjugate at 48 h. This confirmed that the chosen linkage ensured stability of the conjugate and was an appropriate choice to investigate the role of carrier in cell internalization. In addition, EPI release in presence of lysosomes extracts was explored. Different behaviors were observed. HPMA-GFLG-EPI, as expected, and PSA-EPI displayed a time-dependent drug release with about 40% of EPI released in the first 5 hours and 80% and 45% EPI release within 48 h, respectively. Conversely, no or limited drug release was observed from PEG-EPI and HPMA-GG-EPI conjugates. A different pattern was observed for PGA-EPI. About 50% of the starting conjugate was degraded within 48 h but free EPI was not released during this incubation time. The lysosomal enzymes cleaved the PGA polymeric backbone, thus forming a range of PGA-EPI oligomers.

Cytotoxicity assessment of the conjugates in MCF-7 cells (performed by Prof. Greco's group at University of Reading) showed a certain activity (approx 40% reduction of cell viability at 1μM) only in the case of the two biodegradable conjugates (PSA-EPI and PGA-EPI). This behavior can only partially be explained with their ability to release EPI as showed for HPMA-GPLG-EPI when incubated with the lysosomes, but this did not translate into a cytotoxic effect. This data suggest that biodegradability also affects biological activity. It is important to note that release studies are normally carried out in environments mimicking the lysosomal compartment but the percentage of conjugate that reaches such compartment is not taken into account. Conversely, cytotoxicity can be considered as the final outcome of several process in series: internalization, trafficking into the lysosomes, subsequent drug release and lysosomal escape of the drug. The assessment of cytotoxicity in MCF-7/Dx also led to interesting results. PSA-EPI (but not PGA-EPI) retained in this sub-line an activity (approx 30% reduction of viability at 1 μM) comparable to that displayed against parental MCF-7, which suggests that not only biodegradability but also specific features of the carrier can impact on the biological activity of the conjugate. The biological activity against MCF-7/Dx, indicates a therapeutic potential against P-glycoprotein-expressing and anthracycline-resistant breast cancer cells. This finding also suggests that for PSA-EPI, the free drug is efficiently released inside the cell, as an extracellular release would have resulted into no cytotoxicity against MCF-7/ DX.

The drug uptake was also considered. It was clear that the type of carrier did not affect the mechanism of uptake as all conjugates were internalized by a cholesterol-dependent pathway, suggesting, also, that uptake is not responsible for the different pattern of cytotoxicity observed.

Finally, it was interesting to observe that the *in vivo* pharmacokinetics were greatly prolonged for all conjugates. The plasma concentration of free EPI decreased dramatically after 3 min, and at 30 min post injection the drug was not detectable. Conversely, all conjugates were detectable in serum at 5h, showing a marked prolongation of the drug pharmacokinetic.

In conclusion, all data indicate that PSA equaled, or in fact, even outperformed established conjugates that are in clinical trials such as HPMA copolymers and PGA. In particular, PSA-EPI was the only conjugate that retained a certain biological activity against MCF-7/Dx, the resistant cell line, which indicates a therapeutic potential against P-

glycoprotein-expressing and anthracycline-resistant breast cancer cells. In addition, the fact that PSA-EPI was stable in plasma but effectively released the active drug in the presence of lysosomes, without need for a specific biodegradable linker, indicates a high potential for this polymer as PSA-drug conjugates can be prepared easily in a single step approach.

The second study focused on the synthesis and characterization of target polymer-drug conjugates, based on a PEG with a defined dendritic structure for delivery of the anticancer drug paclitaxel (PTX) [113]. The structure of PEG Dendron offer the possibility to obtain defined chemical structure in terms of drug and targeting moiety contents. Furthermore, it was hypothesized that by synthesizing a heterobifunctional PEG-dendrimer, namely $NH_2$-PEG-βGlu-$(βGlu)_2$-$(COOH)_4$, it could be possible to obtain a conjugate with a high degree of homogeneity, thus impacting positively on both the targeting and activity properties. The heterobifunctional PEG allows the subdivision of targeting and activity functions by linking PTX and ALN at the two different end chains of the polymers. This design leads to the obtainment of an amphiphilic conjugate, being PTX highly hydrophobic and ALN hydrophilic. The spatial separation of these drugs, besides offering the possibility to form self-assembled micelles, will maintain all ALN molecules exposed to the water, promptly available for binding to the bone mineral hydroxyapatite.

The derivative designed can target bone neoplasms by dual-targeting as follows: 1) through ALN (active mechanism), and for this reason rapid and elevated targeting to bone tumors are favored by high ALN loadings, and 2) by exploiting the EPR effect (passive mechanism), which is due to the atypically leaky tumor blood vasculature [23-25] that enhances tumor accumulation of the conjugate thanks to its increased size with respect to the free drug.

PTX is a potent anticancer drug used for the treatment of breast, ovarian, non-small-cell lung and prostate cancers [68,109-112]. ALN is a bisphosphonate [79-81], used for the treatment of osteoporosis and bone metastases and also investigated as bone targeting agent [73]. In recent years, it has become evident that both ALN and PTX at low doses can selectively inhibit endothelial functions relevant to angiogenesis [80-82]. Angiogenesis, new capillary blood vessel growth from pre-existing vasculature, is now recognized as important control point in tumor progression and metastasis formation [83-88].

Three derivatives of PEG-β-Glutamic acid dendrimer, bearing ALN and/or PTX were synthesized. The synthesis of PTX-PEG was performed in three main steps: synthesis of SPTX,

synthesis of PEG-dendrimer and binding of SPTX to PEG-dendrimer. SPTX was characterized by: 1) RP-HPLC, showing a pure products without free PTX, 2) UV-VIS spectrometry, showing a spectrum super imposable to PTX spectrum and 3) $^{1}$H-NMR spectroscopy, showing the characteristic signals of PTX together with those of the succinic spacer. The PEG-dendrimer was built at carboxylic activated terminus of commercial Boc-NH-PEG-NHS using β-Glutamic acid (β-Glu) as symmetric bicarboxylic branching unit. PEG-ALN was obtained by firstly linking the ALN targeting residues to the PEG dendrimer carboxylic group and then by removing the Boc protecting group. The coupling of SPTX to PEG-ALN yielded PTX-PEG-ALN. These building blocks for the conjugate are all nontoxic. Indeed the *in vitro* RBC lysis assay demonstrated that PTX-PEG-ALN conjugate had no hemolytic activity at up to 5 mg/ml. In contrast, the commercial vehicle for PTX that contains Cremophor EL had significant hemolytic activity on RBC.

The same conjugates was synthesized inserting FITC in the polymeric structure to obtained labeled conjugates that was used to real time monitor the biodistribution and tumor accumulation of PEG, PTX-PEG, PEG-ALN, and PTX-PEG-ALN following *i.v.* administration to mice bearing MDA-MB-231 tumors in the tibia. FITC was inserted by lysine residue conjugated at carboxylic end of commercial PEG, next, dendron was build in the same condition of PTX-PEG-ALN.

All conjugates was characterized in terms of PTX and ALN content. Through RP-HPLC ad basis hydrolysis assay a total and free PTX was determined. In all cases, was obtained a pure products with a free PTX content below 0,6% w/w total drug therefore compatible for cellular studies instead thanks to a great control over the conjugate chemical structure, was could achieve a higher percent of ALN loading (11% w/w). PTX-PEG-ALN conjugate showed great affinity to HA, used as model mineral mimicking bone tissue. Following 5 min incubation, 80% or 90% of PTX-PEG-ALN or PEG-ALN conjugates, respectively, were bound to HA and reached a plateau. This result confirms that the favorable PEG/ALN ratio and the dendrimer structure, bearing ALN molecules, ensure high and fast binding to the bone mineral HA.

PTX-PEG-ALN conjugate was designed for a strong bone tropism and a faster drug release. In this studies was hypothesized that, with PTX-PEG-ALN conjugate, a cathepsin B-cleavable linker might not be suitable because the derivative *in vivo* will bind to the bone HA matrix. The high affinity to the bone originating from the presence of a bisphosphonate in

the conjugate can affect the conjugate internalization into cancer cells and consequently slow the rate of PTX release, if a cathepsin B-cleavable linker is used. Cathepsin B is overexpressed in lysosomes of many types of tumor cells, but also secreted to the extracellular matrix. In general, enzymatic cleavage is efficient when slow and controlled drug release is required. When a fast release is desired, a different mechanism, such as hydrolysis, is necessary. Therefore, in this case, a PTX-polymer hydrolysis at physiological condition has been preferred because it allows drug release in the surroundings of bone metastasis, where the conjugate will fast accumulate. PTX was linked to PEG through an ester linkage exploiting a succinimidyl spacer, which releases the drug at physiological pH. The PTX release was investigated *in vitro* for PTX-PEG-ALN and PTX-PEG under different conditions (plasma, phosphate buffers at pH 7.4 and 5). As expected, the hydrolysis rate of the ester bond between the drug and the polymer was higher in buffer at pH 7.4 (about 50% of PTX-PEG-ALN and PTX-PEG were degraded within the first 1 h) than in pH 5. Interestingly, the incubation in plasma showed a drug release comparable to that in buffer at pH 7.4, suggesting that PTX is released by a hydrolytically-based mechanism without a significant contribution of esterases. The faster drug release at pH 7.4 affected also the stability of PTX-PEG-ALN and PTX-PEG micelles, which at this pH were less stable than at pH 5. Micelles at pH 7.4 were stable up to about three hours although half of the PTX amount was released within 1 hour. This behavior can be explained with the high hydrophobicity of PTX that limits the PTX escape from the hydrophobic inner core of the micelles, thus prolonging the micelles stability. Probably, this process holds only in simple *in vitro* models whereas *in vivo* these micelles might be less stable due to both the interaction with blood components and the dilution in the bloodstream.

When PEG-β-Glutamic acid dendron was conjugated with PTX and ALN it showed similar cytotoxicity on 4T1 (murine mammary adenocarcinoma) , MDA-MB-231 (human mammary adenocarcinoma) and PC3 (human prostate adenocarcinoma) cells compared with free PTX, suggesting that PTX can be released from the conjugates and achieve tumor cell killing efficacy. Inhibition of the proliferation, capillary-like tube formation, and migration of endothelial cells revealed that the newly synthesized PTX-PEG-ALN conjugate possesses anti-angiogenic properties and is as potent as the combination of free ALN plus PTX at equivalent concentrations (studies performed by Prof. Satchi-Fainaro group at University of Tel Aviv).

Non-invasive intravital FITC optical imaging technology was used to real time monitor the biodistribution and tumor accumulation of FITC labeled PEG, PTX-PEG, PEG-ALN, and PTX-PEG-ALN conjugates following *i.v.* administration to mice bearing MDA-MB-231 tumors in the tibia. A preferred accumulation in tumors was noted in all FITC-labeled conjugates, possibly as a result of the EPR effect. Interestingly, PTX-PEG-ALN-FITC conjugate was accumulated in the tumors mostly. This enhanced accumulation was designed to be reinforced by the addition of the targeting molecule, ALN. Furthermore, both PEG-ALN and PTX-PEG-ALN conjugates were significantly accumulated in bones, probably due to the ALN molecule. An explicit accumulation in the kidneys of all conjugates is due to renal excretion that is profound 8 h following injection of the conjugates (studies performed by Prof. Satchi-Fainaro group at University of Tel Aviv).

The pharmacokinetic profiles of PTX-PEG and PTX-PEG-ALN conjugates in mice showed marked half-lives increase with respect to free PTX solubilized in Cremophor EL (about 5 and 6 times longer, respectively). Interestingly, in the case of PTX-PEG-ALN conjugate, the serum level of PTX was still detectable after 24 h, whereas with PTX-PEG the concentration dropped below the detection limit after 3 h. Likely, this behavior of PTX-PEG-ALN conjugate can be explained by the targeting action of ALN, which induces a strong binding of the PTX-PEG-ALN conjugate to the bones from which PTX is released. Therefore, in the case of PTX-PEG the half-life prolongation is based only on the increased size of the conjugates whereas for PTX-PEG-ALN, beside the role of the carrier, also the ALN targeting effect might reduces the clearance as seen for other targeted conjugates [114].

PTX-PEG-ALN conjugate showed substantial antitumor effects in both syngeneic (4T1-mCherry) and xenograft (MDA-MB-231-mCherry) mouse models. In both mouse models about 50% reduction was recorded in PTX-PEG-ALN conjugate mice treated group. The superiority of this conjugate is evident in its safety compared to free drugs. In both Balb/c and SCID mice, treatment with the combination of free PTX plus ALN was mortal within the first injection. Even treatment with free PTX plus ALN at half the dose was very toxic and caused a reduction of 20% in body weight. However, treatment with PTX-PEG-ALN conjugate did not cause body weight loss. Also, WBC levels normal in mice treated with the conjugate, whereas in mice treated with free PTX, a significant decrease in WBC levels occurred (studies performed by Prof. Satchi-Fainaro group at University of Tel Aviv).

In summary, a well-defined nontoxic conjugate composed of PEG, PTX and ALN was successfully developed. PTX-PEG-ALN demonstrated cytotoxic and anti-angiogenic properties *in vitro*. This conjugate had prolonged circulation time and accumulated preferentially in tumors in the tibia via the dual targeting of EPR effect and the addition of the targeting molecule, ALN. This resulted in enhanced therapeutic efficacy with better safety profiles in both syngeneic and xenograft mouse models. Therefore, PTX-PEG-ALN is a promising drug delivery system that can be exploited to treat breast cancer bone metastases.

This type of bone targeting, also, was studied with the prospects of using these derivatives PEG-alendronate in order to target growth agents for the formation of scaffolds for reconstruction of bone tissue.

# REFERENCES

*Studies on polymer conjugation as versatile tool for drug delivery*

[1] Duncan R., Polymer conjugates as anticancer nanomedicines. *Nature Rev. Cancer*, **6**, 688-701, September2006.

[2] Terada S., Sato M., Sevy A., Vacanti J. P., Tissue engineering in the twenty-first century. *Yonsei Med J.* **41** (6) (2000), 685-91.

[3] Langer R., Vacanti J.P., Tissue engineering. *Science* **260** (1993), 920-926.

[4] Suh H., Tissue restoration, tissue engineering and regenerative medicine. *Yonsei Med J.* **41**(6) (2000), 681-4.

[5] Duncan, R., Polymer conjugates for tumor targeting and intracytoplasmatic delivery. The EPR effect as a common gateway? *Research focus / Reviews* **2 (**1999), 441-449.

[6] Thomas, F., *Scrip. Magazine* May 1998, 42-43.

[7] Folkman, J., *Adv. Cancer Res*. **43**, 175-203.

[8] Lundberg, A.S., Weinberg, R.A., *Eur. J. Cancer* **35** (1999), 531-539.

[9] Sandhu, J.S., Keating, A., Hozumi, N., *Crit. Rev. Biotechnol.* **17** (1997), 307-326.

[10] Robert, K.J., Cheng, Z., Cheng, C.C., *Meth. and Find Exp. Clin. Pharmacol.* **11** (1989), 439-529.

[11] Arnold, I., Freeman, M.D., Mayhew, E., Targeted drug delivery. *Cancer* **58** (1986), 573-583.

[12] Duncan, R., Dimitrijevic, S. and Evagorou, E.G., The role of polymer conjugates in the diagnosis and treatment of cancer. *STP Pharma Sciences*, **6** (1996), 237-263.

[13] Duncan, R., Polymer Therapeutics for tumor specific delivery. *Chemistry & Industry*, **7** (1997), 262-264.

[14] Jayant Khandare, Tamara Minko, Polymer-drug conjugate: Progress in polymeric prodrug. *Prog.Polym.Sci*, **31**, 359-397, 2006.

[15] Hoes, C.J.T., Feijen, J., The application of drug-polymer conjugates in chemotherapy. *Drug Carrier Systems*, **57**-109, 1989.

[16] Cavallaro, G., Pitarresi, G., Licciardi, M., Giammona, G., Polymeric prodrug for release of an antitumoral agent by specific enzymes. *Bioconjugate Chem.* **12**(2), 143-151, 2001.

[17] Ringsdorf, H., Structure and properties of pharmacologically active polymers. *J. Polym. Sci. Polym. Symp.* **51**, 135-153, 1975.

[18] Puttnam, D., Kopeček, J., Polymer conjugates with anticancer activity, *Adv. Polym. Sci.***122** (1995) 55-123.

[19] Shen, W.C., Ryser, H.J.P., Cys-aconityl spacer between daunomycin and macromolecular carriers: a model of pH-sensitive linkage releasing drug from a lysosomotropic conjugate, *Biochem. Biophys. Res. Commun.* **102** (1981) 1048-1054.

[20] Soyez, H., Schacht, E., Vanderkerken, S., The crucial role of spacer groups in macromolecular prodrug design, *Adv. Drug Del. Rev.* **21** (1996) 81-106.

[21] Duncan, R., Hume, I.C., Yardley, H.J., Flanagan, A., Ulbrich, K., Subr, U., Strohalm, J., Macromolecular prodrugs for use in target cancer chemotherapy: melphalan covalently coupled to N-(2-Hydroxypropyl)methacrylamide copolymers, *J. Controlled Release* **16** (1991) 121-136.

[22] Veronese, F.M., Morpurgo, M., Bioconjugation in pharmaceutical chemistry, *Il farmaco* **54** (1999) 497-516.

[23] Maeda, H., Matsumura, Y., Tumoritropic and lymphotropic principles of macromolecular drugs, *CRC Crit. Rev. Ther. Drug Carrier Sys.* **6(3)** (1989) 193-210.

[24] Maeda, H., Sawa, T., Konno, T., Mechanism of tumor-targeted delivery of macromolecular drugs, including the EPR effect in solid tumor and clinical overview of the prototype polymer drug SMANCS, *J. Controlled Release* **74** (2001) 47-61.

[25] Maeda, H., Fang, J., Inutsuka, T., Kitamoto, Y., Vascular permeability enhancement in solid tumor: various factors, mechanisms involved and its implications, *International Immunopharmacology* **3** (2003) 319-328.

[26] Kopeček, J., Kopečková, P., Minko, T., Lu, Z.-R., Peterson, C.M., Water soluble polymers in tumor targeted delivery, *J. Controlled Release* **74** (2001) 147-158.

[27] Lisa M. Bareford, Peter W. Swaan, Endocytic mechanism for targeted drug delivey. *Adv. Drug del. Rev.,* **59**, 748-758, 2007.

[28] Bailey, J.F.E., Koleske, J.V., Poly(etylene-oxide), *Academic Press New York,* (1976).

[29] Dreborg, S., Akerblom, E.B., Immunotherapy with monomethoxypolyethylene glycol modified allergens, *Crit. Rev. Ther. Drug Carrier Syst.* **6(4)** (1990) 315-365.

[30] Powell, G.M., Polyethylene glycol, *Handbook of water soluble gums and resins* (R.L. Davidson, Ed.), pp 18-1-18-31, McGraw-Hill, New York, 1980.

[31] Mutter, M., Bayer, E., *The peptides* Academic Press, New York (1979) 285-332.

[32] Yamaoka,T., Tabata, Y., Ikada, Y., Distribution and tissue uptake of poly(ethylene glycol) with different molecular weights after intravenous administration to mice, *J.Pharm. Sci.* **83** (4) (1994) 601-606.

[33] Molineux, G., Pegylation: engineering improved pharmaceuticals for enhanced therapy, *Cancer Treat. Rev.* **28** (Suppl.A) (2002) 13-16.

[34] Caliceti, P., Veronese, F.M., Pharmacokinetic and biodistribution properties of poly(ethylene glycol)-protein conjugates, *Adv. Drug Deliv. Rev.* **55** (2003) 1261-1277

[35] Zalipsky, S., Functionalized poly(ethylene glycol) for preparation of biologically relevant conjugates, *Bioconjugate Chem.* **6** (1995) 150-165.

[36] Delgado, C., Francis, G.E., Fisher, D., The uses and properties of PEG-linked proteins, *Crit. Rev. Ther. Drug Carrier Syst.* **9** (1992) 249-304.

[37] Bhadra, D., Bhadra, S., Jain, P., Jain, N.K., Pegnology: a review of PEG-ylated systems, *Pharmazie* **57** (2002) 5-29.

[38] Davis, F.F., The origin of PEGnology, *Adv. Drug Deliv. Rev.* **54** (1992), 457-458.

[39] Duncan, R., Polymer–Drug Conjugates, In: D. Budman *et al.*, Editors, *Handbook of Anticancer Drug Development*, Lippincott Williams & Wilkins (2003) 239–260.

[40] Veronese, F.M., Peptide and protein PEGylation: a review of problems and solutions, *Biomaterials* **22** (2001) 405-417.

[41] 12. Veronese, F.M., Pasut, G., Guiotto, A., Protein, peptide and non-peptide drug PEGylation for therapeutic application, *Expert Opin. Therap. Patents* **14** (2004) 859–894.

[42] Roberts, M.J., Bentley, M.D., Harris, J.M., Chemistry for peptide and protein PEGylation, *Adv. Drug Deliv. Rev.* **54** (2002) 459-476.

[43] Ruth Duncan, Development of HPMA copolymer–anticancer conjugates: Clinical experience and lessons learnt,*Advanced Drug Delivery Reviews* **61** (2009) 1131–1148

[44] Ruth Duncan, María J. Vicent, Do HPMA copolymer conjugates have a future as clinically useful nanomedicines? A critical overview of current status and future opportunities,*Advanced Drug Delivery Reviews* **62** (2010) 272–282.

[45] Jindřich Kopeček, Pavla Kopečková, HPMA copolymers: Origins, early developments, present, and future, *Advanced Drug Delivery Reviews* **62** (2010) 122–149.

[46] P.A. Flanagan, R. Duncan, B. Rihova, V. Subr, J. Kopecek, Immunogenicity of protein-N-(2-hydroxypropyl)methacrylamide copolymer conjugates measured in A/J and B10 mice, *J. Bioact. Compat. Polym*. **5** (1990) 151–166.

[47] P. Rejmanova, J. Kopecek, R. Duncan, J.B. Lloyd, Stability in plasma and serum of lysosomally degradable oligopeptide sequences in N-(2-hydroxypropyl) methacrylamide copolymers, *Biomaterials* **6** (1985) 45–48.

[48] R. Duncan, H.C. Cable, J.B. Lloyd, P. Rejmanova, J. Kopecek, Polymers containing enzymatically degradable bonds, 7. Design of oligopeptide side chains in poly [N-(2-hydroxypropyl)methacrylamide] copolymers to promote efficient degradation by lysosomal enzymes, Makromol. Chem. **184** (1984) 1997–2008.

[49] Chun Li, Poly(L-glutamic acid)-anticancer drug conjugates, *Advanced Drug Delivery Review* **54** (2002) 695-713.

[50] Hsin-Cheng Chiu, Pavla Kopečkovà, Sharad S. Deshmane, and Jindřich Kopeček, Lysosomal degradability of poly(a-amino acids), *Journal of Biomedical Materials Research*, Vol. **34** (1997), 381–392.

[51] C.J.T. Hoes,W. Potman,W.A.R. van Heeswijk, J. Mud, B.G. de Grooth, J. Greve, J. Feijen, Optimization of macromolecular prodrugs of the antitumor antibiotic Adriamycin, *J. Control. Release* **2** (1985) 205–213.

[52] C.J.T. Hoes, J. Grootoonk, R. Duncan, I.C. Hume, M. Bhakoo, J.M.W. Bouma, J. Feijen, Biological properties of Adriamycin bound to biodegradable polymeric carriers, *J. Control. Release* **23** (1993) 37–54.

[53] F. Zunino, G. Pratesi, A. Micheloni, Poly(carboxylic acid) polymers as carriers for anthracyclines, *J. Control. Release* **10** (1989) 65–73.

[54] Y. Kato, M. Saito, H. Fukushima, Y. Takeda, T. Hara, Antitumor activity of 1-b-D-arabinofuranosylcytosine conjugated with polyglutamic acid and its derivative, *Cancer Res*. **44** (1984) 25–30.

[55] Jack W. Singer Paclitaxel poliglumex (XYOTAX, CT-2103): A macromolecular taxane *Journal of Controlled Release* **109** (2005) 120– 126.

[56] Chun Li, Sidney Wallace Polymer-drug conjugates: Recent development in clinical oncology, *Advanced Drug Delivery Reviews* **60** (2008) 886–898

[57] C. Li, D.F. Yu, R.A. Newman, F. Cabral, L.C. Stephens, N. Hunter, L. Milas, S. Wallace, Complete regression of well established tumors using novel water-soluble poly(L-glutamic acid)–paclitaxel conjugates, *Cancer Res*. **58** (1998) 2404-2409.

[58] J.W. Singer, P. Devries, R. Bhatt, J. Tulinsky, P. Klein, C. Li, L. Milas, R.A. Lewis, S. Wallace, Conjugation of camptothecins to poly(L-glutamic acid), *Ann. NY Acad. Sci.* **922** (2000) 136–150.

[59] Sanjay Jain1,2, Dale Hreczuk-Hirst1, Peter Laing1, and Gregory Gregoriadis1,2 Polysialylation: the natural way to improve the stability and pharmacokinetics of protein and peptide drugs *dds&s* Vol **4** No 1 July 2004.

[60] Gregory Gregoriadis, Sanjay Jain, Ioannis Papaioannou, Peter Laing, Improving the therapeutic efficacy of peptides and proteins: A role for polysialic acids, *International Journal of Pharmaceutics* **300** (2005) 125–130.

[61] Sanjay Jain, Dale H. Hreczuk-Hirst, Brenda McCormack, Malini Mital, Agamemnon Epenetos, Peter Laing, Gregory Gregoriadis, Polysialylated insulin: synthesis, characterization and biological activity in vivo. *Biochimica et Biophysica Acta* **1622** (2003) 42– 49.

[62] Ana I. Fernandes, Gregory Gregoraadis, Polysialylated asparaginase: preparation, activity and pharmacokinetics, *Biochimica et Biophysica Acta* **1341** (1997) 26-34

[63] Booser, D.J. and Hortobagy, G.N., Antracycline antibiotics in cancer therapy. *Drugs*, **47**, 223-258, 1994.

[64] Robert, J., Clinical pharmacokinetics of epirubicin. *Clin. Parmacok*., **26**, 428-438, 1994.

[65] Marco, A., Casazza, A.M., Gambetta, R., Supino, R. and Zumino, F., Relationship between activity and amino sugar stereochemistry of daunomicin and adriamicin derivates. *Cancer research*, **36** (1976), 1962-1966.

[66] Plosker, G.L. and Faulds, D., Epirubicin. A review of its pharmacodynamic and pharmacokinetic properties, and therapeutic use in cancer chemotherapy. *Drugs*, **45**, 788-856, 1993.

[67] Horwitz, S. B., Cohen, D., Rao, S., Ringel, I., Shen, H. J., and Yang, C. P. (1993) Taxol: mechanisms of action and resistance. *J Natl Cancer Inst Monogr*, 55-61.

[68] Bhalla, K. N. (2003) Microtubule-targeted anticancer agents and apoptosis. *Oncogene* **22**, 9075-9086.

[69] Weiss, R. B., Donehower, R. C., Wiernik, P. H., Ohnuma, T., Gralla, R. J., Trump, D. L., Baker, J. R., Jr., Van Echo, D. A., Von Hoff, D. D., and Leyland-Jones, B. (1990) Hypersensitivity reactions from taxol. *J Clin Oncol* **8**, 1263-1268.

[70] Gelderblom, H., Verweij, J., Nooter, K., and Sparreboom, A. (2001) Cremophor EL: the drawbacks and advantages of vehicle selection for drug formulation. *Eur J Cancer* **37**, 1590-1598.

[71] Sanjeev Kumar, Haider Mahdi, Christopher Bryant, Jay P Shah, Gunjal Garg, Adnan Munkarah, Clinical trials and progress with paclitaxel in ovarian cancer, *International Journal of Women's Health* **2** (2010) 411–427.

[72] Caraglia, M., Santini, D., Marra, M., Vincenzi, B., Tonini, G., and Budillon, A. (2006) Emerging anti-cancer molecular mechanisms of aminobisphosphonates. *Endocr Relat Cancer* **13**, 7-26.

[73] Wang, D., Miller, S., Sima, M., Kopeckova, P., and Kopecek, J. (2003) Synthesis and evaluation of water-soluble polymeric bone-targeted drug delivery systems. *Bioconjug Chem* **14**, 853-859.

[74] Uludag, H. (2002) Bisphosphonates as a foundation of drug delivery to bone. *Curr Pharm Des* **8**, 1929-1944.

[75] Sevcik, M. A., Luger, N. M., Mach, D. B., Sabino, M. A., Peters, C. M., Ghilardi, J. R., Schwei, M. J., Rohrich, H., De Felipe, C., Kuskowski, M. A., and Mantyh, P. W. (2004) Bone cancer pain: the effects of the bisphosphonate alendronate on pain, skeletal remodeling, tumor growth and tumor necrosis. *Pain* **111**, 169-180.

[76] Wang, D., Miller, S. C., Kopeckova, P., and Kopecek, J. (2005) Bone-targeting macromolecular therapeutics. *Adv Drug Deliv Rev* **57**, 1049-1076.

[77] Hirabayashi, H., and Fujisaki, J. (2003) Bone-specific drug delivery systems: approaches via chemical modification of bone-seeking agents. *Clin Pharmacokinet* **42**, 1319-1330.

[78] Segal, E., Pan, H., Ofek, P., Udagawa, T., Kopeckova, P., Kopecek, J., and Satchi-Fainaro, R. (2009) Targeting angiogenesis-dependent calcified neoplasms using combined polymer therapeutics. *PLoS One* **4**, e5233.

[79] Miller, K., Erez, R., Segal, E., Shabat, D., and Satchi-Fainaro, R. (2009) Targeting bone metastases with a bispecific anticancer and antiangiogenic polymer-alendronate-taxane conjugate. *Angew Chem Int Ed Engl* **48**, 2949-2954.

[80] Wang, J., Lou, P., Lesniewski, R., and Henkin, J. (2003) Paclitaxel at ultra low concentrations inhibits angiogenesis without affecting cellular microtubule assembly. *Anticancer Drugs* **14**, 13-19.

[81] Pasquier, E., Carre, M., Pourroy, B., Camoin, L., Rebai, O., Briand, C., and Braguer, D. (2004) Antiangiogenic activity of paclitaxel is associated with its cytostatic effect, mediated by the initiation but not completion of a mitochondrial apoptotic signaling pathway. *Mol Cancer Ther* **3**, 1301-1310.

[82] Fournier, P., Boissier, S., Filleur, S., Guglielmi, J., Cabon, F., Colombel, M., and Clezardin, P. (2002) Bisphosphonates inhibit angiogenesis in vitro and testosterone-stimulated vascular regrowth in the ventral prostate in castrated rats. *Cancer Res* **62**, 6538-6544.

[83] Hanahan, D., Bergers, G., and Bergsland, E. (2000) Less is more, regularly: metronomic dosing of cytotoxic drugs can target tumor angiogenesis in mice. *J Clin Invest* **105**, 1045-1047.

[84] Folkman, J. (2004) Endogenous angiogenesis inhibitors. *APMIS* **112**, 496-507.

[85] Browder, T., Butterfield, C. E., Kraling, B. M., Shi, B., Marshall, B., O'Reilly, M. S., and Folkman, J. (2000) Antiangiogenic scheduling of chemotherapy improves efficacy against experimental drug-resistant cancer. *Cancer Res* **60**, 1878-1886.

[86] Hanahan, D., and Folkman, J. (1996) Patterns and emerging mechanisms of the angiogenic switch during tumorigenesis. *Cell* **86**, 353-364.

[87] Chesler, L., Goldenberg, D. D., Seales, I. T., Satchi-Fainaro, R., Grimmer, M., Collins, R., Struett, C., Nguyen, K. N., Kim, G., Tihan, T., Bao, Y., Brekken, R. A., Bergers, G., Folkman, J., and Weiss, W. A. (2007) Malignant progression and blockade of angiogenesis in a murine transgenic model of neuroblastoma. *Cancer Res* **67**, 9435-9442.

[88] Folkman, J. (1971) Tumor angiogenesis: therapeutic implications. *N Engl J Med* **285**, 1182-1186.

[89] Matthew T. Drake, MD, PhD, Bart L. Clarke, MD, and Sundeep Khosla, MD Bisphosphonates: Mechanism of Action and Role in Clinical Practice, *Mayo Clin Proc*. (2008) **83**(9), 1032–1045.

[90] Fleisch H, Russell RG, Straumann F. Effect of pyrophosphate on hydroxyapatite and its implications in calcium homeostasis. *Nature* (1966); **212** (5065), 901–903.

[91] Russell RG, Muhlbauer RC, Bisaz S, Williams DA, Fleisch H. The influence of pyrophosphate, condensed phosphates, phosphonates and other phosphate compounds on the dissolution of hydroxyapatite in vitro and on bone resorption induced by parathyroid hormone in tissue culture and in thyroparathyroidectomised rats. Calcif Tissue Res (1970) **6** (3), 183–196.

[92] Russell RG. Bisphosphonates: from bench to bedside. *Ann N Y Acad Sci* (2006) **1068**, 367–401.

[93] Dunford JE, Thompson K, Coxon FP, et al. Structure-activity relationships for inhibition of farnesyl diphosphate synthase in vitro and inhibition of bone resorption in vivo by nitrogen-containing bisphosphonates. J Pharmacol Exp Ther (2001), **296** (2), 235–242.

[94] Dingcheng Xin, Ying Wang and Jiannan Xiang The Use of Amino Acid Linkers in the Conjugation of Paclitaxel with Hyaluronic Acid as Drug Delivery System: Synthesis, Self-Assembled Property, Drug Release, and In Vitro Efficiency Pharmaceutical Research (2009), **27** (2), 380-389.

[95] C.J. Schröter, M. Braun, J. Englert, H. Beck, H. Schmid, H. Kalbacher, A rapid method to separate endosomes from lysosomal contents using differential centrifugation and hypotonic lysis of lysosomes, J. Immunol. Methods **227** (1999) 161–168.

[96] Snyder, S. L.; Sobocinski, P. Z. An improved 2,4,6-trinitrobenzenesulfonic acid method for the determination of amines. *Anal. Biochem.* 1975, **64**, 284-288.

[97] Anna Mero, Chiara Clementi, Francesco M. Veronese, and Gianfranco Pasut. Covalent Conjugation of Poly(Ethylene Glycol) to Proteins and Peptides: Strategies and Methods. Sonny S. Mark (ed.), Bioconjugation Protocols: Strategies and Methods, Methods in Molecular Biology, vol. **751**

[98] Kuljanin, J.; Jankovic, I.; Nedeljkovic, J.; Prstojevic, D.; Marinkovic, V. Spectrophotometric determination of alendronate in pharmaceutical formulations via complex formation with Fe(III) ions. *J Pharm Biomed Anal* 2002**, 28**, 1215-1220.

[99] E. Configliacchi, G. Razzano, V. Rizzo, A. Vigevani, HPLC methods for the determination of bound and free doxorubicin, and of bound and free galactosamine, in methacrylamide polymer-drug conjugates, *J. Pharm. Biomed. Anal*. **15** (1996) 123-129.

[100] R. Duncan, L.W. Seymour, K.B. O'Hare, P.A. Flanagan, S. Wedge, I.C. Hume, K. Ulbrich, J. Strohalm, V. Subr, F. Spreafico, M. Grandi, M. Ripamonti, M. Farao, A. Suarato, Preclinical evaluation of polymer-bound doxorubicin, *J. Control. Release* **19** (1992) 331–346.

[101] T. Minko, P. Kopeckova, V. Pozharov, J. Kopecek, HPMA copolymer bound adriamycin overcomes MDR1 gene encoded resistance in a human ovarian carcinoma cell line, *J. Control. Release* **54** (1998) 223–233.

[102] Duncan, R.; Ferruti, P.; Sgouras, D.; Tuboku-Metzger, A.; Ranucci, E.; and Bignotti, F. A polymer-Triton X-100 conjugate capable of PH-dependent red blood cell lysis: a model system illustrating the possibility of drug delivery within acidic intracellular compartments. *J Drug Target* **2** (1994), 341-347.

[103] Ofek, P.; Fischer, W.; Calderon, M.; Haag, R.; and Satchi-Fainaro, R. In vivo delivery of small interfering RNA to tumors and their vasculature by novel dendritic nanocarriers. *FASEB J.* **24** (2010), 3122-3134.

[104] C.J. Langer, CT-2103: a novel macromolecular taxane with potential advantages compared with conventional taxanes, Clin. Lung Cancer **6** (2004) S85–88.

[105] P.A. Vasey, S.B. Kaye, R. Morrison, C. Twelves, P. Wilson, R. Duncan, A.H. Thomson, L.S.Murray, T.E. Hilditch, T. Murray, S. Burtles, D. Fraier, E. Frigerio, J. Cassidy Phase I clinical and pharmacokinetic study of PK1 [N-(2-hydroxypropyl)methacrylamide copolymer

doxorubicin]: First member of a new class of chemotherapeutic agents—drug–polymer conjugates. Clin. Cancer Res. **5** (1999) 83–94.

[106] L. Santucci, A. Mencarelli, B. Renga, G. Pasut, F. Veronese, A. Zacheo, A. Germani, S. Fiorucci, Nitric oxide modulates proapoptotic and antiapoptotic properties of chemotherapy agents: the case of NO-pegylated epirubicin, FASEB J. **20** (2006) 765-767.

[107] S. Jayant, J. J. Khandare, Y. Wang, A. P. Singh, N. Vorsa, T. Minko, Targeted Sialic Acid - Doxorubicin Prodrugs for Intracellular Delivery and Cancer Treatment, Pharm. Res., **24** (2007) 2120-2130.

[108] G. Gregoriadis, B. McCormacka, Z. Wang and R. Lifeiyb, Polysialic acids: potential in drug delivery, (1993) Febs Letters 315 (1993) 271-276.

[109] Arbuck, S. G., Dorr, A., and Friedman, M. A. Paclitaxel (Taxol) in breast cancer. *Hematol Oncol Clin North Am* **8** (1994), 121-140

[110] Cetnar, J. P., Malkowicz, S. B., Palmer, S. C., Wein, A. J., and Vaughn, D. J.. Pilot trial of adjuvant paclitaxel plus estramustine in resected high-risk prostate cancer. *Urology* **71** (2008), 942-946.

[111] Hennenfent, K. L., and Govindan, R., Novel formulations of taxanes: a review. Old wine in a new bottle? *Ann Oncol* **17** (2006), 735-749.

[112] Sanfilippo, N. J., Taneja, S. S., Chachoua, A., Lepor, H., and Formenti, S. C. Phase I/II study of biweekly paclitaxel and radiation in androgen-ablated locally advanced prostate cancer. *J Clin Oncol* **26** (2008), 2973-2978.

[113] Clementi C, Miller K, Mero A, Satchi-Fainaro R, Pasut G. Dendritic poly(ethylene glycol) bearing paclitaxel and alendronate for targeting bone neoplasm. Mol Pharm. **8** (4) (2011), 1063-72.

[114] Canal, F.; Vicent, M. J.; Pasut, G.; Schiavon, O. Relevance of folic acid/polymer ratio in targeted PEG-epirubicin conjugates. *J. Control. Release* **146 (**2010)*,* 388-399.